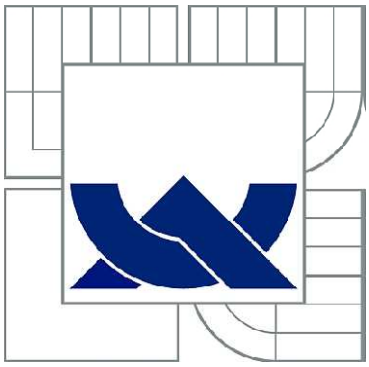

VYSOKÉ UČENÍ TECHNICKÉ V BRNĚ

BRNO UNIVERSITY OF TECHNOLOGY

FAKULTA ELEKTROTECHNIKY A KOMUNIKAČNÍCH TECHNOLOGIÍ
ÚSTAV BIOMEDICÍNSKÉHO INŽENÝRSTVÍ

FACULTY OF ELECTRICAL ENGINEERING AND COMMUNICATION
DEPARTMENT OF BIOMEDICAL ENGINEERING

POTLAČENÍ BALISTOKARDIOGRAFICKÉHO ARTEFAKTU V SIGNÁLU EEG

BALLISTOCARDIOGRAM ARTIFACT REMOVAL FROM EEG SIGNAL

DIPLOMOVÁ PRÁCE
MASTER´S THESIS

AUTOR PRÁCE — Bc. VÍT DOLEŽAL
AUTHOR

VEDOUCÍ PRÁCE — doc. Ing. JANA KOLÁŘOVÁ, Ph.D.
SUPERVISOR

BRNO 2010

VYSOKÉ UČENÍ TECHNICKÉ V BRNĚ

Fakulta elektrotechniky a komunikačních technologií

Ústav biomedicínského inženýrství

Diplomová práce

magisterský navazující studijní obor
Biomedicínské a ekologické inženýrství

Student: Bc. Vít Doležal ***ID:*** 114858
Ročník: 2

Akademický rok: 2009/2010

NÁZEV TÉMATU:

Potlačení balistokardiografického artefaktu v signálu EEG

POKYNY PRO VYPRACOVÁNÍ:

Prostudujte princip merení fMRI a EEG pro funkcní vyšetrení mozku. Seznamte se s možnými zdroji rušení EEG záznamu behem hybridního merení fMRI-EEG. Navrhnete algoritmus pro potlacení balistokardiografického artefaktu a realizujte jej. Funkcnost algoritmu overte na reálných datech získaných na pracovišti konzultanta.

Práce musí obsahovat teoretický úvod do problematiky vzniku balistokardografického artefaktu a prehled používaných prístupu jeho potlacení. Pro výslednou programovou aplikaci a namerená data doloženou dokumentaci a vyhodnocení funkcnosti navrženého postupu.

DOPORUCENÁ LITERATURA:

[1] Kim KH, Yoon HW, Park HW: Improved ballistocardiac artifact removal from the electroencephalogram recored in FMRI. J Neourosience Methods 135: 193-203, 2004
[2] Niazy RK et al: Removal of FMRI environment artifacts from EEG data using optimal basis sets. NeuroImage, in press 2005
[3] Allen PJ, Josephs O, Turner R: A Method for Removing Imaging Artifact from Continuous EEG Recording during Functional MRI. NeuroImage 12: 230-239, 2000.

Termín zadání: 12.10.2009 ***Termín odevzdání:*** 23.7.2010

Vedoucí práce: doc. Ing. Jana Kolárová, Ph.D.

prof. Ing. Jirí Jan, CSc.
Predseda oborové rady

LICENČNÍ SMLOUVA
POSKYTOVANÁ K VÝKONU PRÁVA UŽÍT ŠKOLNÍ DÍLO

uzavřená mezi smluvními stranami:

1. Pan/paní

Jméno a příjmení: Bc. Vít Doležal
Bytem: Vinohrady 2540, Kyjov, 697 01
Narozen/a (datum a místo): 26. ledna 1986 v Kyjově

(dále jen „autor“)

a

2. Vysoké učení technické v Brně

Fakulta elektrotechniky a komunikačních technologií
se sídlem Údolní 244/53, Brno, 602 00
jejímž jménem jedná na základě písemného pověření děkanem fakulty:
prof. Ing. Ivo Provazník, Ph.D. předseda rady oboru Biomedicínské a ekologické inženýrství
(dále jen „nabyvatel“)

Čl. 1
Specifikace školního díla

1. Předmětem této smlouvy je vysokoškolská kvalifikační práce (VŠKP):

- □ disertační práce
- □ diplomová práce
- □ bakalářská práce
- □ jiná práce, jejíž druh je specifikován jako .....

(dále jen VŠKP nebo dílo)

Název VŠKP: Potlačení balistokardigrafického artefaktu v signálu EEG
Vedoucí/ školitel VŠKP: doc.Ing. Jana Kolářová, Ph.D.
Ústav: Ústav biomedicínského inženýrství
Datum obhajoby VŠKP:

VŠKP odevzdal autor nabyvateli v*:

tištěné formě – počet exemplářů: 2
elektronické formě – počet exemplářů: 2

---

* hodící se zaškrtněte

2.Autor prohlašuje, že vytvořil samostatnou vlastní tvůrčí činností dílo shora popsané a specifikované. Autor dále prohlašuje, že při zpracovávání díla se sám nedostal do rozporu s autorským zákonem a předpisy souvisejícími a že je dílo dílem původním.
3. Dílo je chráněno jako dílo dle autorského zákona v platném znění.
4. Autor potvrzuje, že listinná a elektronická verze díla je identická.

Článek 2
Udělení licenčního oprávnění

1. Autor touto smlouvou poskytuje nabyvateli oprávnění (licenci) k výkonu práva uvedené dílo nevýdělečně užít, archivovat a zpřístupnit ke studijním, výukovým a výzkumným účelům včetně pořizovaní výpisů, opisů a rozmnoženin.
2. Licence je poskytována celosvětově, pro celou dobu trvání autorských a majetkových práv k dílu.
3. Autor souhlasí se zveřejněním díla v databázi přístupné v mezinárodní síti

- □ ihned po uzavření této smlouvy
- □ 1 rok po uzavření této smlouvy
- □ 3 roky po uzavření této smlouvy
- □ 5 let po uzavření této smlouvy
- □ 10 let po uzavření této smlouvy

(z důvodu utajení v něm obsažených informací)
4. Nevýdělečné zveřejňování díla nabyvatelem v souladu s ustanovením § 47b zákona č. 111/ 1998 Sb., v platném znění, nevyžaduje licenci a nabyvatel je k němu povinen a oprávněn ze zákona.

Článek 3
Závěrečná ustanovení

1. Smlouva je sepsána ve třech vyhotoveních s platností originálu, přičemž po jednom vyhotovení obdrží autor a nabyvatel, další vyhotovení je vloženo do VŠKP.
2. Vztahy mezi smluvními stranami vzniklé a neupravené touto smlouvou se řídí autorským zákonem, občanským zákoníkem, vysokoškolským zákonem, zákonem o archivnictví, v platném znění a popř. dalšími právními předpisy.
3. Licenční smlouva byla uzavřena na základě svobodné a pravé vůle smluvních stran, s plným porozuměním jejímu textu i důsledkům, nikoliv v tísni a za nápadně nevýhodných podmínek.
4. Licenční smlouva nabývá platnosti a účinnosti dnem jejího podpisu oběma smluvními stranami.

V Brně dne: 15. července 2010

……..	……
Nabyvatel	Autor

Abstrakt

Diplomová práce se zabývá hybridním vyšetřením fMRI-EEG. V EEG signálu jsou přítomny dva základní artefakty, gradientní a balistokardiografický. Po odstranění gradientního artefaktu a detekce R vln v kanálu EKG byl navržen postup pro odstranění balistokardiografického artefaktu, pomocí metody odečtu artefaktového vzoru, pomocí metody ICA (metody nezávislých proměnných) a metody spojující obě uvedené. Byla vyhodnocena úspěšnost všech metod a jejich vliv na evokované potenciály v signálu EEG.

Klíčová slova

balistokardiografický artefakt, gradientní artefakt, metoda nezávislých proměnných, evokované potenciály

Abstract

Master´s thesis deals with hybrid examination fMRI-EEG. Two main artifacts are present in EEG, imaging (gradient) and ballistocardiographic. After gradient artifact removal and R wave detection in ECG channel, approach for ballistographic artifact removal was proposed, with help of artifact template subtraction method, ICA and combined method. Efficiency and influence on evoked potentials of all methods were evaluated.

Keywords

ballistocardiographic artifact, gradient artifact, independent component analysis, evoked potentials

DOLEŽAL, V. *Potlačení balistokardiografického artefaktu v signálu EEG.* Brno: Vysoké učení technické v Brně, Fakulta elektrotechniky a komunikačních technologií, 2010. 72 s. Vedoucí diplomové práce doc. Ing. Jana Kolářová, Ph.D.

Prohlášení

Prohlašuji, že svou diplomovou práci na téma Potlačení balistokardigrafického artefaktu v signálu EEG jsem vypracoval samostatně pod vedením vedoucího diplomové práce a s použitím odborné literatury a dalších informačních zdrojů, které jsou všechny citovány v práci a uvedeny v seznamu literatury na konci práce.

Jako autor uvedené diplomové práce dále prohlašuji, že v souvislosti s vytvořením této diplomové práce jsem neporušil autorská práva třetích osob, zejména jsem nezasáhl nedovoleným způsobem do cizích autorských práv osobnostních a jsem si plně vědom následků porušení ustanovení § 11 a následujících autorského zákona č. 121/2000 Sb., včetně možných trestněprávních důsledků vyplývajících z ustanovení § 152 trestního zákona č. 140/1961 Sb.

V Brně dne 15. července 2010 . .....
podpis autora

Poděkování

Děkuji vedoucímu diplomové práce Ing. Janě Kolářové, Ph.D. za účinnou metodickou, pedagogickou a odbornou pomoc a další cenné rady při zpracování mé diplomové práce.

V Brně dne 15.července 2010 .....
podpis autora

Table of contents

List of Figures

1 Introduction

Combined recording and analysis of electroencephalography (EEG) and functional magnetic resonance imaging(fMRI) provide non-invasively information about functional state of brain. EEG has a very good temporal resolution, but suffer from poor spatial resolution. fMRI has an advantage in good spatial resolution, but due to nonzero duration of data acquisition we cannot reach a suitable temporal resolution. Combined measurement has been used for the examination of event-related potentials, spontaneous sleep, epileptic activity as well as alpha rhytms.

EEG data suffer in this case from two major artifacts. The gradient artifact is caused by switching of magnetic fields during MRI image aquisition. The second, ballistocardiogram artifact (BCG) is a bigger methodological challenge. It is related to cardiac related movements of the body, small, but firm movement of the electrodes and scalp due to expansion and contraction of scalp arteries. Also fluctiations of the Hall-voltage due to pulsatile speed changes of the blood in arteries plays it´s role.

In this thesis, whole artifact removal process will be described. Firstly, imaging artifact must be removed. Secondly, QRS intervals in ECG channels must be well detected. In third part, possible methods for BCG artifact removal are proposed. On the end, effect on the evoked potentials is described.

2 Theoretical part

2.1 fMRI

Functional magnetic resonance imaging measures the hemodynamic response related to neural aktivity in the human brain. This idea has been presented since 1890s. Since the neural cells has been active, consumption of oxygen increases and at this time the metabolism switches to anaerobic glycolysis, the local response is increasing blood flow to these regions of increased neural activity. This response has a latency of approximately 1-5 s. After this interval blood flow falls slightly to baseline. This leads to local changes in the relative concentration of hemoglobin and oxyhemoglobin.
In 1990 Dr. Seiji Ogawa reported the blood oxygenation level dependent (BOLD) contrast mechanism. The basis of this technique is the fact, that deoxyhemoglobin acts as own natural intravascular paramagnetic agent. This means, it alters the magnetic field in its vicinity. The effect is directly equal to the concentration of deoxyhemoglobin. Detectable local distortion of the magnetic field surrounding the red blood cells and surrounding blood vessel is produced. This has effect on decreasing in both transverse relaxation time (T_2) and the apparent transverse relaxation time (T_2^*). It caused attenuation of the signal intensity.

2.2 EEG

Electroencephalography is a recording of the electrical activity of brain produced by firing neurons. Signals from the scalp have, in general, amplitudes ranging from a few μVs to approximately 100 μV and frequencies, which extent from 0,5 to 30-40 Hz. EEG rhythms are conventionally classified into five frequency bands.
Content of different types of rhythms depends on the age and mental state of the subject. Newborn EEG is different from adult one, it contents significantly higher frequencies.

2.2.1 Rhytms

These rhytms are present:

a) δ (<4 Hz)

This rhythm has a large amplitude. It occurs mostly during deep sleep. It is usually not observed in the awake, normal adult, but may occur during cerebral damage or brain disease(encephalopathy).

b) θ (4-7 Hz)

We can find this rhythm during drowsiness and in certain stages of sleep.

c) α (8-13 Hz)

This rhytms is typical in normal subjects who are relaxed and awake with closed eyes. This activity decreases when the eyes are open. Largest amplitude is measured in the occipital regions.

d) β (14-30 Hz)

Fast rhythm with low amplitude. It occurs during certain sleep stages. It occurs mainly in the frontal and central regions of the scalp and it is connected to the activated cortex.

e) γ (> 30 Hz)

Gamma rhythm is related to the state of active information processing of the cortex.

Most of the above rhythms may persist up to several minutes, while others occur only for a few seconds, such as γ rhythm. It is important to realize that one rhythm is not present at all times, but an irregular, arrhytmic-looking signal may prevail during long time intervals.

2.2.1 Recording techniques

The clinical EEG commonly uses the international 10/20 system, which is standardized. This system means, that 21 electrodes are attached to the surface of the scalp. The numbers 10 and 20 are percentages signifying relative distances between different electrode locations on the skull perimeter. Bipolar and also unipolar electrodes are used in clinical routine. Unipolar electrodes require a reference electrode, either positioned distantly or taken as the average of all electrodes. The spacing is relatively sparse. The distance is 4,5 cm between electrodes. Using too few electrodes may result in aliasing in the spatial domain and consequently, the electrical activity will be inaccurately represented. Sufficient number of electrodes are 64 or higher in order to provide sufficient details. Sampling interval is usually selectected at 200 Hz. More detailed characteristics analysis of transient evoked waveforms may, however, necessitate a substantionally higher sampling rate.

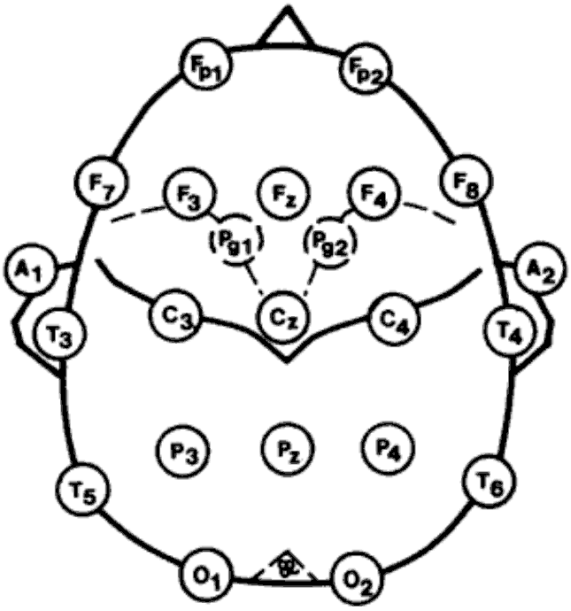

Fig 1 International 10-20 EEG electrode systém (redrawn from [1]). Odd numbers are on the left, even numbers on right and with Z in the center.

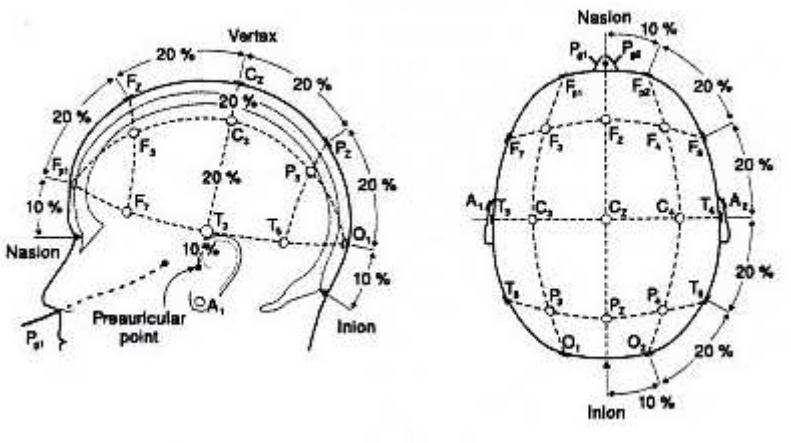

Fig 2 International 10-20 EEG electrode systém[2]

Main EEG applications are study of epilepsy and sleep disorders.[2]

2.3 Evoked potentials

Evoked potentials represent an event-related activity. I occurs in form of electrical response from the brain or the brainstem. Various types of sensory stimulation exist, visual and auditory are most commonly used. We can get information about sensory pathways abnormalities, disorders related to language and speech. Electrode configuration is similar to that of the EEG recording. The potentials are transient waveforms. Morphology of these waveforms depends on the type and strength of the stimulus, the electrode positions on the scalp and also mental state of the subject. (wakefulness, expectation and attention).

EPs typically extent from 0,1 to 10 μV. They are hidden in the ongoing activity, because this aktivity ranges from 10 up to 100 μVs. Ongoing activity is here considered as "noise". This noise must be suppressed. EPs occur regurarly after a delay, related to the time of stimulus presentation. Ensemble averaging can be used to reduce the noise level. This averaging is not without complications. Evoked response undergoes dynamic changes. Considerable research has been directed toward findingtechniques which can track dynamic changes, while at the same time providing sufficient noise reduction.

One popular approach consist of assumption, that each response can be modeled as a linear combination of a subset of orthogonal basis functions. The response is obtained by reconstruction of the response from a small number of basis functions. The weights of the linear combination result from fitting the basis functions to the observed response.

The peak (wave komponent) of the EP is referred to the letters P (positive amplitude) and N (negative amplitude). Number means the latency in miliseconds from the time at which the stimulus was elicited.

Evoked potentials usually results from visual (VEP), auditory (AEP) and somatosensory (SEP) stimulation. Normative values of these potentials are stringly dependent on age. We can mark these potentials as abnormal, when they have increased latency, decreased amplitude or are missing.

Isopotential maps

EPs are often analyzed in individual channels with respect to temporal and amplitude waveform properties without involving information recorded in other channels. Additional information can be derived on the spatial distribution of voltages on the scalp by simultaneously analyzing the data in a multichannel recording. Each map is created by connecting points on the scalp with equal voltages, this creates the isopotential map. Interpolation is usually performed to make the map continuous-looking for ease of interpretation. The resulting series of maps can be used to localize the underlying sources, that would generate the maps, sources which usually are considered in terms of a dipole model.

2.4 Hybrid fMRI/EEG

Hybrid simultaneously fMRI/EEG examination connects advantages of both methods. At the same time information from both methods is aquired. Optimal suppression of MR-induced artifacts require complex and time-demanding processing. The length of session reduces both subject´s discomfort and data processing restrictions. Due to this conditions several researchers are focussing on different techniques to combine EEG and fMRI separately. Simultaneous recording of EEG and MRI is necessary, when some time-depending effects (learning, habituation) occurs within the experimental design. Some brain processes are unpredictable. Some examples of this processes are abnormal activities in epileptic patients, sleep stages and spontaneous fluctuations of different EEG rhytms. When e.c. some cognitive process need to be explored, an additional sensory stimulation represents source of difference with the data collected outside. Reproducibility of cognitive experiments is discussed, therefore simultaneous aquisition is desired. fMRI does not affect latencies and amplitudes of the main waveforms, as well as scalp distribution of brain activity, that´s an argument for separate aquisition. In the contrary when analysis is focused on single-trial responses to nociceptive stimulation, variability induced a degree of unpredictability, therefore simultaneous acquisition is also desired. Simultaneous aquisition has an effect on between-trial variations, this could clarify better the relationship between the nature of the signal measured by EEG and fMRI. This could be shown on example, that latency jitter of LEPs strongly decreases the amplitude of the average signal as compared to the average of single-trial amplitudes. New approach has an aim of identifying EEG characteristics that correlate most closely with fMRI measures. Most of the studies describing evoked potentials accept the interleaved approach, that means relatively long periods of fMRI acquisition with similar periods without scanning. Second choice of the interleaved approach is performing "sparse" fMRI. Single images are collected with a delay that allows the registration of the predicted peak of an evoked hemodynamic response.
Both temporal and spatial resolution increase.[2]

Unfortunately, a lot of problems elicite. Experimental setup is difficult, EEG hardware must comply with conditions of patients safety and quality of collected data.

E.c. patients safety: During this examination some safety hazards can occur. The main is induction of currents in the EEG electrodes and leads by the various electromagnetic fields in fMRI. Avoiding loops in electrode leads and putting current-limiting resistors in series with each electrode lead may avoid danger. In contrast, maximization of the EEG signal-to-noise ratio is desired. F. e. when rf head coils is using, magnitude of B_1 near the head coil is sine-modulated. B_1 increases symmetrically as a function of the distance from the central axial plane with a gain about 60 % near the edges of the coil. Field must be lowest near the imaged body and maximum near the headcoil. Values differs not so significantly. Also power may be deposited inside body due to eddy currents from the RF pulses.[3]

The biggest problem during hybrid fMRI/EEG examination means artifacts.

Artifacts

Artifact in general is a structure or feature not normally present but visible as a result of an external agent or action, such as one seen in an image produced by radiology.
Artifacts in EEG can be divided into several major categories.

Firstly, machine and impedance artifact may destroy images. The electrode could be broken or improperly attached to the head. The most common machine artifact is so called 60-cycle artifact, either from common ground loop, when the patient has been grounded more than once or from nearby equipment. Ground electrode could be shorted to one of the active electrodes, it may appear in many different channels. Only when the bridge between ground and scalp electrodes is removed, this problem is eliminated.[1]

Multiple types of artifacts could be present at the same time. Certain types of artifacts are more frequently encountered in certain recording situaction, e.g. during sleep. Main types are muscle artifacts, less common artifacts have origin in respiration, tongue movements, tremor and skin potential.

Most common physiological artifacts are oculographic and cardiac.

The measured voltage is proportional to the angle of gaze. Eye is relative dipole, cornea is more positive, retina negative. The strength of the interfering EOG signal depends primarily on the proximity of the electrode to the eye and the direction in which the eye is moving. EOG artifact can sometimes be confused with slow EEG activity, theta and delta.EOG may interfere also when rapid movements occur during sleep. Eye movement artifact is easier to detect, when it develops from vertical eye movement. It suggest the possibility of bilaterally synchronous δ waves. Cortical activity have the same phase both above and below the eye.

Most troublesome artifact from cardiac artifacts is the artifact resulting from QRS complex. It produces a sharp wave or spike in the EEG. The constant rhythm is not a sufficient discriminator. A particular QRS complex will be observed, then several complexes will be missed and then another complex will be visible. It is crucial to apply EEG monitor to every patient, because otherwise it is not possible to differentiate ECG artifact and spikes. Only EEG electrode on the shoulder referenced to the ear is appropriate.
The next artifact is pulsation artifact. It results from the blood pulsing through a vessel under an electrode. Slow wave in EEG occurs. Slight movement of the electrode off the pulsating vessel is sufficient to eliminate this artifact.
The last is ballistocardiographic artifact.(Sometimes, all these artifacts are considered as cardiac related artifacts.)[2]

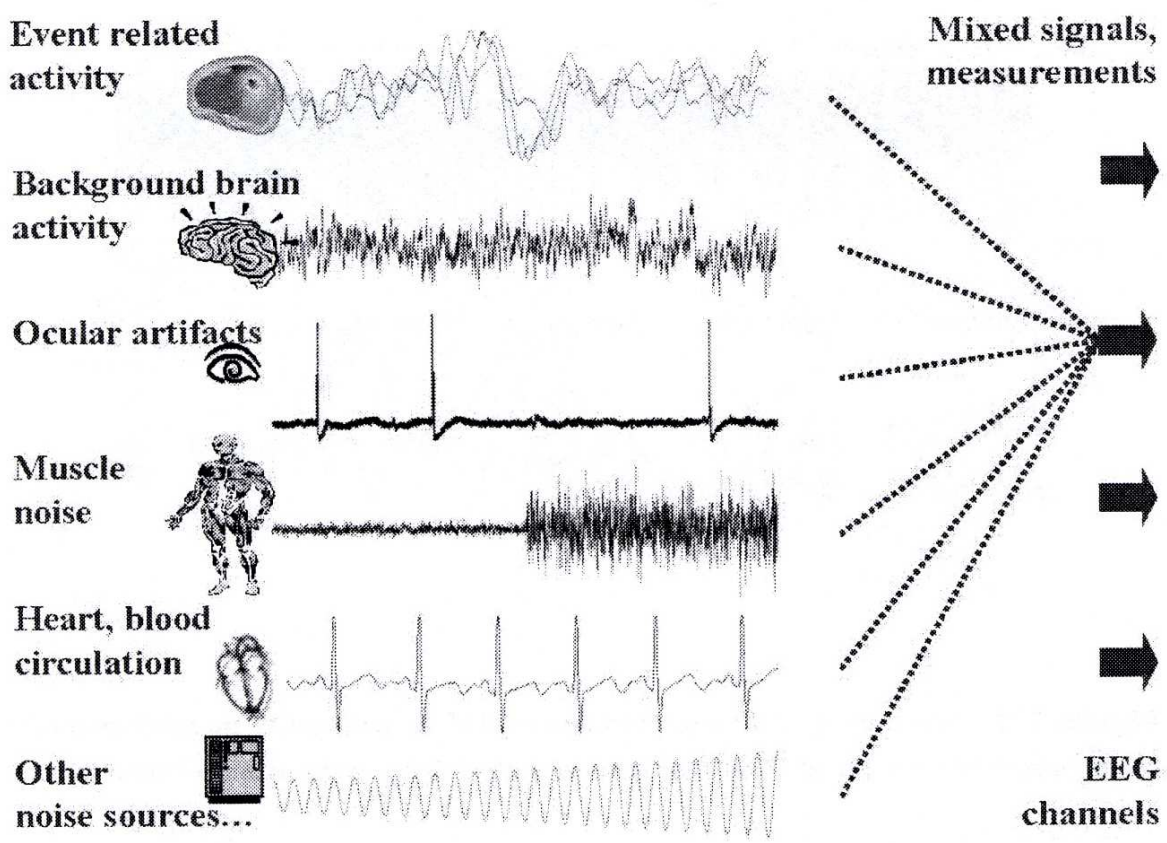

Fig 3 Noise sources in event related measurements [4]

2.4.1 Gradient (imaging) artifact

Magnetic field changes during the MRI examination due to switching of the magnetic field gradients. Normally, gradient switching is repeated during the acquisition of each slice. The amplitude of this artifact can be 100 times greater than the EEG signal. Also frequency range overlaps with EEG. Artifact amplitude and shape varies from one EEG channel to another depending on the location of the electrode and the wire connection. [5]

Although the artifact is a consequence of sequential RF and gradient pulses, which time scale is about microsecond time scale, original artifact usually consist of components with a much higher frequency than those of EEG. To obtain the real artifact waveform, 3-5 kHz sampling rate must be used. In [6] it was concluded, that the artifact can have complicated but consistent waveforms, and each peak component corresponds precisely to an RF or a gradient pulse. The artifacts caused by gradient pulses are much larger than those by RF pulses. An artifact component typically consist of
of a pair of peaks, one positive or negative and the other inverse to the previous. This implies, that the gradient artifact has its origin in electromagnetic coupling (Faraday's law). [6]

A detailed analysis of RF (radio frequency) and gradient artifact allows us to remove them through an online "sample by sample" subtraction.

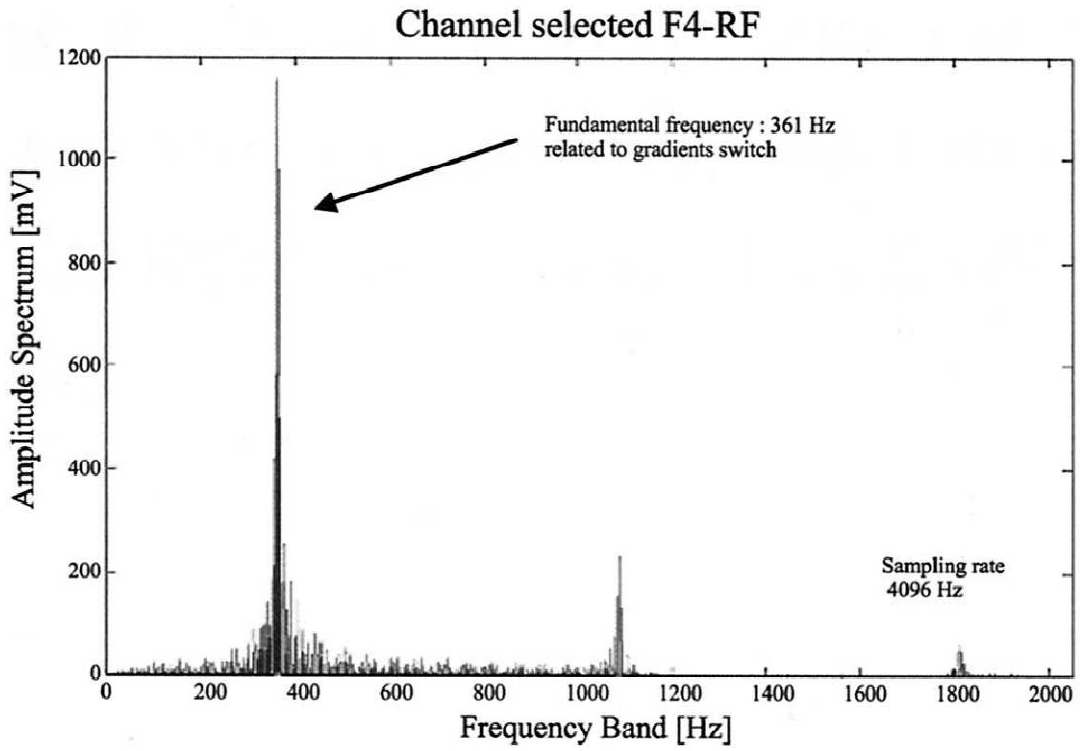

Fig 4 Main dominant frequencies carry out from gradient switching events.(source: [7])

It was estimated, that maximum gradient artifacts amplitude is of about a few tens of mV (12 mV for EEG signals and 120 mV for ECG signal, respectively). [7]
Another estimate of artifact size caused by switched gradient is of 600 mV in the EEG. The interference which come from the RF alone is 50 mV. [8]

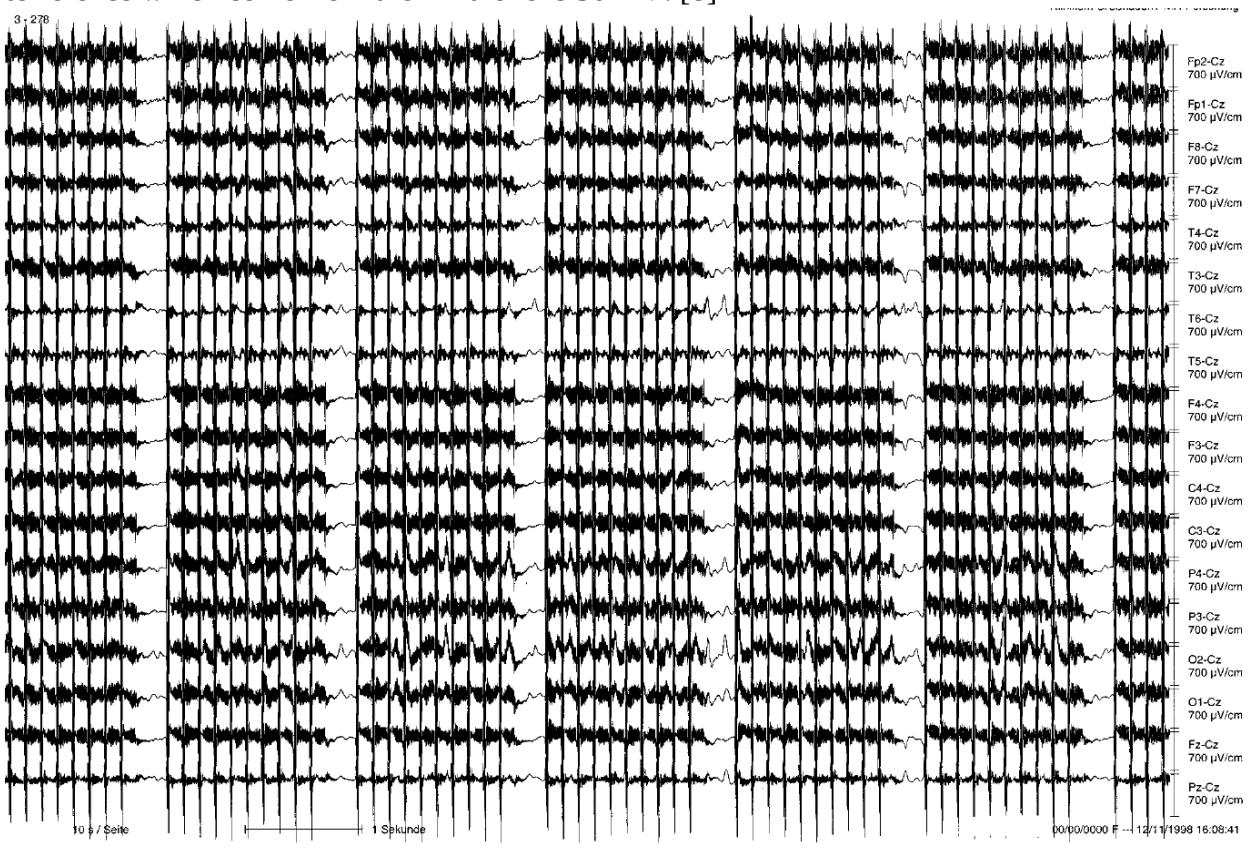

Fig 5 Example of typice shape of imaging artifact (source: [7])

2.4.2 Ballistocardiographic artifact

The large ballistocardiogram artifact is correlated to the current, which is induced by a wire-like blood movement in a magnetic field. [9] This artifact is originated by the slight micromovements of the head due to heartbeat and consist of potentials, that are sometimes higher than the EEG amplitude.[7] Pulse artifact can be induced by blood flow inside the heads veins, in normal direction to the static magnetic field. [8]

The exact properties of the BCG artefact are still poorly characterized, BCG became a methodological challenge. [10]

From the beginning of fMRI/EEG examination, in first EEG recordings substantial, heart-beat-related artifact was present [11][12]. As a reason pulsatile whole body motion, time-locked to cardiac activity was identified. [11] Body motion was caused by the abrupt reversal and acceleration in blood flow in the aortic arch. [12]

Study on interpretation of the possible origins of the BCG artefact lead to creating of of various BCG removal methods.

It is agreed, that motion causes the BCG, but it is still not clear, what particular motion is most relevant. Some researchers indicate cardiac-related head rotation, which is caused by axial body motion, as the major cause [11][13]. Other studies consider the pulsatile movement of the scalp as a main reason. Thus also EEG electrodes and cables movement is caused by the expansion and contraction of adjacent blood vessels. In [14] a motion sensor was placed on the temporal artery. This was used in combination with an adaptive filter, which lead to succesfull removal of the algorithm. Blood as a conductive fluid induces electrical potentials while moving [15] Blood flow itself could cause the BCG [16] [10]

Axial movement of the body can cause, with a delay, a nodding head rotation (pitch). Nodding head rotation leads to opposite polarity voltages at left and right hemisphere electrodes and also inverse polarity voltages in a later time due to the rotation of the head back to originál position.

If both of these effects (electrodes movement adjacent to blood vessels and current which is induced by blood flow) contribute to the artifact, BCG will be more spatially dependent than axial rotation alone. Areas, where electrodes are adjacent to blood vessels (frontal-temporal and occipital channels) would show larger BCG-related artifacts. Lateral electrodes would be pushed outwards by vessels. If these mechanisms, which have different tempoval and spatial properties, contribute to the to the BCG, this leads to removal methods, which are operating on a channel-by-channel instead of a spatial template basis. [10]

Head rotation is consider as a major contribution to the BCG [13] in both EEG and ECG channels, during the 200- to 400-ms interval. Some of these effects may also be caused by the momentu of the blood flow in axial direction towards the brain.
[10]

Average subtraction method assumes that all BCG waveforms are very simile during the gin recording session, which is unrealistic for movement. The assumption of regularity is obviously violated and average subtraction can actually cause distortion of the EEG. In EEG data, there may be artifacts, which are related to cardiac pulse and which should be dependent on BCG. [13]

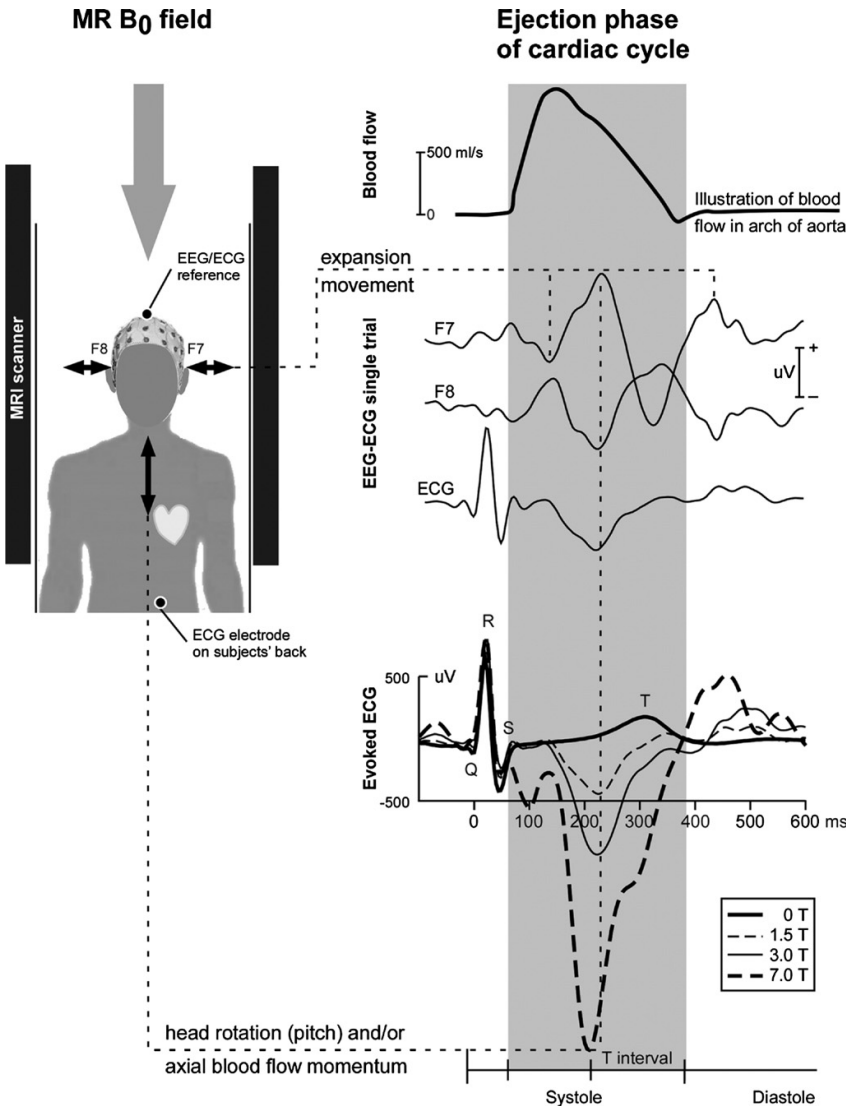

Fig 6 Two major contributions to the BCG artifact [10]

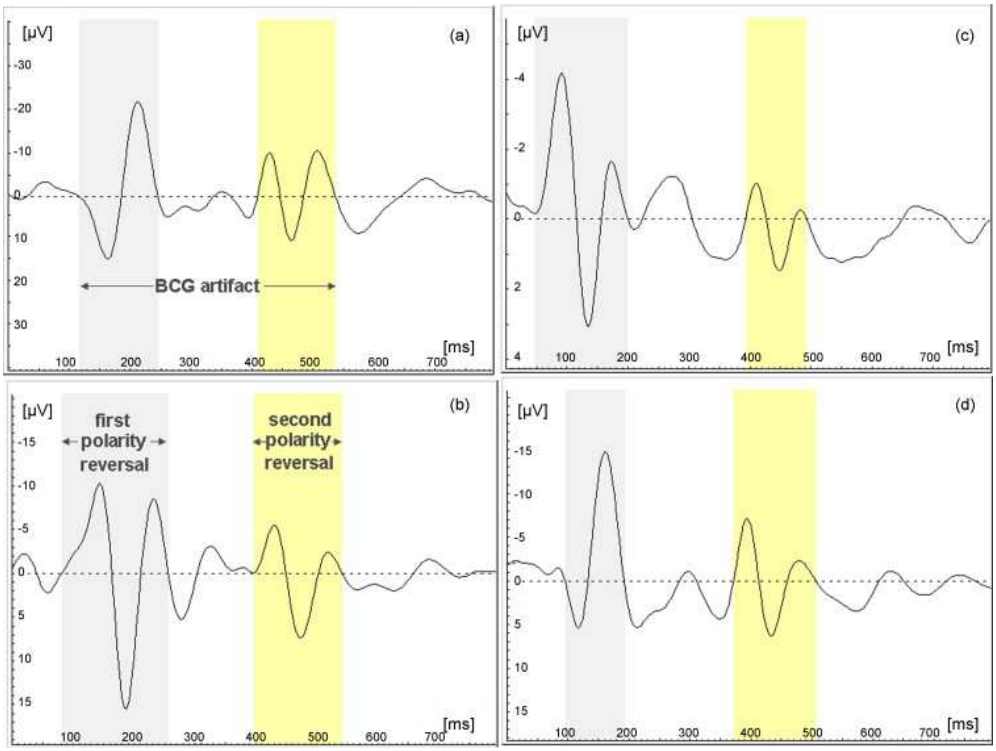

Fig 7 The averaged time courses of the BCG artifact in Cz for four representative subjects (source: [17])

E.g. BCG artifact can have in channel Cz characteristic time course. BCG mainly influenced the signal between 80 ms and 500 ms post-QRS complex. It can be defined as two successive polarity reversals. First high polarity reversal appears about 147 ms after the QRS complex and second, which is smaller, occurs 304 ms after the first one. Mean amplitude of first polarity reversal is 13,8 μV. Second has only 8 μV. [17]
Major artifact is present in ECG at a peak latency of about 210 ms [9] and does not start before 150 ms after the QRS complex. In one study, major artifact peak in the EEG become is visible, with a prominent left/right polarity reversal at about 230 to 240 ms [10]
Several removal methods are proposed in its origin by using the spatial properties of the bipolar montage. One possibility is to make a suitable wire setting patient head locking. [7]
Simple recomendation sounds: If the wires are fixed on the head and bound together to the amplifier more properly, amplitude of the ECG-synchronous pulse artifact and of the interference due to scanner aktivity can be decreased. The area of the inductive loop, which is formed by the
electrodes, the head, and the amplifier is decreased. Padding under the electrode wires and the amplifier can reduce the artifact amplitude in addition. [8]

2.4.2.1 Intensity of magnetic field and amplitude of BCG

Theoretically, considering the Lorentz' law it can be predicted that the amplitude of the BCG artefact is directly proportional to the strength of the magnetic field. [15] Also practically, in [10] the BCG artifact scaled linearly with the static magnetic field strength. Also spatial variability is increased at higher field strength as a consequence of increased magnitude of the BCG. Also because of the BCG is dynamic, it changes topography over time more at higher field strength. [10]

2.5 Methods

2.5.1 Basic noise removal algorithms

Noncerebral noise sources are eye blinks, eye and eyelid movements, muscle activity, 50/60 Hz powerline interference, instrumentation noise, poor electrode atachment etc.

Linear, time-invariant, bandpass filtering is sometimes used for removing noise, whose spectral content is outside that of the EP. It is imperative to use filters with a linear phase response in order to avoid distorting the interpeak latencies. E.c. band-pass filtering of the averaged signal of BAEP (brain auditory evoked potentials) have the lower and upper cut-off frequencies of the filter located approximately at 25 and 2000 Hz. Band-pass filtering characteristics arises, when the goal is to construct filter to maximize the signal-to-noise ratio (SNR). The avering methods are not succesfull, when the artifacts are related to the time of stimulus. The averaging methods requires that eye movement is first reliably detected in an EOG. Electrical activity of the heart is another noise source, which we cannot cancel with ensemble averaging methods. It is particularly difficult, when the heart rate coincide with the stimulus rate. Solving is to select suitable timing of stimulus, to avoid the coincidence or using aperiodic presentation of the stimulus. [2]
All disturbing frequencies outside the frequency windows of the EEG (0.5–40 Hz) could be eliminated by high- or low-pass filters without damage to the EEG, but within this range all frequencies generated by MRI must be selectively removed! [8]

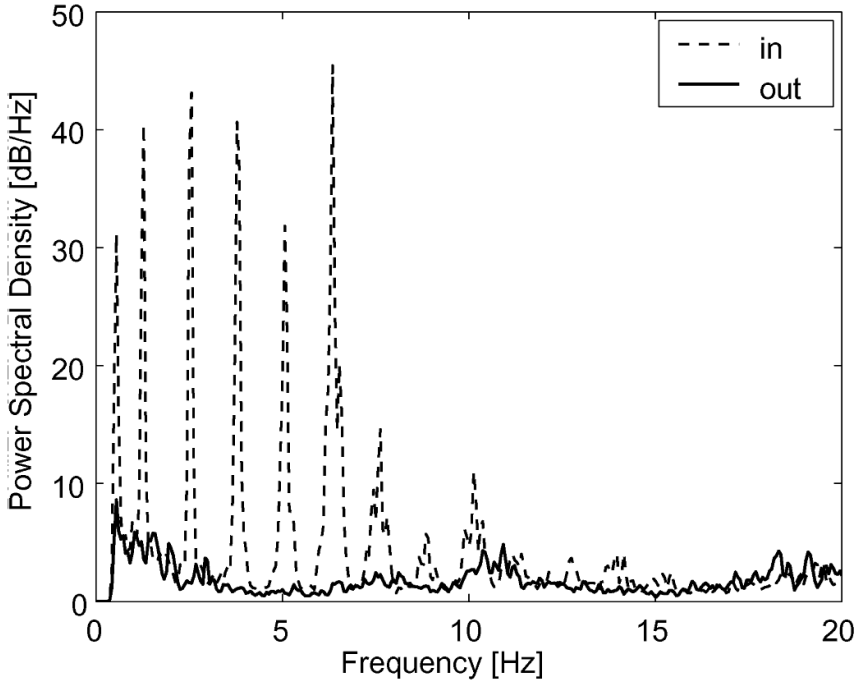

Fig 8 Example of power spectral densities of EEG data recorded inside(in) and outsider(out) the scanner (source: [13])

2.5.2 QRS detection algorithm

2.5.2.1 QRS detection algorithm in BrainVision

QRS is normally searched in ECG channel or EEG channel with well-defined pulse artifacts can be used instead. Firstly, template is counted. Normally, from first 15 s of the record. After „correlation trigger level“ setting, in the intervals, in which the current correlation is bigger than this level, is searched for maximum correlations. If the valu is between the minimum and maximum amplitude triggers, this value is identified as the pulse peak. [18]

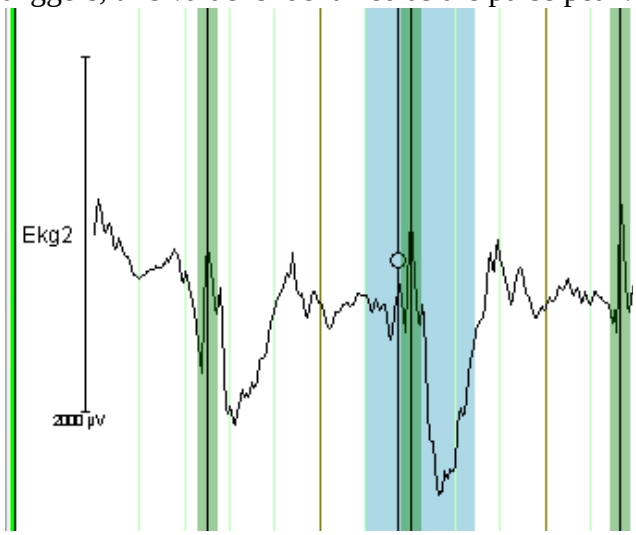

Fig 9 Qrs detection in BrainVision [18]

2.5.2.2 QRS detection algorithm by [19]

First step is complex lead constructing. It is done from several ECG channels. By most simultaneous EEG/fMRI measurements ECG channel is recorded from a single bipolar channel and thus another alternative complex lead is needed. ECG is first band-pass filtered from 7 to 40 Hz. Moving averaging of samples in 28 ms interval for electromyogram noise suppression is performed. The filter has first zero at about 35 Hz. The complex lead is calculated by applying the k-Teager energy operator (k-TEO) to the filtered ECG. Then a setting of these values to zero is applied.

$$\boldsymbol{X}(n) = max(\boldsymbol{E^2}(n) - \boldsymbol{E}(n-k)\boldsymbol{E}(n+k), 0) \quad (1)$$

X is the complex lead, **E** is the filtered ECG, *k* is the frequency selection parameter and *n* is the time index. *k* can be set to emphasize the desired frequency

$$k = \frac{f_s}{4f_d} \quad (2)$$

f_s is the sampling frequency and f_d is the desired frequency.

f_d is set to the 10th harmonic frequency of the ECG (Usually it is set to 10 Hz). Then, adaptive threshold method (MFR) is applied to the complex lead **X.**
Method used by [19] introduces absolute values of a threshold *MFR = M + F + R*, which is a combination of three independent adaptive thresholds. F is integrating threshold for high-frequency signal, M means steep-slope threshold and the last one, R, the beat expectation threshold.

Moving averaging filter averages samples in one period of the powerline interference frequency with first zero at this frequency. Then next moving averaging filtering is applied on the complex lead. It is done in 40 ms intervals. This filter has first zero at about 25 Hz. It´s function is suppressing the noise.

Complex lead is in cases of 12-standard leads, synthesis of the three quasi-orthogonal Frank leads. The complex lead is a spatial vector. It can be obtained by

$$Y(i) = \frac{1}{L}\sum_{j=1}^{L}\left|X_j(i+1) - X_j(i-1)\right| \quad (3)$$

Xj(i) is the amplitude value of the sample *i* in lead *j* and *Y(i)* is the current complex lead.

2.5.2.3 Adaptive steep-slope threshold – M

On the begining we set $M = 0{,}6 \cdot \max(Y)$ for the first 5 s of the signal. At least 2 QRS complexes are present. A buffer with 5 steep-slope threshold values is preset:

$$MM = [M_1 M_2 M_3 M_4 M_5] \quad (4)$$

where $M_1 \div M_5$ are equal to *M*

If $Y_i \geq MFR$, then QRS or beat complex is detected. At the time 200 ms after the current detection is no next detected. In this gap a new value of M_5 is calculated via:

$$newM_5 = 0{,}6 \cdot max(Y_i) \quad (5)$$

The *newM*5 value may increase strongly, if steep slope premature ventricular contraction or artifact appeared. Then we set $newM_5 = 1{,}1 \cdot M_5$ if $newM_5 > 1{,}5M_5$
Then we exclude the oldest MM buffer component and include $M_5 = newM_5$. *M* is then an average of MM. In an interval from 200 to 1200 ms M value decreases. After 1200 ms *M* doesn´t change.

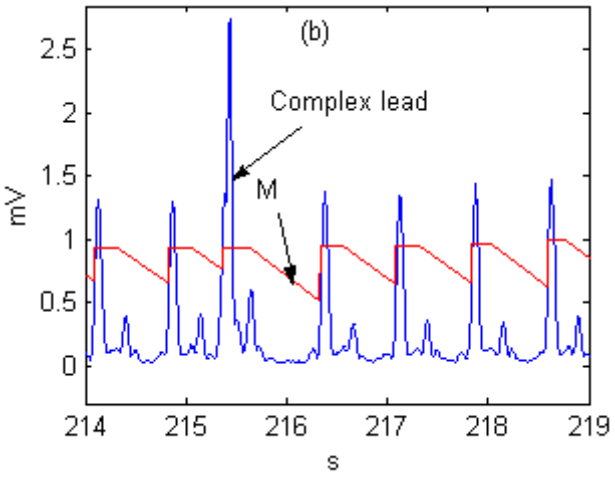

Fig 10 Adaptive steep-slope threshold (source: [19])

2.5.2.4 Adaptive integrating threshold – F

If electromyogram noise is present together with ECG, this integrating threshold increases combined threshold. On the begining *F* is the mean value of the pseudo-spatial velocity *Y* for 350 ms. Sample-by-sample is F:

$$F = F + \frac{\left(max(Y_{in\ latest\ 50\ ms\ in\ the\ 350\ ms\ interval}) - max(Y_{in\ earliest\ 50\ ms\ in\ the\ 350\ ms\ interval})\right)}{150} \quad (6)$$

Not every sample in the 350 ms interval is integrated, just the envelope of the pseudospatial velocity *Y*. The weight coefficient 1/150 is derived empirically.

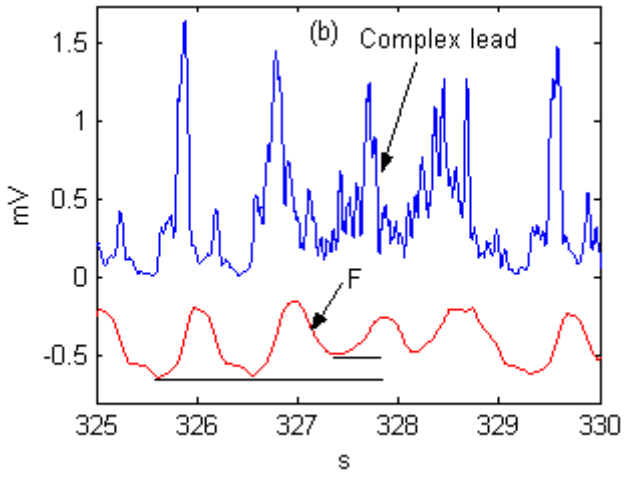

Fig 11 Adaptive integrating threshold (source: [19])

2.5.2.5 Adaptive beat expectation threshold – R

This threshold is useful with heartbeats of normal amplitude followed by a beat with very small amplitude slew rate. This can be observed for example in cases of electrode artifacts. *R* protects against 'QRS misdetection'. A buffer with the 5 last RR intervals is updated at any new QRS detection. R_m is the mean value of the buffer. R is a zero in the time from the detected QRS to $\frac{2}{3}$ of the expected R_m. In the interval from $QRS + \frac{2}{3}R_m$to $QRS + R_m$, M decreases 1,4 times faster then the R. After $QRS + R_m$interval the decrease of *R* is stopped.

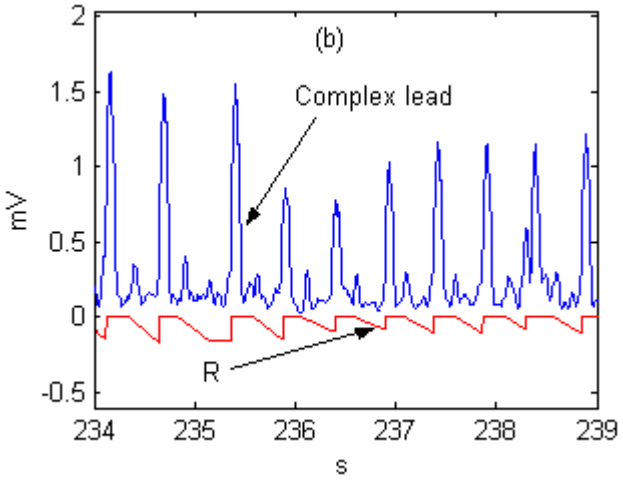

Fig 12 adaptive beat expectations threshold [19])

2.5.2.6 Combined adaptive threshold – MFR

The combined adaptive threshold is a sum of the adaptive steep-slope threshold, adaptive integrating threshold and adaptive beat expectation thresholds.

$$MFR = M + F + R \quad (7)$$

A QRS peak is detected, when X(n) is higher than MFR(n).

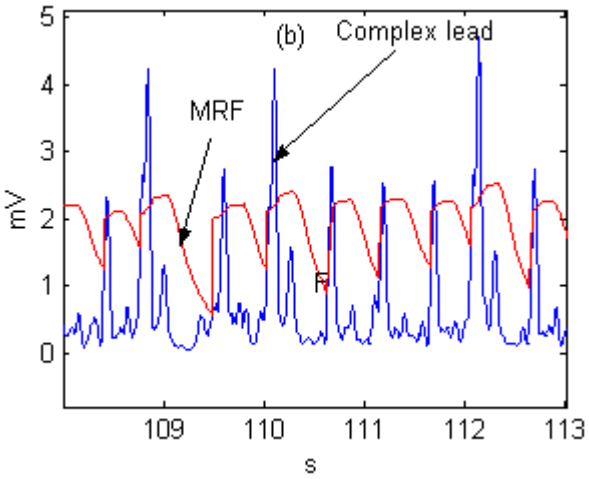

Fig 13 Combined threshold [19])

2.5.2.7 QRS peak correction algorithm

We have a binary vector, 1 indicates a QRS peak. Median $\tilde{X}_{RR}$ and standard deviation, σ_{RR}, are calculated. P is divided into 20-s sections, P_u^s, where u=1,2,...,U. These sections overlap by 5 s. For Q ones in the section, there is Q - 1 RR intervals. These RR are calculated, For any $RR(r) < \left(\tilde{X}_{RR} - 3\sigma_{RR}\right)$ is $P_u^s\left(n_{RR(r)}\right)$ set to zero. This means, if the difference between two consecutive peaks is less than the median of RR minus 3 times the standard deviation of all RR intervals, the second peak is set to zero, that means this peak is removed. The original P is updated before the next section is processed. The original ECG is then divided into equal segments according to the corrected peaks in P and the segments are averaged to form an average ECG beat waveform. The peaks are then adjusted to maximize the correlation between heart waveforms and the reference waveform. As we saw, P is then again divided into 20-s sections. For any $RR(r) > \left(1{,}5\tilde{X}_{RRu}\right)$ is $\mathrm{P_u^s\left(n_{RR(r-1)} + \tilde{X}_{RRu}\right)}$ set to 1. When the difference between two consecutive peaks is more than 1,5 times the median RR for that section, a peak is added at time $\tilde{X}_{RR}$ after the first peak. False negative are corrected. The original P is again updated, before the next section. [19] [5]

2.5.2.8 Quality of QRS detection

For each ECG recording, the total number of QRS complexes/heart beats was counted manually. This total number is T_P. F_N means any QRS complex not detected by this algorithmus. $F_N$represents number of false positive, that means QRS complex is detected, but in real measurement is absent. If a QRS complex was detected but its position had a time-shift error, the algorithm indicated the location of the QRS a little early or late, this was considered both as false negative and a false positive.

sensitivity: $$S_E = \frac{T_P}{T_{P+F_N}} \quad (8)$$

2.5.3 Image artifact removal

2.5.3.1 FASTR

fMRI artifact slice template removal is based on constructing a unique template for each artifact segment, in each channel during a single fMRI slice. The algorithm has four parts.

.2.5.3.1.1 First part

During the acquisition, the triggers from MRI machine are sent at the start of each slice acquisition. MRI and EEG are driven by separate clocks, some degree of misalignment - "jitter", may occur. The jitter is worse as the EEG sampling rate is reduced. EEG channel data is sinc interpolated (up-sampled) to bring the sampling rate to about 20 kHz and then divided into segments according to the slice-timing triggers. Artifact segment means the window covering the duration of a single slice artifact occurrence. The first artifact segment is taken as a reference. Trigger location is adapted to maximize the correlation with the reference.

.2.5.3.1.2 Second part

It is useful for any channel, to high-pass filter (1 Hz) them. It removes any slow drifts in the EEG. Different artifact segments used in the average artifact estimation have the same baseline. High-pass filtered version $\boldsymbol{Y}^h$ is then segmented into *N* (*N = volumes x slices*) equal sized segments according to the adjusted/aligned slice-timing triggers. Each of these segments is a 1 x q vector, where q is the number of time points spanning each artifact interval
The local moving average artifact template for each segment is then:

$$\boldsymbol{A}_j = \frac{1}{|I(j)|}\sum_{l\in I(j)} \boldsymbol{Y}_l^h (9)$$

j=1,2,…,N are indexes the slice artifact segments, $\boldsymbol{A}_j$ is *1 x q* vector of the local moving average artifact template for segment *j* and *l* is an index of the different artifact segments to be averaged.

I(j) is an index function, which determines which segments are included in the average. The slice segments in *I(j)* are centered around segment j and are chosen so, that there is sufficient time gap between them to ensure that there is no EEG autocorrelation between segments included in the template computation. This approach removes any data that correlates with the fMRI slice acquisition indiscriminately. The user set only how many elements to include in *I(j)*, the length of the moving average window and how much gap to leave between the selected segments. Shorter window will increase the adaptivity of the algorithm, and also the more noisy the artifact template, more real EEG data is removed. The gap should fit the closeness the segments in time. Finally, the computed template, $\boldsymbol{A}_j$, is scaled by a constant α to minimize the least squares between the template and the data. Then we subtract the scaled artifact from $\boldsymbol{Y}^h$ to generate a signal $\boldsymbol{Y}^r$. It is then cleaned EEG data with residual artifacts. This stage is useful to remove the bulk of the artifact variance and is adaptive to sudden changes in the artifact shape. This stage does not capture the exact artifact shape.

.2.5.3.1.3 Third part

From $\boldsymbol{Y}^r$ is extracted a set of basis functions for the residuals. $\boldsymbol{S}_{p\times q}$ is a residual matrix. p is the number of artifact segments. PCA is then performed on **S.** PC as principal component is projection of **S** onto the principal component coefficients. The first C of the PCs represents an optimal basis set (OBS), $\boldsymbol{B}_{q\times C}$. The number of C components is derived on the amount of variance explained by the PCs. C is chosen conservatively, since including unnecessary components may result in the loss of data.

$$\boldsymbol{Y}_j^{r'} = \boldsymbol{B}\beta_j + \varepsilon'_j (10)$$

$\beta_j$is a C x 1 vector of weights to fit **B** to □^{r}and ε_j is an error term for the segment.

The weights are estimated by least squares and added to the artifact noise found the local slice artifact template subtraction to create the final estimation of the gradient artifacts, **Z**, and an artifact-subtracted EEG data $\boldsymbol{Y}^n$. Final estimated noise is subtracted from the original interpolated EEG data,

not the high-pass filtered version. Both **Z** and $\boldsymbol{Y}^n$ are low-pass filtered at 70 Hz, then down-sampled back to the original sampling frequency, then $\boldsymbol{Z}^d$ and $\boldsymbol{Y}^d$, respectively. Residuals matrix **S** needs to have as many entries as possible for the PCA to produce an accurate OBS. The second and third stage should be adaptive and accurate. This stage is useful for removing the details of the residuals.

.2.5.3.1.4 Fourth part

Adaptive noise cancellation.
Signal contaminated with the noise constitutes the input to the filter, **Y**. The source of the noise is assumed to be known. The noise in the signal is correlated with the reference noise. The weights of the filters are hold and updated at each time point with least mean-square (LMS) algorithm. The accuracy of estimation is limited by the quality of the reference noise and choise of μ (step size) and L (length of the weight vector). Final artifact estimation, $\boldsymbol{Z}^d$, is the reference for ANC. The subtracted noise **Z** provides more accurate reference for this purpose and was found to have less effect on real data. The input to the ANC filter is a high-pass filtered version $\boldsymbol{Y}^d$. Cut-off frequency is set to be half of the fundamental gradient artifact frequency, $f_c = \frac{slices}{2TR}$. The output is then subtracted from the original $\boldsymbol{Y}^d$ to produce the final clean data. It fails to adapt quickly enough to adequately remove all residuals. ANC occasionally diverges, when applied to channels with high amplitude residuals. Basis functions in the OBS do not perfectly describe all residual variations. [5]

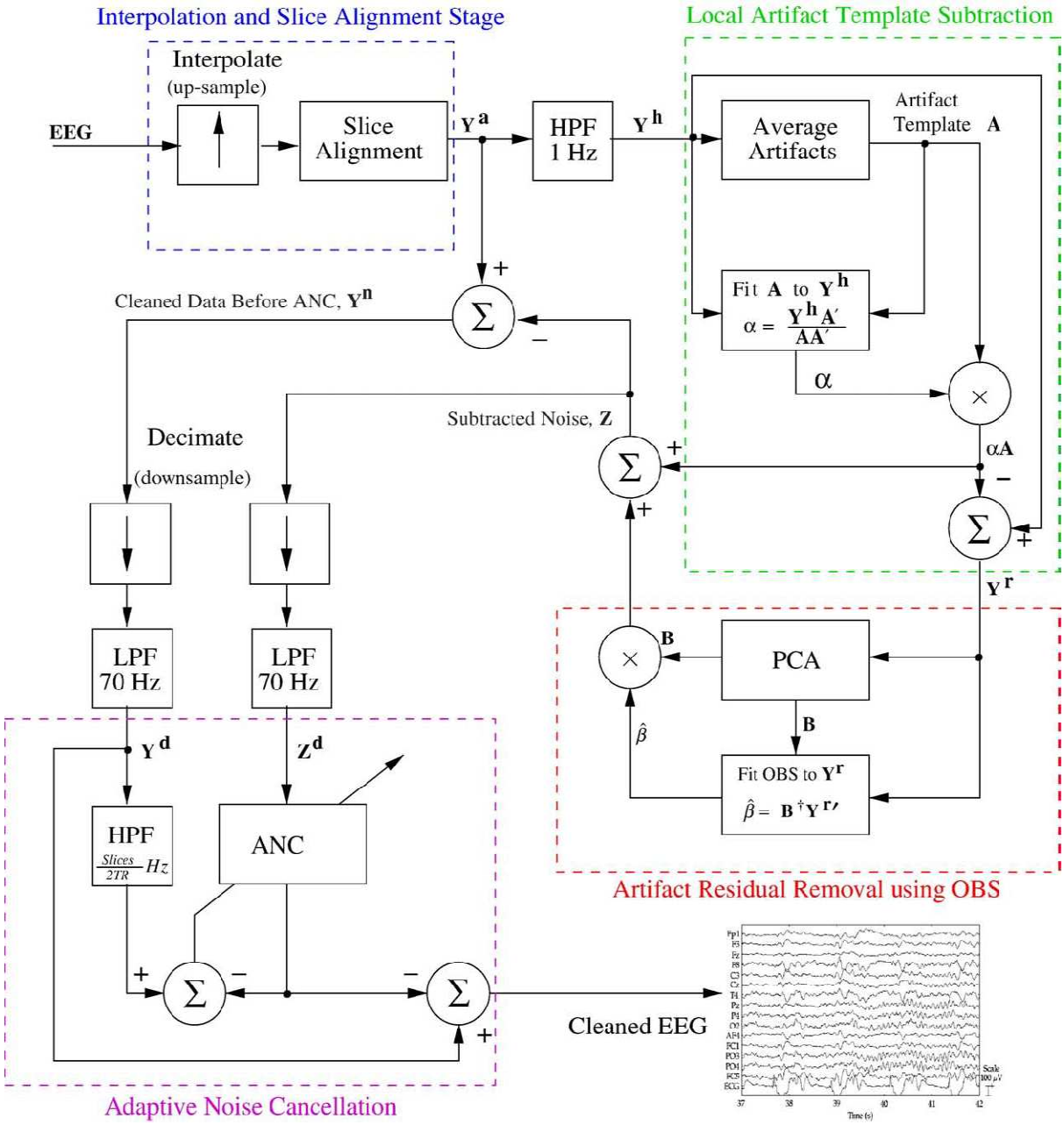

Fig 14 FASTR [5]

2.5.3.2 Image artifact reduction used in Brain vision analyzer

First stage of imaging (gradient) artifact removing is based on calculating an average imaging artifact waveform a subtraction from the EEG each epoch. Second part introduces adaptive noise canceling. Volume repeat time, TR is defined as an epoch. EEG recording is divided into sections of 25 epochs. There is an assumption, that EEG is uncorrelated between epochs. 25 epochs is sufficient to obtain an accurate average. For continuous fMRI acquisition, an epoch is defined as one slice. One slice takes less than 100 ms, correlation between epochs is relative likely. EEG is uncorrelated over 0,3 s. EEG is then divided into sections of 25 x 0,3 = 7,5 s. The averaging time includes also a period, when no gradient changes are applied, because artifact is present also. This is caused due to subject movement in the static fields. The first five epochs in each section were always included – subsequent epochs were included only if the cross correlation function between the epoch and current average exceeded 0,975. Although not optimal is this scheme was a computationally efficient method for reducing averaged artifact corruption by atypical epoch signals, for example, those in which a subject

movement occurred. EEG is interpolated by sinc function, to be synchronous with the slice-timing signal. Similar interpolation is performed in the reverse direction to synchronize the averaged waveform to the EEG samples. After subtracting, smoothing is performed to reduce the danger of aliasing in the next process. Additional low-pass filtering was then performed (55 coefficient, finite impulse response, cut-off 50 Hz). Adaptive noise cancelling can reduce signal components correlated with a reference signal and was considered appropriate for removing this residual artifact. By ANC the EEG signal with averaged artifact subtracted was used as the primary input. Reference signal has 1 on the positions, where slice-timing signals occurred, other values are set to zero. Adaptive filter´s length is 20 and it is adapted for every input sample using the Widrow-Hoff least mean squares algorithm to minimize the error between the filter output and the primary signal. Step size (μ) is set to 0,05. The filter is applied only to the EEG coincident with imaging,as residual artifact is present only during these periods. To reduce the discontinuity between these periods, the reference signal was tapered (raised cosine function) over the first and last 0,5 of each period. The EEG output was taken as the difference between the primary signal and the adaptive filter output, that is, the EEG signal minus components correlated with the reference signal.

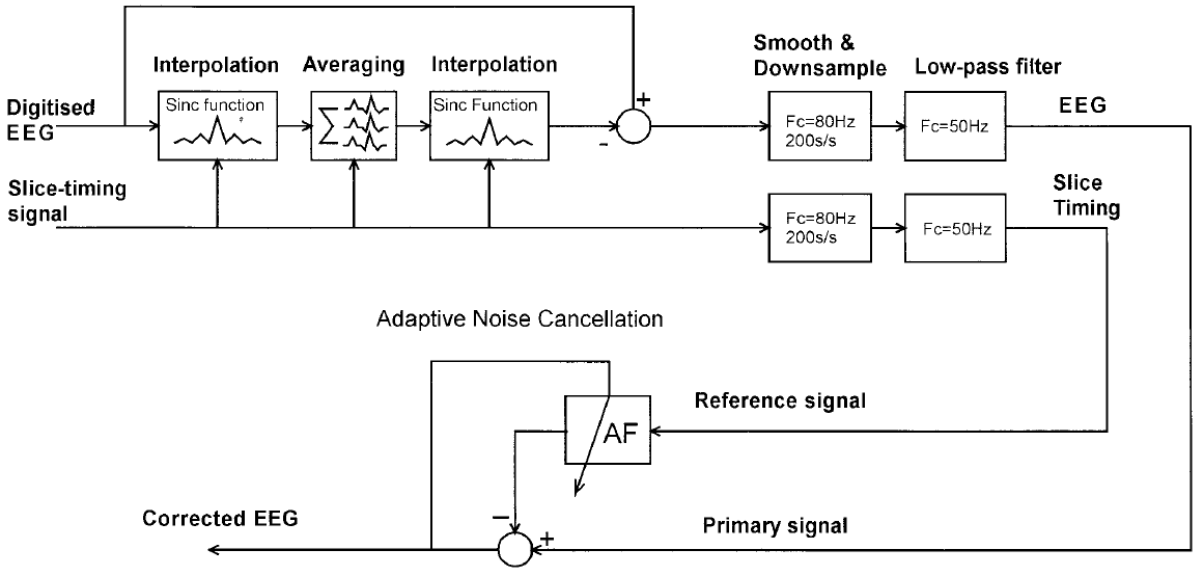

Fig 15 Brainvision method for gradient artifact removal [16]

2.5.4 Ballistocardiographic artifact removal

2.5.4.1 „Allen method“- artifact template subtraction method

One classical approach is subtraction algorithm developed by [9]. Firstly, ECG peaks in the previous 10 s are identified. The average waveform is time-locked to the ECG peaks in this period. This waveform is calculated for each referential EEG signal. The algorithm delays the display of EEG by at least 1 s. There is a compromise in duration of 10-s period, it must be long enough to separate the artifact from the underlying EEG, but short enough to adapt to changes in the artifact waveform. The time delay (0,21 s) exist between QRS complex and artifact peak. Before including sections of EEG in the average, each section is tested for artifacts which could corrupt the average artifact waveform. EEG sections with a mean magnitude more bigger than average could contain artifacts such as eye blinks or musle activity. This averaging could reject non-artifact activity from the waveform to be subtracted.

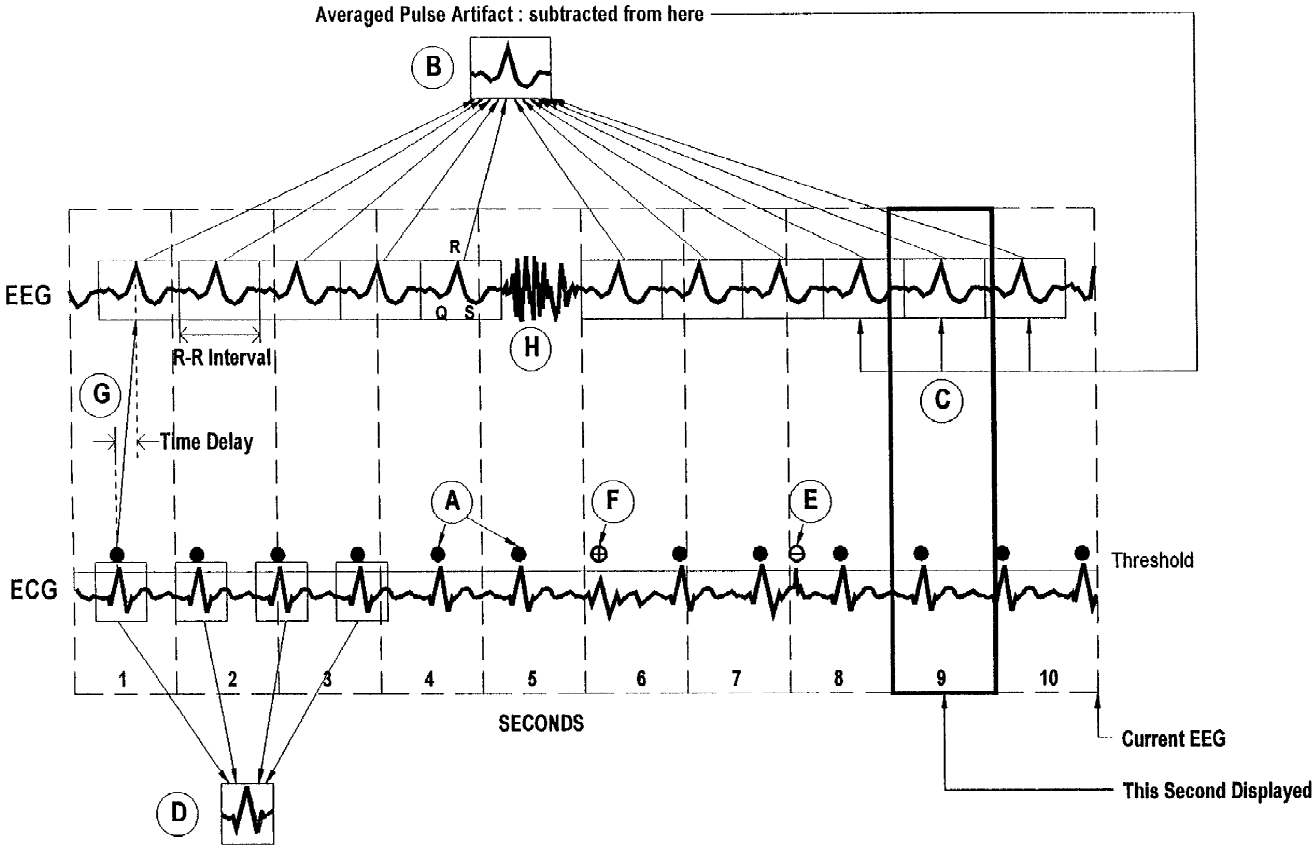

Fig 16 Allen method[9].

2.5.4.2 „Kim method“

Algorithm based on [20] uses 10 seconds segments of the input signal. Each heartbeat is detected from the derived BCG signal obtained by subtracting the left EOG from the right EOG, using a slight modification of Teager energy operator (TEO). This heartbeat detector is defined as

$$\psi\{x(n)\} = x^2(n) - x(n+k)x(n-k) \quad (11)$$

k is set to k=1

The mean waveform is obtained by averaging the segmented waveforms centered at the detected heartbeat time points. Only when the assumption is valid, that pulse wave form varies only slightly within the time interval, this averaging by [9] is succesfull. Therefore significant parts of the artifacts still remained in the output waveform. Wavelet transformation is used for the elimination of the residual artifact. Its coefficients are selectively removed (eliminated). This elimination is applied at specific scales and specific time points. Input signal is decomposed into eight dyadic scales by discrete wavelet. On the scales d1 and d2 are the coefficient thresholded to reduce high frequency random noise. It must be paid attention, whether the input wave form doesn´t contain important frequency components. In cases, when important frequency components of the signal may be excluded, adaptive filter must be turned on. It is also used, when the artifact subtraction is not well done. To decide, whether or not to turn the adaptive filter on, ratio between the power spectrum in the 0,5 – 7 Hz subband and the total power. If this ratio is larger than 0,6, the adaptive filter is switched on. Also when correlation between the k-TEO outputs of the processed wave form and the original input wave form is larger than 0,5. The RLS adaptive filter is used. In this case the length of the finite impulse response adaptive filter tap was 80.

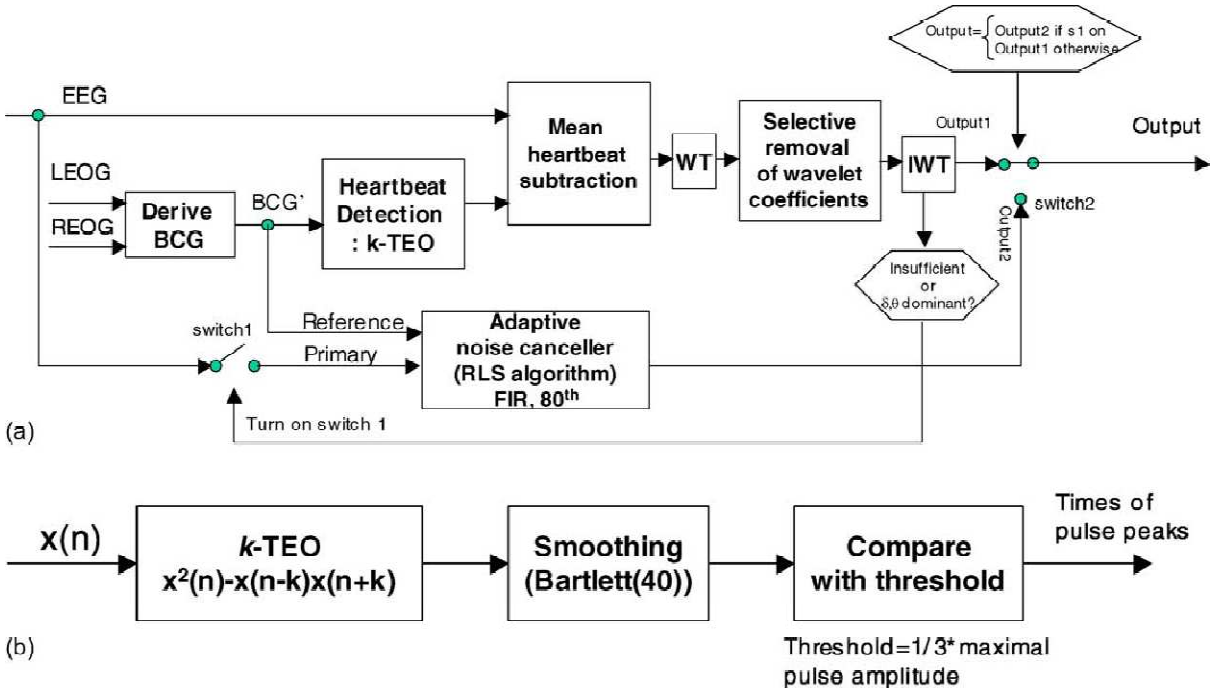

Fig 17 a) Block diagram of the proposed ballistocardiac artifact removal system. (b) Heartbeat detector using *k*-TEO [20]

2.5.4.3 "Bonmassar method"

Specific way of the ballistographic artifact removal is chozen in [14]. A set of control VEP data are recorded at earth magnetic field strength. Additional motion sensor is applied, it is piezoelectric transducer on the subject´s temporal artery. Own gradient echo sequence suitable for interleaved fMRI and EEG acquisition is introduced. All EEG recordings were short-chained bipolar from the modified cap. Analog bandpass filtering was performed from 0,5 to 35 Hz prior to sampling. Epoch selection was performed by comparing the maximum voltage excursion of each epoch for each active channel to the $\pm 50\ \mu V$ threshold level, rejecting epochs that exceeded this threshold. Before this method is applied on the real data, simulated biphasic epileptic spikes with approximately $\pm 200\ \mu V$ peak amplitude and 100 ms duration were randomly added to the EEG recording, to control the capability of artifact correction. Input signal $y(t)$ is sum $y(t) = s(t) + n(t)$, of underlying EEG signal $s(t)$ and $n(t)$, which contains motion and ballistocardiogram components. Relationship between the motion signal sensor $m(t)$ and the noise signal is

$$n(t) = \sum_{k=0}^{N-1} w_t(k)(t-k) \quad (12)$$

$w_t(k)$ is finite impulse response kernel (FIR) with order N. Then adaptive filtering is applied.

$$\hat{n}(t) = \sum_{k=0}^{N-1} \hat{w}_t(k) m(t-k) \quad (13)$$

$$\hat{s}(t) = y(t) - \hat{n}(t) \quad (14)$$

If the true underlying signal $s(t)$is uncorrelated with the motion signal $m(t)$. The input signal may be downsampled, to reduce the order of the FIR filter and therefore to improve the computationally efficiency.

2.5.4.4 "Sun method"

Another idea introduced Sun L. in [21] His idea is based on MNF.
First model: Observed data matrix $X = [x_1, x_2, \dots, x_n]$ is linear mixture of the source matrix $S = [s_1, s_2, \dots, s_n]$ to fulfill equation $X = SA$. Each component $x_i^T = \{x_{ij} | j = 1, \dots, k\}$ represents one measured EEG channel and each $s_i^T = \{s_{ij} | j = 1, \dots, k\}$ is one underlying source component channel at k sampling times.
Second model: Signal data matrix X can be split into a signal part P and an independent noise part Q like $X = P + Q$. These are orthogonal $Q^T P = P^T Q = 0$. As we count with typical BCG artifact, artifact is there treated as the "signal" and ongoing EEG as the "noise". Success of MNF method does not depend on relation of BCG and EEG artifacts. The basic concept underlying MNF approach is to derive components(eigenvectors) ψ under the constraint of maximizing the signal to noise ratio (SNR) according to

$$SNR = max_{\varphi \neq 0} \frac{\|P_\psi\|}{\|Q_\psi\|} = max_{\varphi \neq 0} \frac{\psi^T P^T P \psi}{\psi^T Q^T Q \psi} = max_{\varphi \neq 0} \frac{\psi^T X^T X \psi}{\psi^T Q^T Q \psi} - 1 \quad (15)$$

Source matrix is

$$S = XA^{-1} \quad (16)$$

Sources s_i^T are ordered according to their SNR. Artifact is always captured by the sources exhibiting the largest SNR according to the minimum noise fraction, so long as the BCG is the dominant artifact.

$$\hat{X} = STA = XA^{-1}TA \quad (17)$$

T is the selection matrix, and it is diagonal ($T(i,i) = 0$ for the sources to be excluded and $T(i,i) = 1$ for another sources). MNF components are ordered by their signal to noise ratio (indicated by their eigenvalue), the last or the first are set to zero before application of $X = SA$.
Main idea of selecting the MNF-components for artifact removal is the problem of defining the number of components to reject. It must be set the suitable number to remove the whole artifact, but not to suppress the ongoing signal. 29 values of variance were measured in- and outside the scanner and then normalized resulting in relative variances. BCG EEG signal has significantly larger variance than BCG-free EEG signal. Therefore, when the sufficient number of components have been removed, the variance of the EEGs observed inside the scanner should approach the variance observed outside the scanner.
After first application of MNF procedure some residual artifacts remain. A subsequent subtraction method can serve to remove this residual BCG artifact provided that the BCG template is reproducible. For this purpose, additional measurement of ECG was applied. It has two parts:
In the first part, the ECG onset must be identified.
In the second part, place of artifact template is defined as interval of mean RR duration around the ECG onsets. For each artifact, an artifact template is counted by averaging over the 50 BCG epochs (25 preceding and 25 following). This average of mean RR duration was subtracted from the actual BCG epoch to remove the artifact.

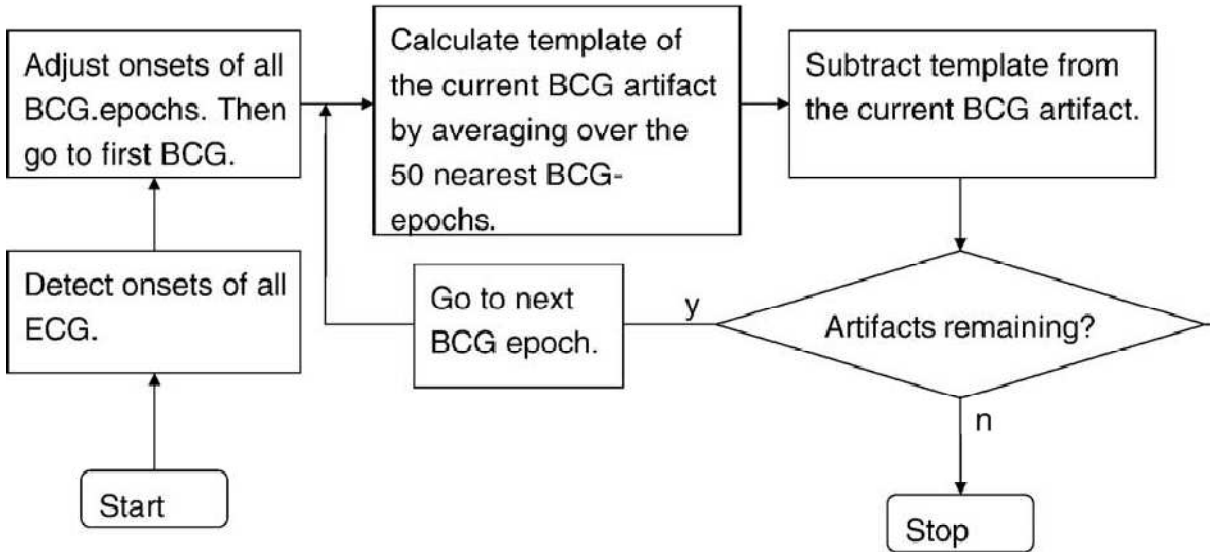

Fig 18 „Sun method“ [21]

2.5.4.5 “Ellingson method”

EEG is set to zero amplitude, during periods when gradient-switching is performed. A specific wide window of EEG data is located 200 ms after the R peak in ECG. This windowed EEG waveform was then zero-meaned. Template is derived from a certain number of consecutive artifact contaminated EEG epochs and from the median BA amplitude on a point-by-point basis. The median-filtered BA template and the section of EEG from which the artifact is to be subtracted are then both zero-meaned. Before subtraction the amplitude of the template is scaled to each section of BA-contaminated EEG data using least-square minimization. This scaled template is finally subtracted from the current section of EEG data. [22]

2.5.4.6 “Benar method 2”

Another method was introduced in [23]. The PCA is introduced by singular value decomposition on raw data:

$$X = USV^T \quad (18)$$

X represents the data matrix (n time points × m channels), U (n × m) the matrix of normalized time courses of the PCA components (one per column), S (m × m) the diagonal matrix of eigenvalues or amplitudes of the components, and V (m × m) the matrix of spatial distributions of each components (one per column).

The ICA results in the following decomposition:

$$X^T = W^{-1}u \quad (19)$$

u (m × n) means the matrix of component time courses (one per row). W^{-1} (m × m) the matrix of spatial distributions of the component (one per row) (W is usually referred to as the ‘unmixing’ matrix).
Then suitable filters for ICA and PCA is introduced. These excludes the components corresponding to ballistocardiogram in the spatial matrices.
For PCA filter:

$$A = VI_0V^T \quad (20)$$

And for ICA filter also:

$$A = W^T I_0 (W^T)^{-1} \quad (21)$$

I_0 represents the diagonal matrix with elements set to zero when the component was retained and zero when the component was excluded.

$$Y' = YA \text{ (22)}$$

Y represents the matrix of original data and Y' filtered data.

2.5.4.7 "Negishi method"

In an alpha wave detection experiment, we used the temporal PCA-based noise removal algorithm to remove cardiac artifacts. Cardiac trigger pulses(1 for R peak) has been computed. First PCA filter must be applied. Principal components capture component waveforms whose amplitude variations accounts for the largest variations of BCG waveforms. The basic idea behind using PCA is that if the gradient artifact waveform consists of multiple components whose amplitudes do not co-vary with each other, they would be captured in different PCs. Activations of PCs are computed, along with the moving average and the associated standard deviation of PC activation. The mean and the standard deviation is computed from the EEG data, inside scanner, but no scanning. PC activations, which are associated with gradient artifacts are estimated using the PC activations and statistics. An estimated BCG artifact at each frame is then computed as a sum of PCs weighted by estimated PC activations for each frame, and is subtracted from the original frame. Then 80 Hz low-pass filtering is performed. For further details [24]

2.5.4.8 Basic ICA

Time varying observed signal is denoted as $x(t) = (x_1(t), \dots, x_n(t))^T$. The source signal consists of independent components by $s(t) = (s_1(t), \dots, s_n(t))^T$. Linear ICA supposes, that the signal $x(t)$ is linear mixture of independent components:

$$x(t) = As(t) \text{ (23)}$$

The algorithm, which must be found to separate or unmix components, leads to

$$s(t) = Wx(t) \text{ (24)}$$

In which W is denoted as an unmixing matrix.
Inverse ICA can be performed as:

$$\acute{x}(t) = W^{-1}s(t) \text{ (25)}$$

[25]
Independent component analysis creates same number of independent component as channels. All independent components should be as independent as possible. Before ICA application, gradient artifact should be well removed, otherwise gradient artifact may be present in more components and be dominant at all. ICA is well described in [26]. If the spatial topography remains unchanged over the cardiac cycle, ICA can be well applied. Several studies referred over the the application of ICA for BCG removal. [23][27][28][13][29]. Some negative experiences are described in [30][10]. Some authors state, that ICA alone could not separate completely. BCG normally contains only lower frequency components, another was to perform ICA is first to low-pass filter EEG and then apply ICA.[13]

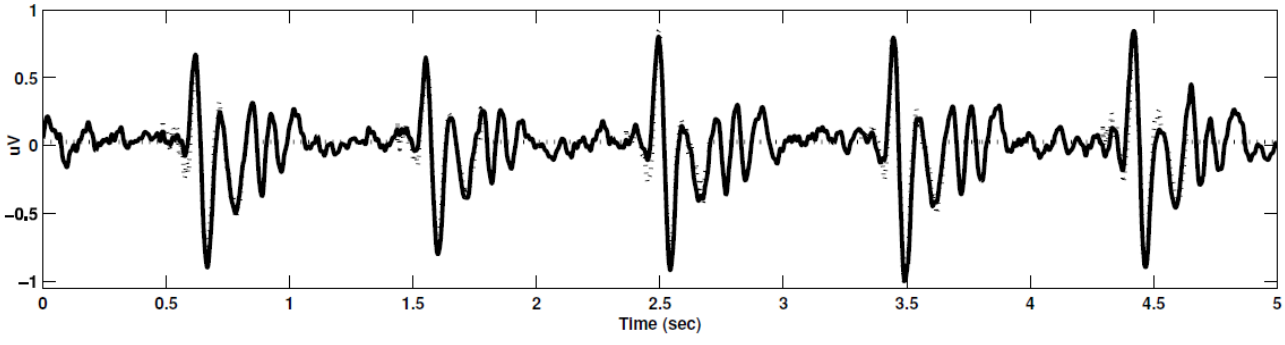

Fig 19 Independent component, which shows significant connection to heart rate [25]

2.5.4.9 ICA connected with "Allen method"

Relatively new approach to BCG artifact removal was performed. ICA was performed as before, but now we apply "Allen method on IC components, which show significant connection to heart beat rate. Delay can be set to 0,21 as before, or as described before in 3.2.3.2.1. Artifact template can be counted as before, from 10, 20 or 30 previous and following waveforms, as described above.

2.5.4.10 Comparison

In [13] four ICA algorithms of BCG artifact were performed. ICA-based methods show the same efficiency as the „Allen method". Signals differs in values of the power spectrum density in 4–8 Hz frequency band. But the diference is not statistically significant. These ICA methods has some advantages, e.g. it doesn´t depem on cardiac pulses rhythm(short or irregular) and it removes BCGs regardless of the fluctuation of BCG waveforms.

2.5.1 Evoked potential processing

Stimulus causes a brain response time-synchronized to the stimulus. The stimulus are elicited at equidistant points in time. The observed EEG signal can be transformed into an ensemble of M different potentials, with each potential $x_i(n)$ described by N samples

$$x_i\,(n), i = 1, \dots, M; n = 0, \dots, N-1 \quad (26)$$

The ensemble is represented by $N \times M$ matrix X

$$X = [x_1\, x_2 \dots\, x_M\,] \quad (27)$$

where the i^{th} potential is contained in the column vector

$$\boldsymbol{x}_i = \begin{bmatrix} x_i(0) \\ x_i(1) \\ \dots \\ x_i(N-1) \end{bmatrix} \quad (28)$$

The assumption of perfect time synchronization between stimulus and response is not always valid. Variations in latency can be attributed, to various degrees, to the inherent phenomenon of biological variability. It may, therefore, be necessary to introduce techniques that can estimate and compensate for such variations prior to ensemble averaging. For further details, see [2]

2.5.2 P300

P 300 is a wave, which is elicited by infrequent and task-relevant stimuli. It is considered to a person´s reaction to the stimulus, to the stimulus evaluation or categorization, respectively. Typically, it occurs, when oddball paradigm is applied. By this paradigm, low-probability target items are inter-mixed with high-probability standard items. In EEG, it occurs as a positive deflection in voltage with a latency 300 to 600 ms. In [31] mean parameters present in channels Pz and Cz are:

peak	Amplitude(μV) - Cz	Latency(ms) - Cz	Amplitude(μV) - Pz	Latency(ms) - Pz
P3	13,7	308	14,2	302
P2	6	173	5,5	172
N2	-1,3	219	-1,8	218
N1	-7,9	96	-8,5	98

Fig 20 Characteristics of P300

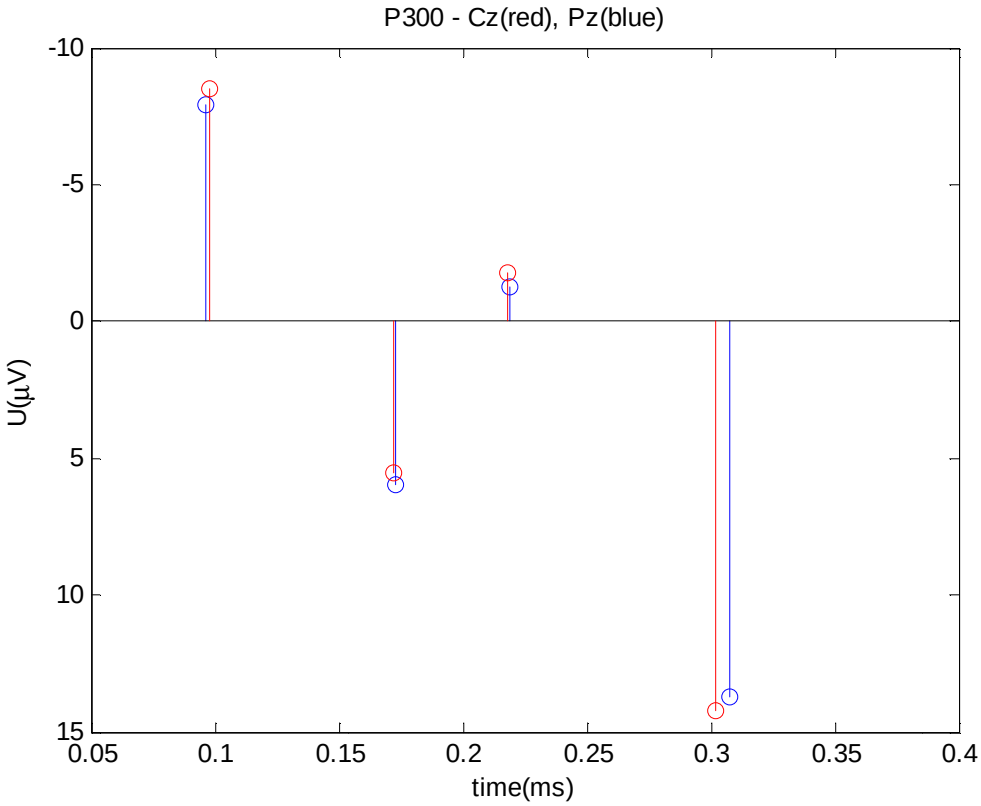

Fig 21 amplitudes and latencies of P300, Cz(red) , Pz(blue)

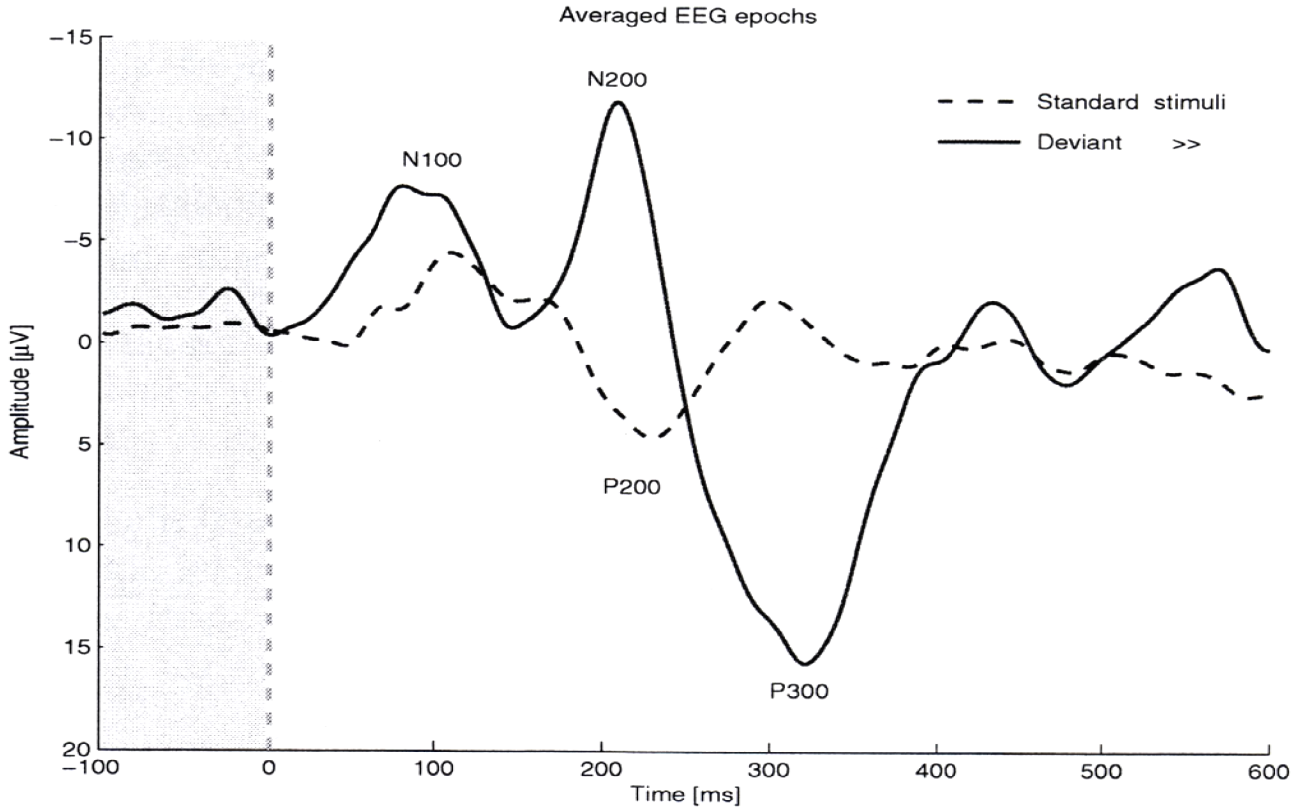

Fig 22 Average responses from an oddball paradigm. [4]

3 Practical part

3.1 Data

Data were collected at KYS (Kuopio university hospital). The subjects were scanned with 1,5T scanner (Siemens MAGNETOM Avanto, Erlangen, Germany) with a T2*-weighted EPI sequence (TR = 2500ms + 100 ms , TE = 50 ms , FOV = 192 mm, matrix = 64x64 , 29 slices, slice thickness=3mm, inter-slice gap=1mm). The experimental task was a typical go-nogo task with visual stimuli. The subjects were informed to press a button for green squares and ignore the red squares. Simultaneous EEG measurement was performed with Brain Products BrainAmp MR+ and cap providing 31 channels of EEG, EOG and ECG electrodes. In the thesis, 6 measurements were used. For 3 subjects also measurements of EEG outside the scanner were performed. Sampling frequency was set to 5000 Hz, due to presence of imaging artifact and further possibility of it´s removal. Normally, this high frequency rate is not needed.

3.2 Methods

3.2.1 EPs outside the scanner

For 3 subjects, n.4, n.5 and n.6 EEG measurements outside the scanner exist. In each subject and each channel another shape, amplitude and latency of P300 occurs, this is strongly subject dependent. For later EPs estimation from the artifact destroyed signal, image of EPs from measurement outsider the scanner is useful. Basic ensemble averaging was performed and then pass-band filtered (Butterworth, 0.5-40 Hz) for noise and trends removal.

3.2.2 EPs inside the scanner

For all 6 subjects, n.4, n.5, n.6, n.9, n.10, n.11, EPs estimation was performed, with help of basic ensemble averaging and pass-band filtering (Butterworth, 0.5-40 Hz) for noise and trends removal.

3.2.3 Imaging artifact removal

At the beginning, imaging artifact has to be removed. BrainVision was used. It offers a special application for this purpose. BrainVision use an artifact template subtraction method. For each epoch, which si defined as TR (repetition time), artifact template was computed. It can be set, if this artifact template is computed from all epochs or just from the previous few epochs (moving average). Second possibility seemed to be better choice for the artifact removal, the quality of the signal after the artifact removal was significantly better. The reason for this is movement of patients head. If the subject moves his head even slightly, the resulting EEG artifacts are modified, in some cases considerably. This substantially reduces the quality of a template calculated across all intervals. The number of intervals to be used for calculating the correction template can be set here. An odd number was recommended. 21 was set here.

3.2.4 QRS complex detection

QRS detection was performed with help of BrainVision. Also Matlab script, which use method introduced by [19] was performed. Sensitivity of these QRS algorithm were counted.

Sensitivity is denoted as $SE = \frac{TP}{TP+FN} = \frac{number\ of\ True\ Positives}{number\ of\ True\ Positives+number\ of\ False\ Negatives}$ (29)

Let explain what exactly means this components.

True positive means well detected R peak. False negative means undetected peak in case, where exists peak in real.

3.2.5 Ballistographic artifact removal

3.2.5.1 BrainVision

Brainvision was used to remove the ballistographic artifact. Time delay can be set, or can be counted from the channels. If computation of the time delay was not possible, time delay was set to 0,21 s normally.

3.2.5.2 „Allen method“

Method uses artifact template, which was computed from the 10 previous waveforms and then this template is subtracted from the EEG signal. This method is useful only then, when all trends are removed. Before Allen method application, basic linear filter was applied (Butterworth,bandpass 0,1-40 Hz). Range of this filter is set due to ERPs, which are present mainly in this frequency range. Filter can also remove the rest of imaging artifact, noise connected to power-supply (50 Hz), etc.

.3.2.5.2.1 Delay

The delay between time of R wave in ECG and presence of the artifact in EEG signal was not easy to set. In general, 0,21 s is recommended. Artifact waveforms and mean of artifact waveforms were plotter to show character of this artifact. According to [17], BCG artifact mainly consist of two polarity reversals. Interval, in which „Allen method“ is performed, was set from the beginning to the end of present BCG. Mean artifact is plotted in Annex in fig 41-52.

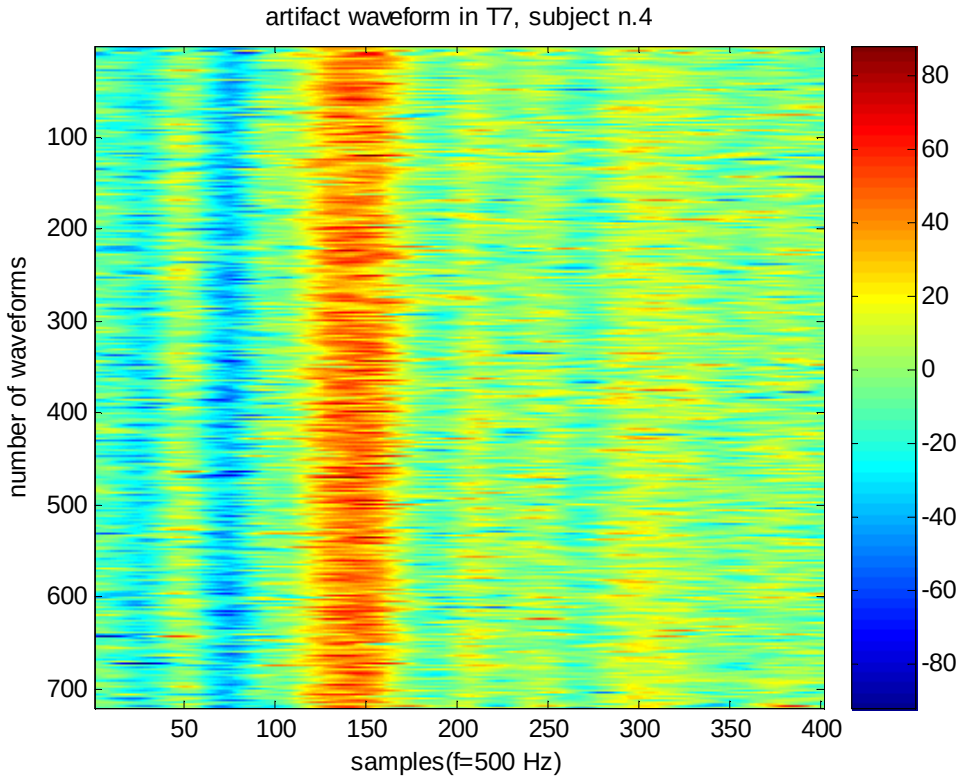

Fig 23 artifact waveforms in T7, subject n.4

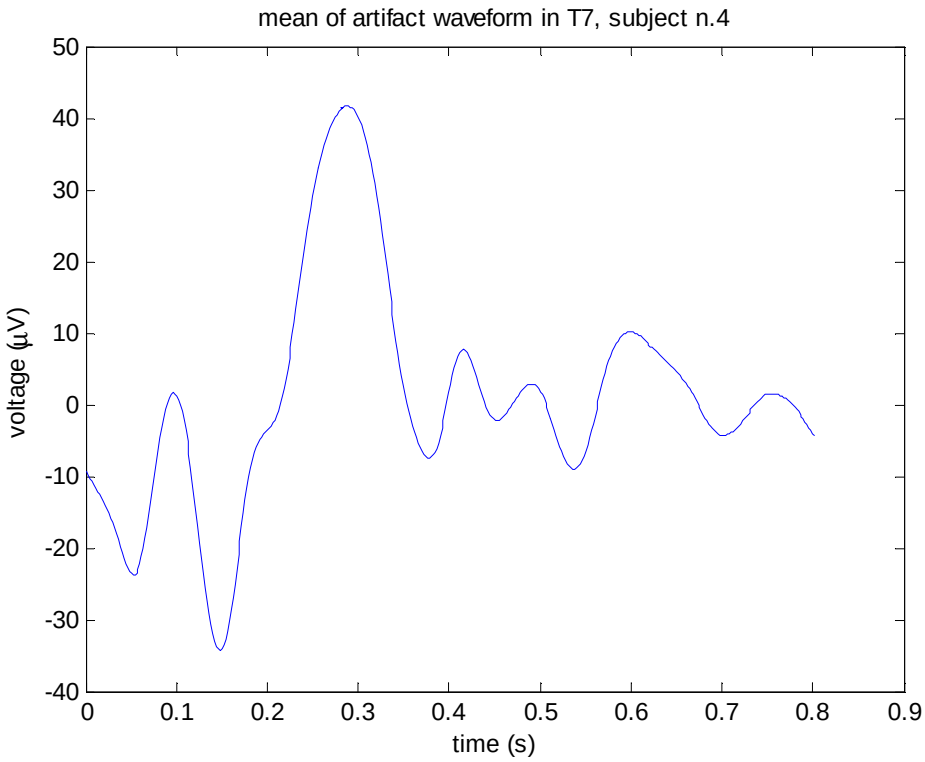

Fig 24 mean artifact waveform in T7, subject n.4

subject	begin(ms)	middle(ms)	end(ms)
4	100	325	550
5	30	265	500
6	40	295	550
9	50	275	500
10	90	295	500
11	80	280	480

Figure 25 Delay settings during artifact template subtraction method

3.2.5.3 ICA

ICA was performed by BrainVision and with help of EEGLAB.

.3.2.5.3.1.1 ICA - Brainvision

In Brainvision, ICA transforms EEG channels in analogon to EEG channels in time domain. ICA transformation creates transformation matrix. Fast ICA algorithm or infomax algorithm is used for determining the weight matrix. Infomax algorithm is iterative gradient method used to estimate maximum likelihood. In addition, fast ICA algorithm is an iterative fixed-point method used to minimize negentropy. „Fast“ is slightly different from that used in the Fast Fourier transform(FFT). Fast ICA has stricter requirements in terms of separability of components. If these requirements are fullfilled, ICA is calculated more quickly than conventional methods. Otherwise is calculation slower than with other methods in general.
Two types of sphering can be used: classic and probabilistic. In classic case, conventional sphering by means of PCA is used, this method treats all components equally. In probabilistic method, probabilistic sphering by means of PCA is performed. This sphering, while used with any ICA method is referred to in the literature as probabilistic ICA. The noise is normally filtered out of EEG data, using the probabilistic method.

Two approaches can be performed by ICA: Restricted and extended. Special case is Biased infomax method. At each ICA calculation step an additional method is used. It improves the quality of the ICA separation by highlighting particular characteristics of individual components.
ICA computation is performed until the modification of matrice sis smaller than Convergence bound, that means, that ICA is processed until result is sufficiently accurate. But, in contrast, number of training steps should not exceed value: Number of steps. For fast ICA, number of step sis set to 150 normally, for infomax method is the default value 512.
When the probabilistic ICA should be performed, Number of components or Components with eigenvalue at least can be set. If one of these numbers is too low, loss of infomation may occur. That´s because only few components in the probabilistic PCA interprest a large portion of the data as noise. It may be eliminated.
Two sort criteria can be set: Kurtosis or Energy, both in descending order. Kurtosis means a numerice estimate of the peakedness of a curve. $K = 0$ is denoted as a normal peak. $K > 0$ means steep peaks, it can be denoted as super-Gaussian or leptokurtic also. $K < 0$ shows flat peak. Restricted infomax method, can separate components only with positive kurtosis ($K > 0$).
In general, ICA transform consist of these steps: Mean values of the channels are subtracted from the data set. Then computation of sphering matrix is performed and it is applied to the data set. Data are then trained until the ICA matrix is not sufficient precise. Independent components are determined by applied ICA matrix. Components are sorted according to appropriate sort criterion.[19]

By visual inspection, few channels, which showed signifiant connection to the heart rate, were set to zero and inverse ICA was performed.

.3.2.5.3.2 ICA - EEGLAB

EEGLAB computes sphere and weigth matrix, which lead to computing of unmixing matrix:

$$unmixing\ matrix = weights \cdot\ sphere \quad (30)$$

Independent components are computed then as:

$$IC = unmixing\ matrix \cdot data \quad (31)$$

.3.2.5.3.1 Combined ICA – Allen method

Second possibility was to perform „Allen method“ on these independent components, to save more information from EEG channel. First choice was to perform Allen method only on channels, which was set as a significantly connected to BCG. By more proper visual inspection was found, that more channels contain BCG and therefore Allen method was applied to all channels.

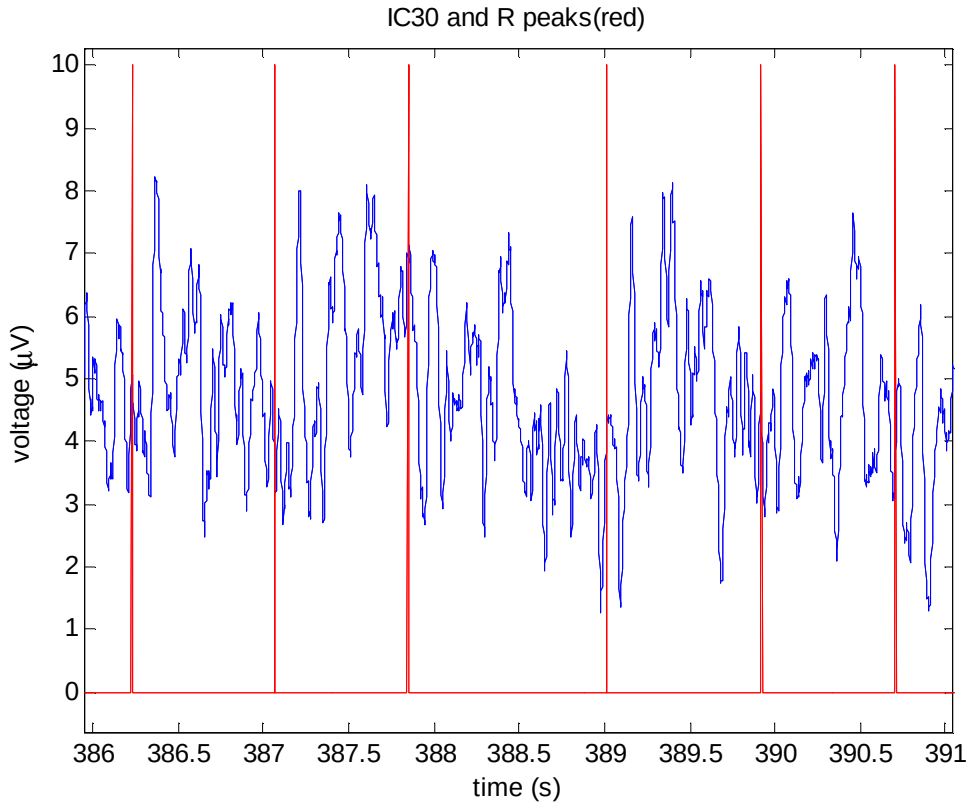

Fig 26 IC30, whic contain BCG, R peaks(red), (subject n.4)

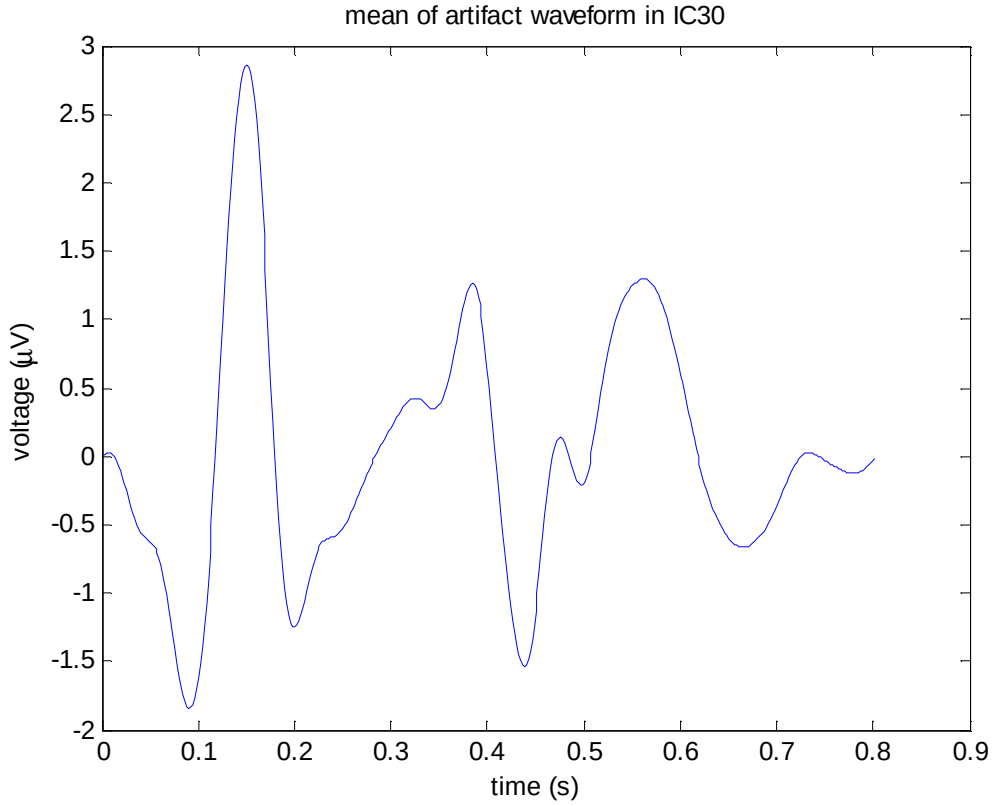

Fig 27 mean of artifact waveform by IC30, (subject n.4)

3.2.6 EP estimation

Data contained markers, which shows time of stimuli. With help of ensemble averaging, basic EPs were computed. Normally, polarity of voltage is shown inversely. Time interval 0,1 s before and 0,8 s after stimuli was shown. In this data set, P300 should be present. It is the dominant and has connection to visual stimulation.

4 Results

4.1 EPs outside the scanner

Due to filtering, EPs waveforms have smaller amplitude than real. Small waveforms with amplitude of 5-10 μVs occurs. EPs are plotted in annex, fig 1-6. In subject n.4, in channels Cz, C3, C4, CP1, CP2, CP5, CP6, FC1, FC2 is the P300 present. Analogically in subject n. 5, in channels C4, CP2, CP6, F3, F4, F7, F8, Fp1, Fp2, Fz, O1, O2, P4, P8, T8, TP10 and in subject n.6, in channels F3, F4, F7, F8, FC2, FC5, FC6, Fp1, Fp2, Fz, T7, T8, TP10 and TP9 small positive deflection as P 300 occurs.

4.2 EPs inside the scanner

In any channel, no signifiant P300 peak was found. Due to filtering, EPs waveforms have smaller amplitude than real. In real, big gradient artifact peaks occur. Amplitude ranges from 20 – 200 μVs. EPs are plotted in annex, fig 7-18.

4.3 Imaging artifact removal

EPs are plotter in annex in fig 19-30. In subject n.4 in C3,C4,CP1, CP2, CP6, FC1, FC2, FC5, P3, P4, P7, P8, T7, T8, TP10, TP9 positive deflection was present. Also in subject n. 5, in channels F7, F8, FC1, Fp1, Fp2, P7, P8, T7, T8, TP10, TP9 is P300 present. In subject n. 6, P300 occurs in channels F4, F8, FC6, Fp1, Fp2, Fz, O1, O2, P4, P7, P8, Oz, T7, T8, TP10, TP9. In subject n. 9, little delayed P300 is in F7, F8, FC1, FC5, Fz, T7, T8, TP10. In subject n. 10, in channels Cz, C3, CP1, CP2, CP5, F7, FC1, FC5, O1, P4, P7, Oz, Pz, T7, TP9 is P300 visible. In subject n. 11, in channels Cz, C3, C4, CP2, CP5, CP6, F3(little delayed), F4, F7, F8, FC1, FC2, FC5, FC6, Fp1, O2, P3, P4, P7, P8, T7, T8, TP10, TP9 P300 can be seen.

4.4 QRS detection

4.4.1 BrainVision

Sensitivity SE was computed for a QRS detection with help of BrainVision.

$$SE_5 = \frac{845}{845 + 4} = 99{,}5\ \%$$

$$SE_6 = \frac{908}{908 + 3} = 99{,}7\ \%$$

$$SE_9 = \frac{652}{652 + 5} = 99{,}2\ \%$$

4.4.2 „Christov method“

Sensitivity SE was computed for a QRS detection using „Christov method

$$SE_4 = \frac{770}{770 + 15} = 98{,}1\ \%$$

$$SE_5 = \frac{845}{845 + 17} = 98\%$$

$$SE_6 = \frac{908}{908 + 16} = 98{,}3\ \%$$

$$SE_9 = \frac{652}{652 + 18} = 97{,}3\ \%$$

$$SE_{10} = \frac{602}{602 + 62} = 90{,}7\%$$

$$SE_{11} = \frac{409}{409 + 73} = 84{,}9\%$$

4.5 Ballistocardiographic artifact removal

4.5.1 BrainVision

Results are plotted in fig 31-40. After BCG artifact removal with help of BrainVision, in subject n. 5, in channels F7, FC1, Fp1, Fp2, Fz, O1, O2, P7, P8, Oz, Pz, T7, T8, TP10, TP9 is P300 present. In subject n. 6, in channels C4, CP2, CP5, CP6, F3, F4, F7, F8, FC1, FC2, FC5, FC6, Fp1, Fp2, Fz, T7, T8, TP10, TP9 is P300 seen. In subject n. 9, in channels little delayed in C3, C4, CP6, F3, F4, F7, F8, FC1, FC2, FC6, Fp1, Fp2, Fz, T7, T8, TP10, TP9 can be seen.

4.5.2 „Allen method“

Artifact template subtraction method was used for BCG artifact removal. It was performed on all subjects. Results are shown in Annex in figures 53-64. This method significantly decrease amplitude of BCG, but it doesn´t remove it on its own. Artifact waveform shape remains the same. Second disadvantage is due to finiteness of the subtraction interval, it doesn´t remove all artifacts, which are connected to heart rate, just that, which was denoted as BCG.

To increase the efficiency of BCG artifact removal with help of artifact template subtraction method, this algorithm can be performed more times. This approach has few disadvantages, there is no clear condition, when is the whole BCG artifact removed and when some parts remain. In some channels, discontinuity at the beginning and at the end of the subtraction interval occurs. Signal must be filtered, to remove trends, otherwise artifact template subtraction method has no sense, because the whole signal must be at the same level and mean of whole signal should be close to zero.

4.5.3 ICA (BrainVision)

Main problem with use of BrainVision elicited after computation of IC. IC looks discrete, which shows, that unmixing matrix was badly computed. Another possible reason is bad settings before ICA computation in BrainVision. Also characteristics of the signal can lead to this type of results.

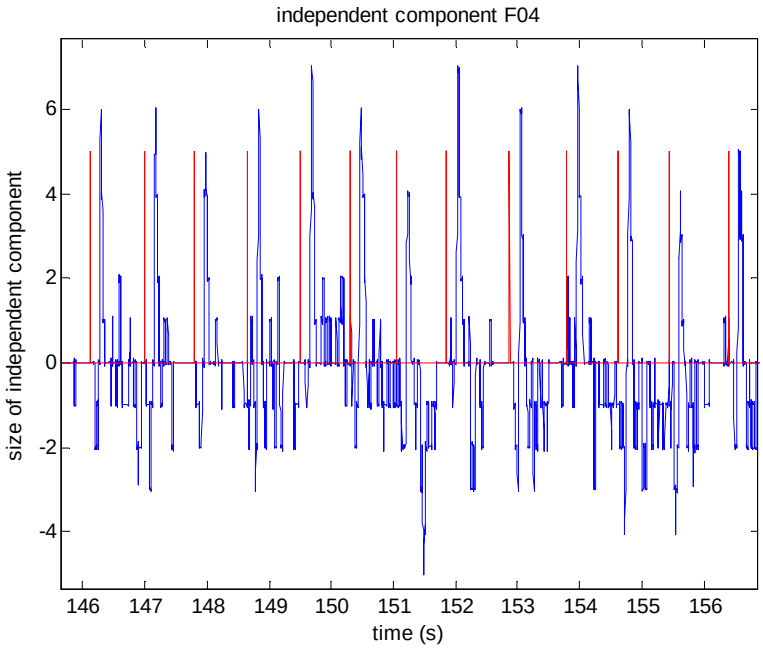

Fig 28 IC, which has significant connection to heart rate, in subject n.4

Results are seen in fig 65-74. Subject n.4 in Cz, C3, C4, CP1, CP2, CP5, CP6, FC1, FC2, FC6, Fp2, Fz(little delayed), O1, O2, P3, P4, P7, P8, Oz, Pz, T7, T8, TP10, TP9 P 300 is present. In subject n.5 approximately 20 components contain BCG part, therefore, performed inverse ICA will destroy information vigorously. In subject n.6, channels C3, CP5, F3, F4, F7, F8, FC1, FC2, FC5,FC6, Fp1, Fp2, Fz, O1, P7, T7, TP9 contain P300. In subject n.9 in channels C3, CP5, F3, F7, FC1, FC5, Fp1, Fp2, P7, T7, TP10, TP9, P300 ocurrs. Subject n.10, positive-P3, P4, P7, T7, TP9. In subject n.11, CP5, F7, F8, FC1(delayed), O1, O2, P7, Oz, T7 are present.

4.5.4 ICA (EEGLAB)

ICA transform computes appropriate regular unmixing matrix only in subjects n.4 and n.6. Otherwise complex, close to regular or badly scaled matrix was computed. 3 IC in subject n. 4, 7 IC in subject n. 6 were set to zero. Inverse ICA was applied and channels are displayed in Appendix in fig 79-82 .In subject n.4 in C3, C4, CP1, CP2, CP5, CP6, F4, FC1, FC2, FC5, FC6(small), Fp2(small), P3, P4, P7, P8, T7, T8, TP10, TP9, 300 are present. In subject n. 6, channels C3(200 ms), C4, CP2, CP5, CP6, F3, F4, F7, F8, FC2, FC6, Fp1, Fp2, Fz, P4, P8, Oz, Pz, T8, TP10 contain P300.

4.5.5 ICA connected with „Allen method“

Combined method was performed only by subjects n.4 and n.6, for the same reason as by normal ICA method on its own. Allen method was performed on all channels. Intervals, where artifact subtraction template was performed was the same as for the basic Allen method. It was set according to artifact templates shown in Appendix in figure .

Combined method shows good efficiency only in subject n.4. Combined method shows the same disadvantages as seen before in simple artifact template subtraction method. In subject n.6, only in a few channels performed combined method decreased level of BCG artifact, in other channels, decreasing of amplitude of BCG was succesfull, but due to filtering of IC and inverse ICA, these channels are shifted by 10-50 μVs up or down. Results are shown in annex in fig 75-79.

4.5.6 Comparison of all artifact removal techniques

In fig in annex it was shown comparison of EPs after all removal techniques. It was shown, that artifact template subtraction method and combined ICA-artifact template subtraction method don´t destroy the character of EP. Small decrease in amplitude of EPs after BCG artifact removal was seen due to subtraction.
ICA performed with help of both EEGLAB and BrainVision, when some IC are removed show destroyment of mean peaks. In several channels, this method didn´t destroy mean peak, P300.

5 Conclusion

Master´s thesis deals with problem of ballistocardiographic artifact in EEG signal by simultaneously performed hybrid fMRI-EEG examination. Main goal was studying of BCG artifact removal methods and proposal of algorithms, which leads to successfull removal of this artifact. Another goal was studying of effects of BCG removal on present EPs.

Assumptions of good BCG artifact removal are succesfull imaging artifact removal and QRS peak detection.

Unsufficiently removed imaging artifact negatively influences pass-band filtering. Amplitude of filtered signal is shifted in some parts of signal. Imaging artifact remains manifested in artifact template and then, parts of signal not corresponding to BCG. Another bad influence is while performing ICA on EEG signal. Imaging artifact manifests as a main part if independent components. Decided whether or not to remove(set to zero) concrete independent component is more difficult. Also more independent components have to be removed due to presence of imaging artifact removal.

Succesfull QRS peak detection is most important assumption of BCG artifact removal. Detection of not present peaks or detection, which is shifted cause bad computation of artifact template and also leads to bad removal of ICA.
Both methods of QRS peak detection shows high sensitivity.

Clean EEG, without artifacts, looks randomly, has mean close to zero. Well done BCG removal looks like that, but preserves frequency contain and don´t affect EPs.

First method used to remove BCG artifact was artifact template subtraction method. It leads to decrease in artifact amplitude, but shape and character of BCG remains. In contrast, this method don´t destroy EP.

ICA performed with help of BrainVision was the least succesfull method for BCG removal. It leads to decrease in BCG artifact, EEG signal then looks more randomly, but ICA strongly affects EPs.

ICA performed with help of EEGLAB was more succesfull. It decreased the BCG artifact amplitude, but don´t affect EPs severely. It preserves P300 very clearly.

Combined ICA-artifact template subtraction method shows the same effect as basic artifact template subtraction method. It requires well done ICA, this assumption is not always fullfilled.

There are no sufficient methods to prove BCG artifact removal success rate. Main reason is, that no exact definitions and parameters of BCG artifact exist. BCG artifact is also strongly subject dependent, also technical conditions and examination environment play important role.

In future, importance of hybrid examination methods will increase due to need of synthesis of data from more examination methods. BCG artifact belongs to the big challenges in field of EEG signal processing.

6 References

[1] NIEDERMEYER, E., DA SILVA L.: Electroencephalography: Basic principles, clinical applications, and related fields, 1998

[2] SORNMO L., LAGUNA P., Bioelectrical Signal Processing in Cardiac and Neurological Applications

[3] LEMIEUX L., ALLEN PJ., FRANCONI F. Recording of EEG during fMRI experiments: patient safety Magn Reson Med. 1997 Dec;38(6):943-52.

[4] GEORGIADIS, S. State-space modeling and bayesian methods for evoked potential estimation, Kuopio university publications C. Natural and environmental science 213. 2007. 179 p.

[5] NIAZY R.K., BECKMANN C.F: Removal of FMRI environment artifacts from EEG data using optimal basis sets, Neuroimage. 2005 Nov 15;28(3):720-37. Epub 2005 Sep 16.

[6] ANAMI K.,MORI T., TANAKA F.: Stepping stone sampling for retrieving artifact-free electroencephalogram during functional magnetic resonance imaging, 2002, Neuroimage. 2003 Jun;19(2 Pt 1):281-95.

[7] GARREFFA G., CARNI M. Real-time MR artifacts filtering during continuous EEG/fMRI acquisition, 2003, Magn. Reson. Imaging. 2003 Dec;21(10):1175-89.

[8] HOFFMANN A., JAGER L. Electroencephalography During Functional Echo-Planar Imaging: Detection of Epileptic Spikes Using Post-processing Methods, Magn Reson Med. 2000 Nov;44(5):791-8.

[9] ALLEN P.J., POLIZZI G., KRAKOW K. Identification of EEG Events in the MR Scanner: The Problem of Pulse Artifact and a Method for Its Subtraction, NeuroImage Volume 8, Issue 3, October 1998, Pages 229-239

[10] DEBENER S., MULLINGER K.J., Properties of the ballistocardiogram artefact as revealed by EEG recordings at 1.5, 3 and 7 T static magnetic field strength, Int J Psychophysiol. 2008 Mar;67(3):189-99. Epub 2007 Jul 12.

[11] HUANG-HELLINGER F.R:, BREITER, F.R. McCORMACK, G. . Simultaneous functional magnetic resonance imaging and electrophysiological recording. 1995. Human Brain Mapping 3 (1), 13–23.

[12] IVES JR, WARACH, S., SCHMITT, F., Monitoring the patient's EEG during echo planar MRI. 1993. Electroencephalogr Clin Neurophysiol 87 (6), 417–420.

[13] NAKAMURA, W., ANAMI, K., MORI, T. Removal of ballistocardiogram artifacts from simultaneously recorded EEG and fMRI data using independent component analysis. 2006.IEEE Transactions in Biomedical Engineering 53 (7), 1294–1308.

[14] BONMASSAR, G., PURDON, P.L., JAASKELAINEN, I.P. Motion and ballistocardiogram artifact removal for interleaved recording of EEG and EPs during MRI. 2002.Neuroimage 16 (4), 1127–1141.

[15] TENFORDE, T.S., GAFFEY, C.T., MOYER, B.R. Cardiovascular alterations in Macaca monkeys exposed to stationary magnetic fields: experimental observations and theoretical analysis. 1983.Bioelectromagnetics 4 (1), 1–9.

[16] ALLEN, P.J.., JOSEPHS, O. TURNER R.. A method for removing imaging artifact from continuous EEG recorded during functional MRI. 2000.Neuroimage 12 (2), 230–239.

[17] ERTL M., KIRSCH V., LEICHT G. Avoiding the ballistocardiogram (BCG) artifact of EEG data acquired simultaneously with fMRI by pulse-triggered presentation of stimuli. J Neurosci Methods. 2010 Feb 15;186(2):231-41. Epub 2009 Nov 27.

[18] BrainVision, user manual

[19] CHRISTOV, I.I. Real time electrocardiogram QRS detection using combined adaptive threshold.Biomed Eng Online, Vol. 3, No. 1. 27 August 2004

[20] KIM H.K, YOON H.W., PARK H.W. Improved ballistocardiac artifact removal from the electroencephalogram recorded in fMRI. Journal of Neuroscience Methods Volume 135, Issues 1-2, 30 May 2004, Pages 193-203
[21] SUN L., RIEGER J., HINRICHS H. Maximum noise fraction (MNF) transformation to remove ballistocardiographic artifacts in EEG signals recorded during fMRI scanning Neuroimage. 2009 May 15;46(1):144-53. Epub 2009 Feb 6.
[22] ELLINGSON ML, LIEBENTHAL E., SPANAKI, MV. Ballistocardiogram artifact reduction in the simultaneous acquisition of auditory ERPS and fMRI Neuroimage. 2004 Aug;22(4):1534-42
[23] BÉNAR CH-G, AGHAKHANI Y., WANG Y. Quality of EEG in simultaneous EEG-fMRI for epilepsy, Volume 114, Issue 3, Pages 569-580
[24] NEGISHI M, ABILDGAARD M. Removal of time-varying gradient artifacts from EEG data acquired during continuous fMRI. Clin Neurophysiol. 2004 Sep;115(9):2181-92.
[25] RASHEED T., HO IN M., LEE Y-K Constrained ICA Based Ballistocardiogram and Electro-Oculogram Artifacts Removal from Visual Evoked Potential EEG Signals Measured Inside MRI, lemure notes in computer science, Bibliographic details 2006, NUMB 4232, pages 1088-1097
[26] HYVARINEN A., KARHUNEN J., OJA E. Independent component analysis, 2001 , 505 pages.
[27] BRISELLI E., GARREFFA G. BIANCHI L. An independent component analysis-based approach on ballistocardiogram artifact removing. 2006. Magnetic Resonance Imaging 24 (4), 393–400.
[28] MANTINI, D., PERRUCCI M.G, CUGINI S Complete artifact removal for EEG recorded during continuous fMRI using independent component analysis. Neuroimage 34 (2), 598–607 (Jan 15)
[29] SRIVASTAVA, G., CROTTAZ-HERBETTE S., LAU K.M. ICA-based procedures for removing ballistocardiogram artifacts from EEG data acquired in the MRI scanner. 2005.Neuroimage 24 (1), 50–60
[30] DEBENER S., STROBEL, A., SORGER, B., Improved quality of auditory event-related potentials recorded simultaneously with 3-T fMRI: removal of the ballistocardiogram artefact. 2007.Neuroimage 34 (2), 590–600
[31] POLICH J., KOK A. Cognitive and biological determinants of P300: an integrative review Biol Psychol. 1995 Oct;41(2):103-46.

7 Annex

7.1 Annex 1 - Comparison of EPs

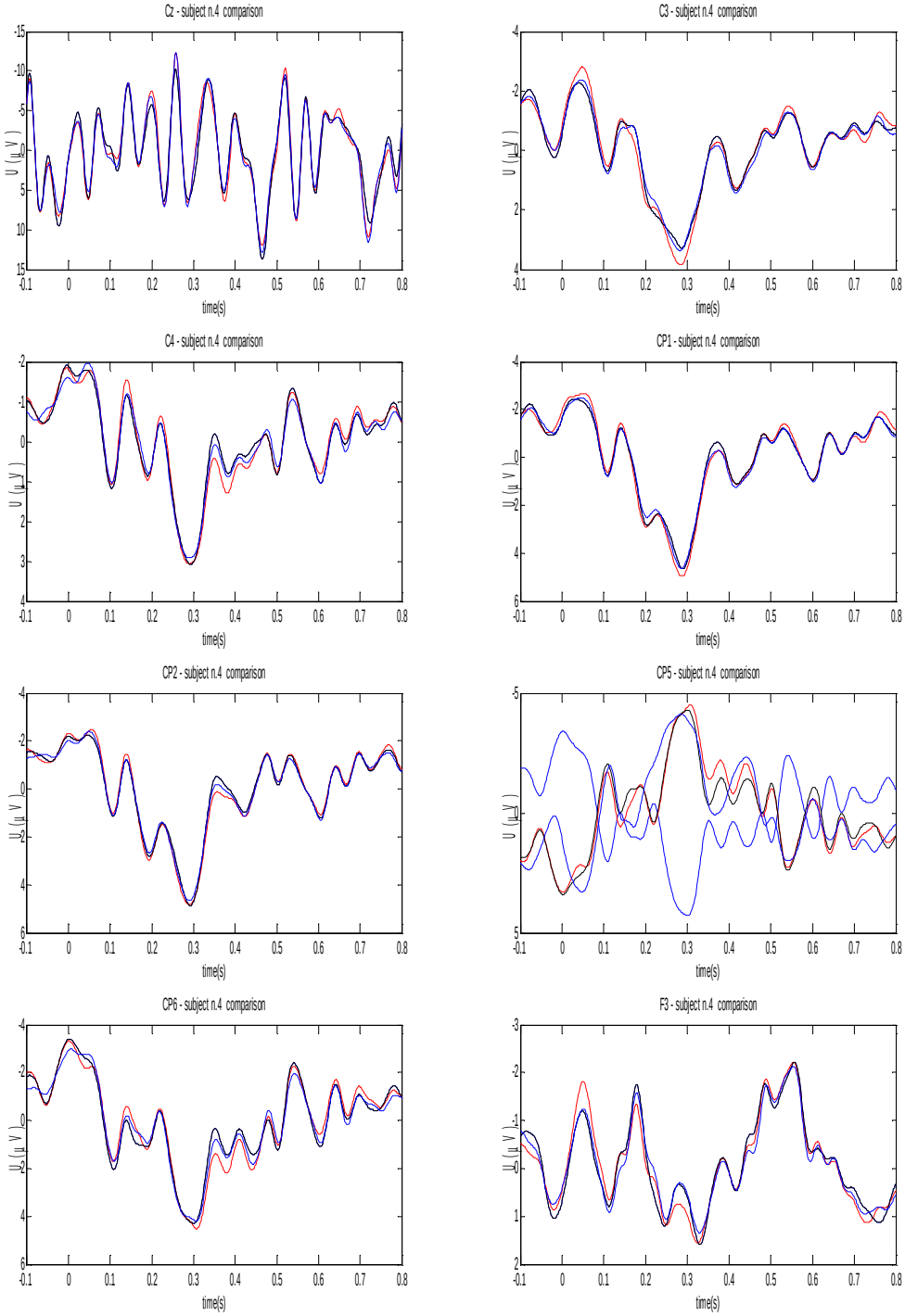

Fig 1 Comparison of EPs, red(after imaging artifact removal), blue(after BCG removal with ICA(EEGLAB)), black(after artifact template subtraction method) – subject n.4(1/4)

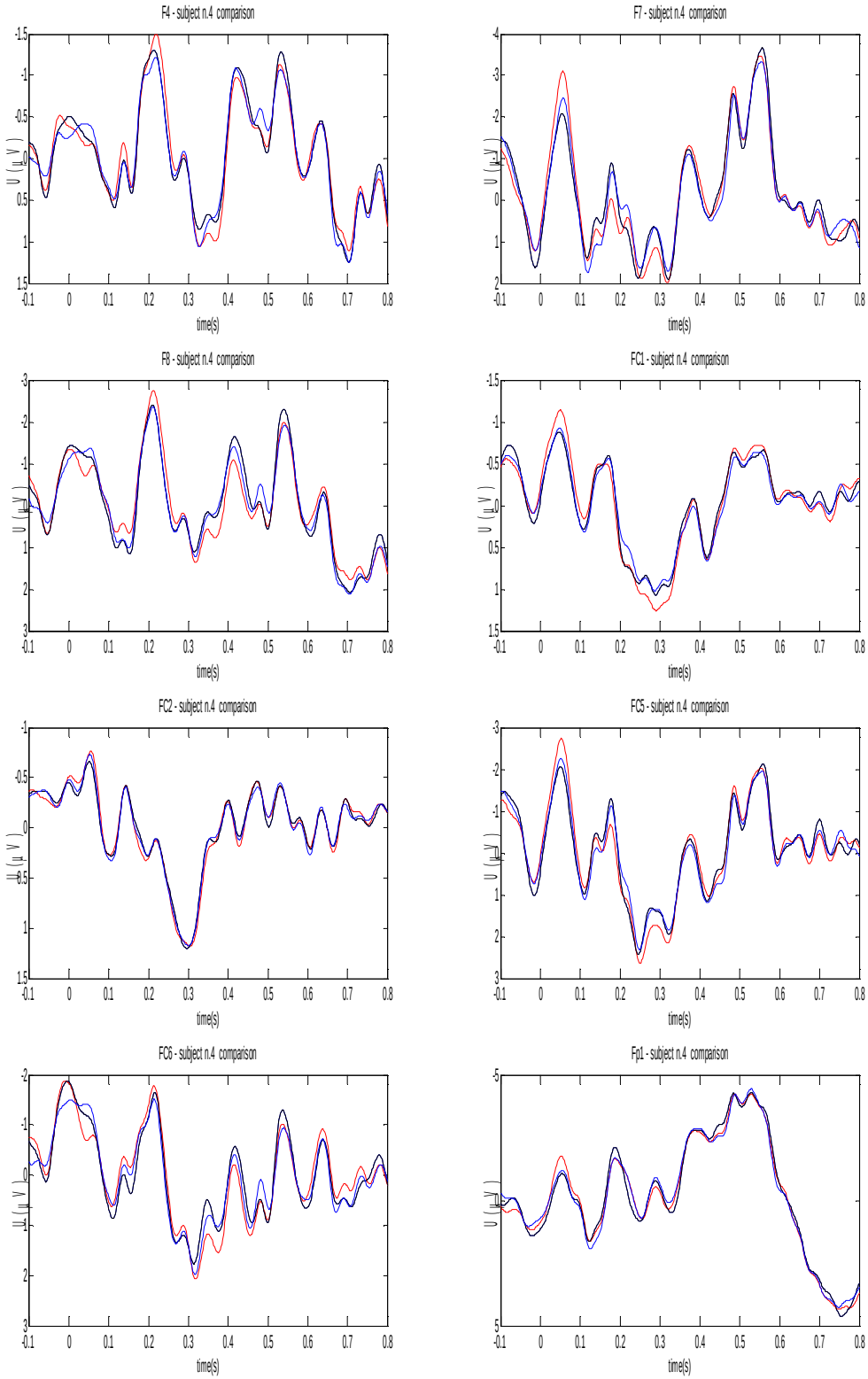

Fig 2 Comparison of EPs, red(after imaging artifact removal), blue(after BCG removal with ICA(EEGLAB)), black(after artifact template subtraction method) – subject n.4(2/4)

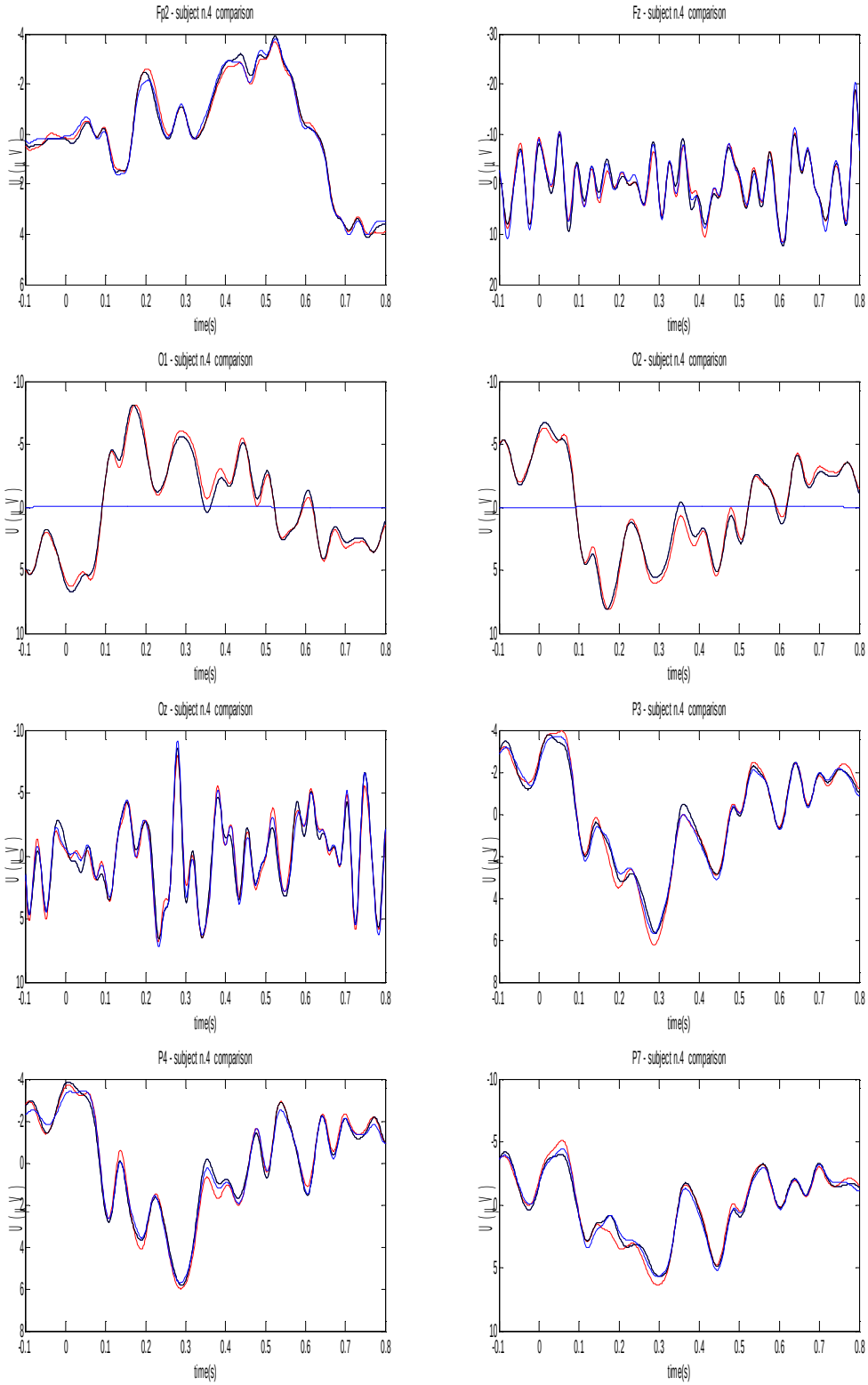

Fig 3 Comparison of EPs, red(after imaging artifact removal), blue(after BCG removal with ICA(EEGLAB)), black(after artifact template subtraction method) – subject n.4(3/4)

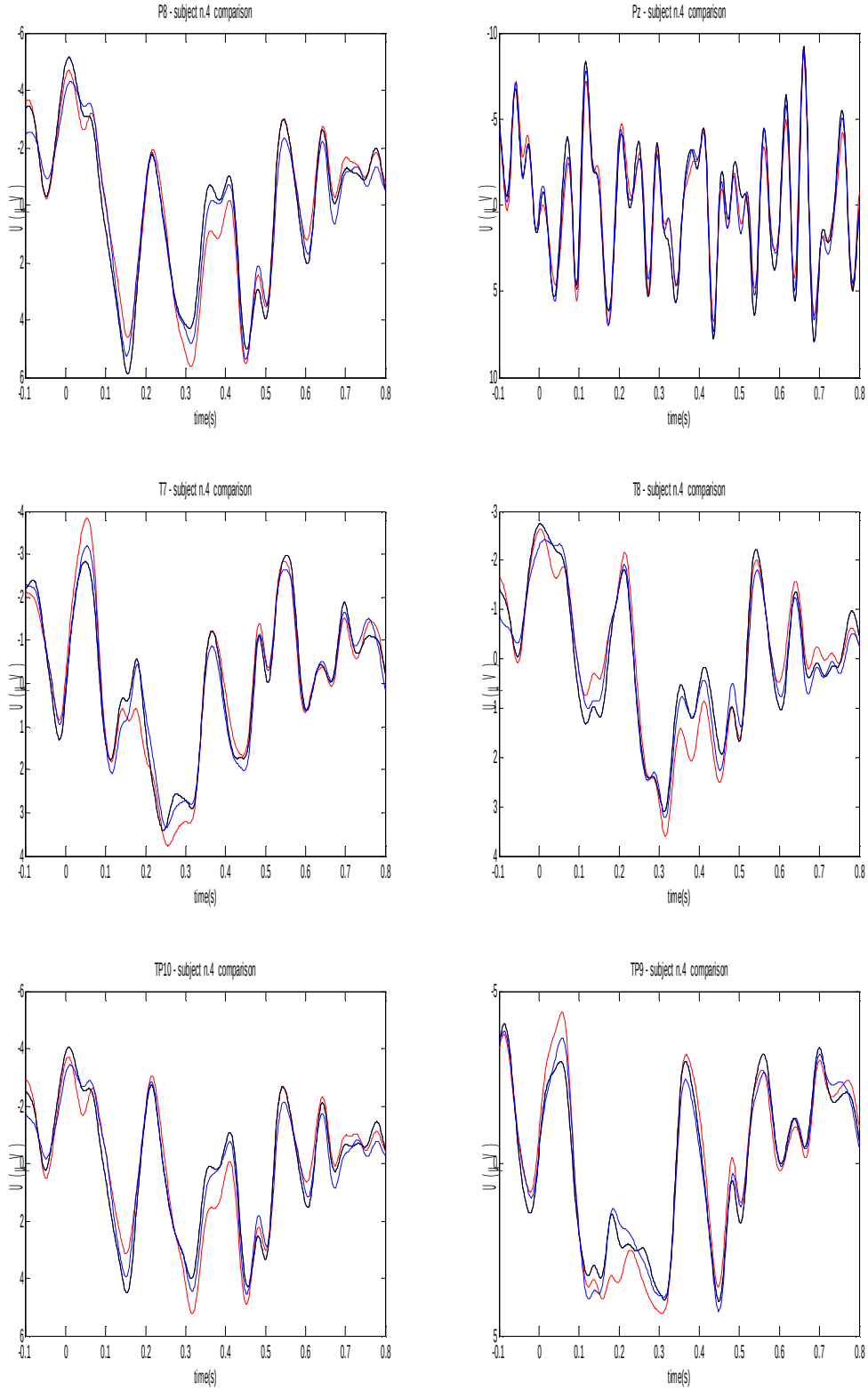

Fig 4 Comparison of EPs, red(after imaging artifact removal), blue(after BCG removal with ICA(EEGLAB)), black(after artifact template subtraction method) – subject n.4(4/4)

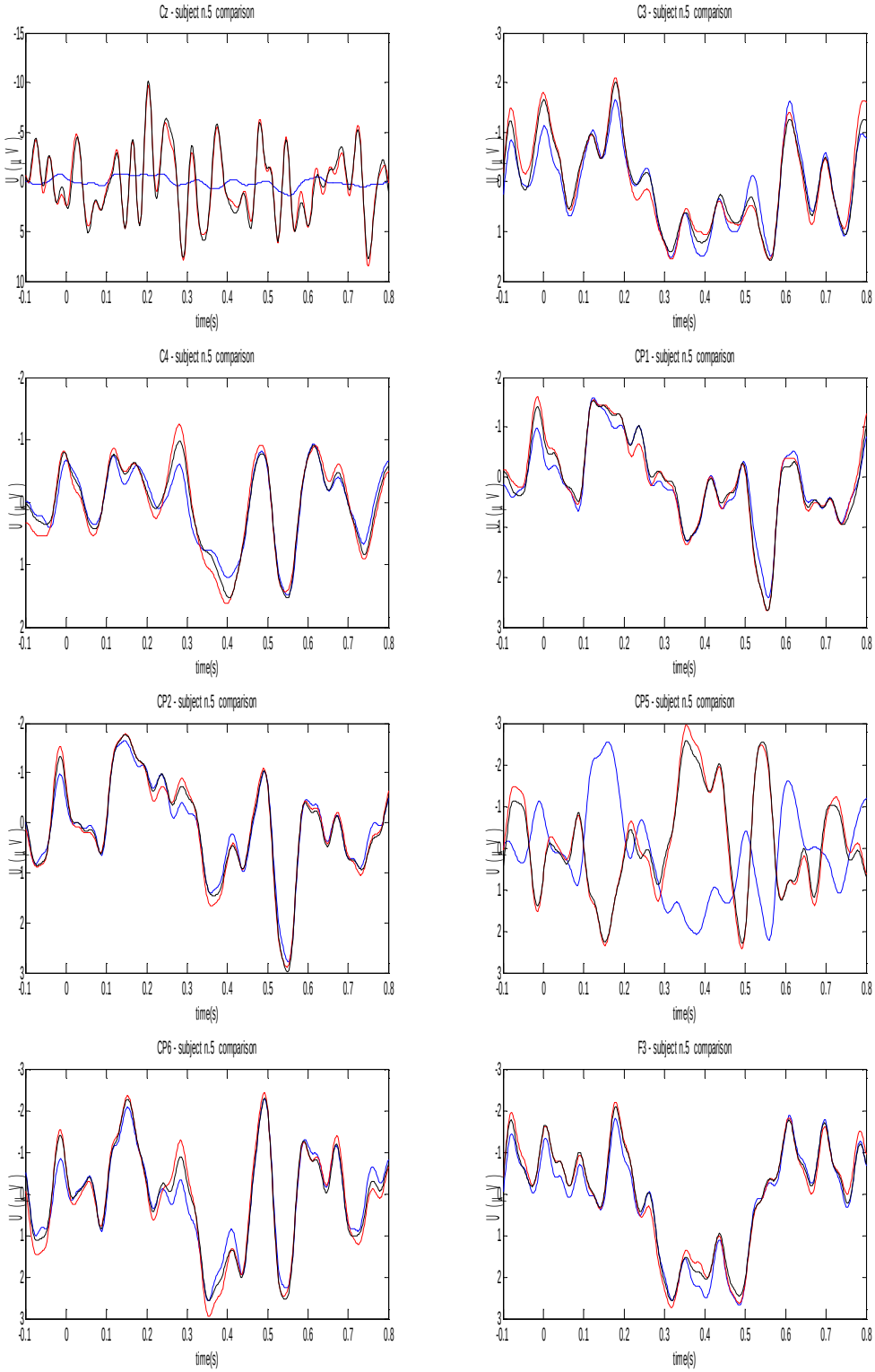

Fig 5 Comparison of EPs, red(after imaging artifact removal), blue(after BCG removal with BrainVision, black (after artifact template subtraction method) – subject n.5(1/4)

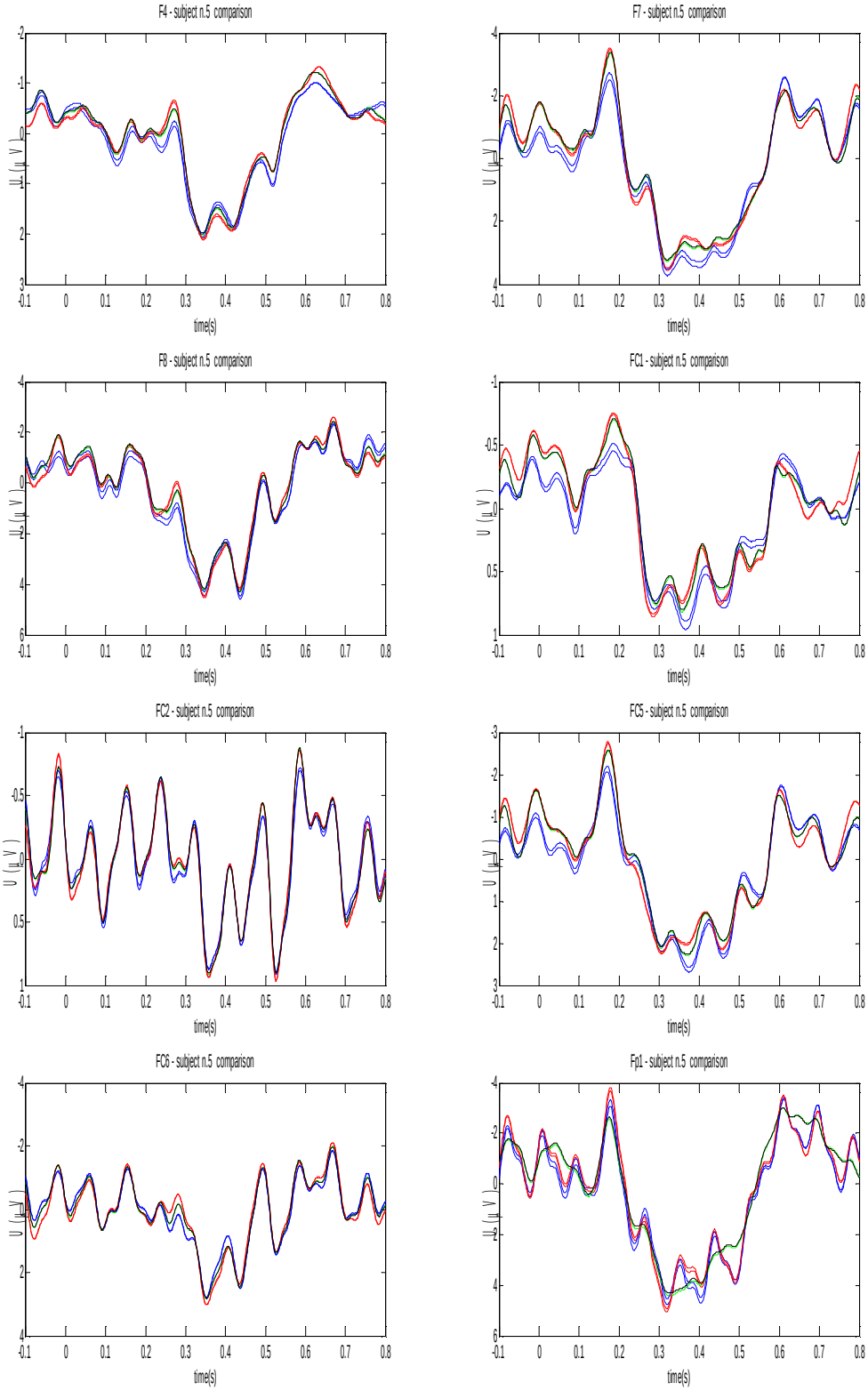

Fig 6 Comparison of EPs, red(after imaging artifact removal), blue(after BCG removal with BrainVision, black (after artifact template subtraction method) – subject n.5(2/4)

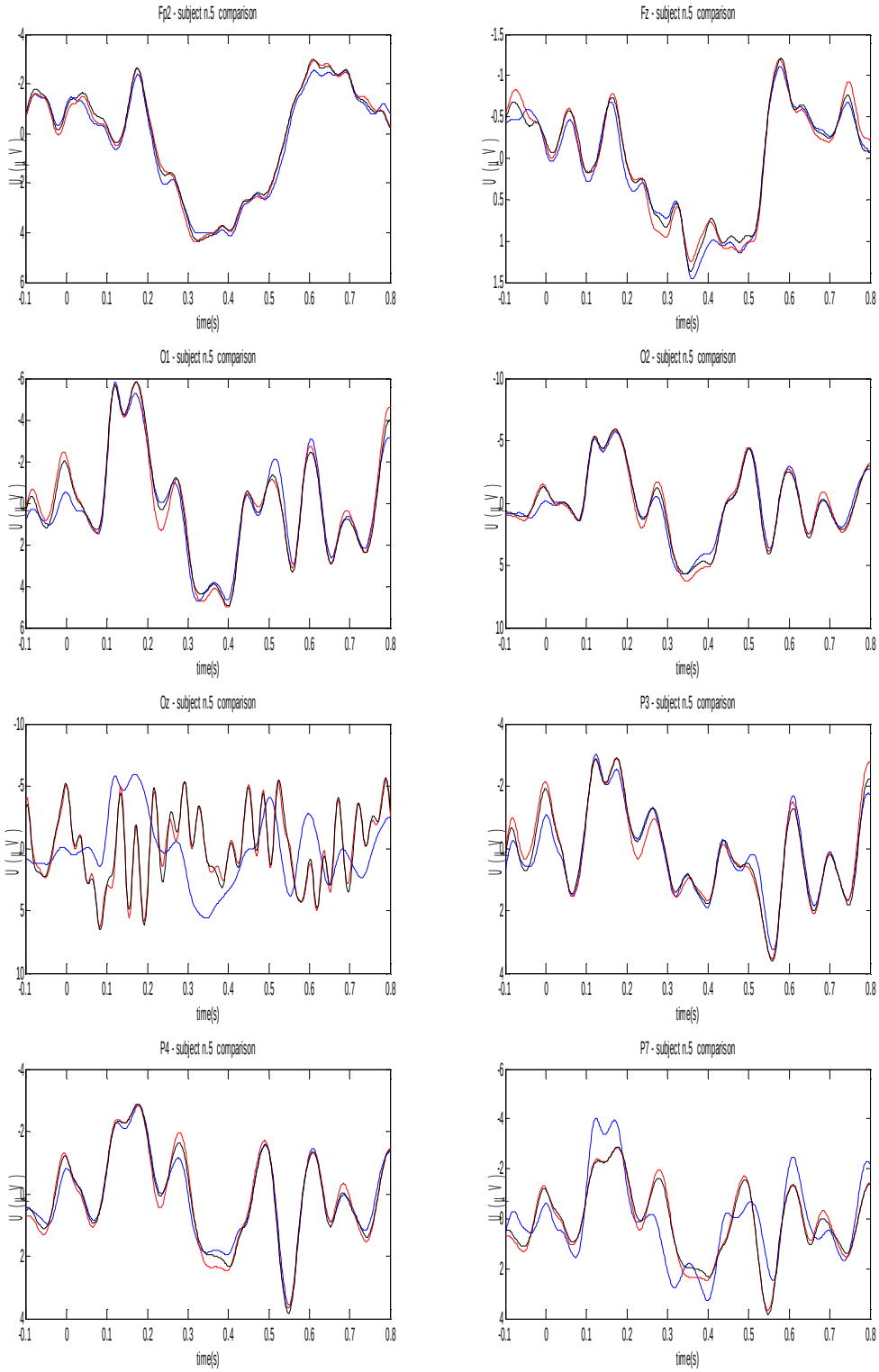

Fig 7 Comparison of EPs, red(after imaging artifact removal), blue(after BCG removal with BrainVision, black (after artifact template subtraction method) – subject n.5(3/4)

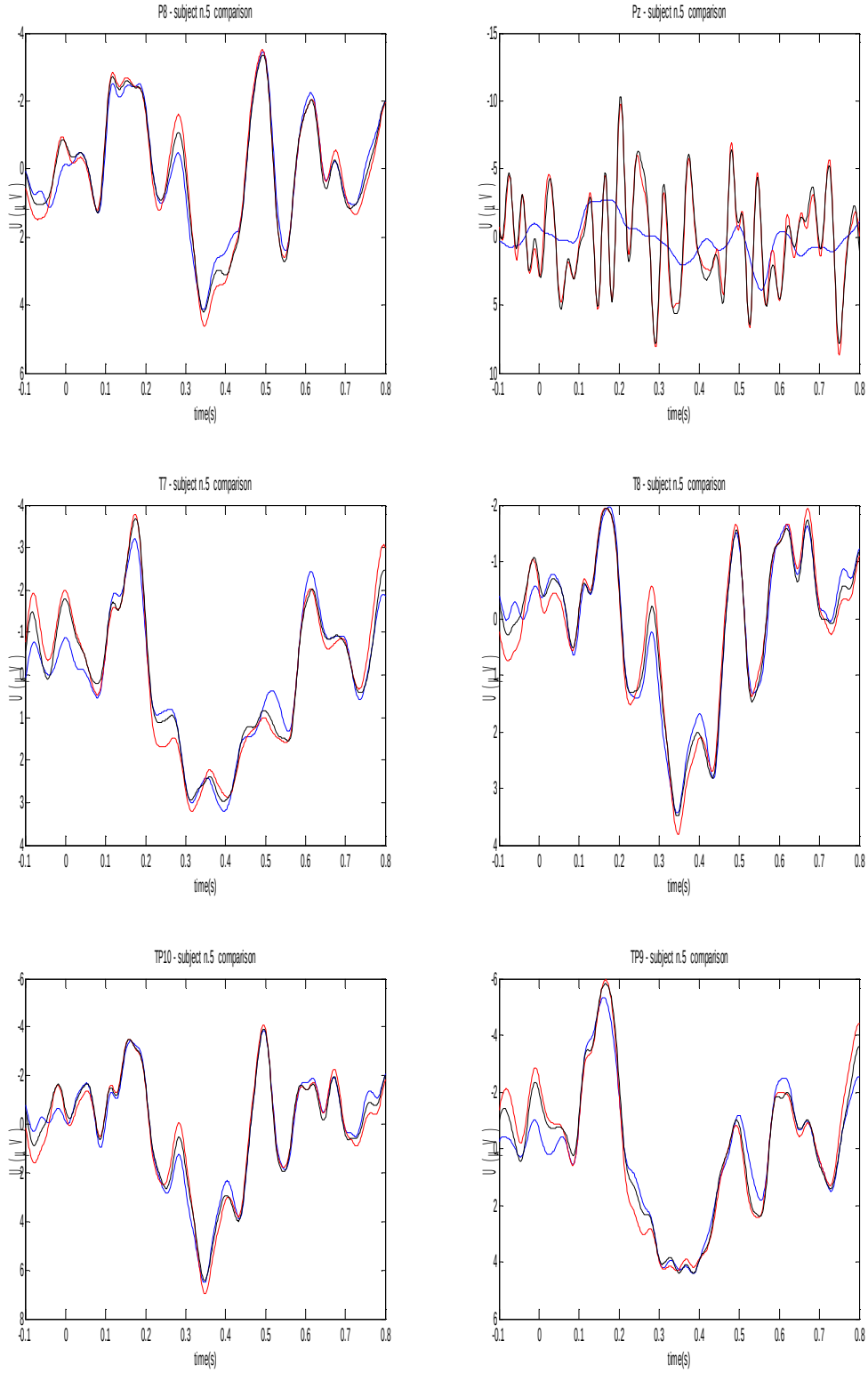

Fig 8 Comparison of EPs, red(after imaging artifact removal), blue(after BCG removal with BrainVision, black(after artifact template subtraction method) – subject n.5(4/4)

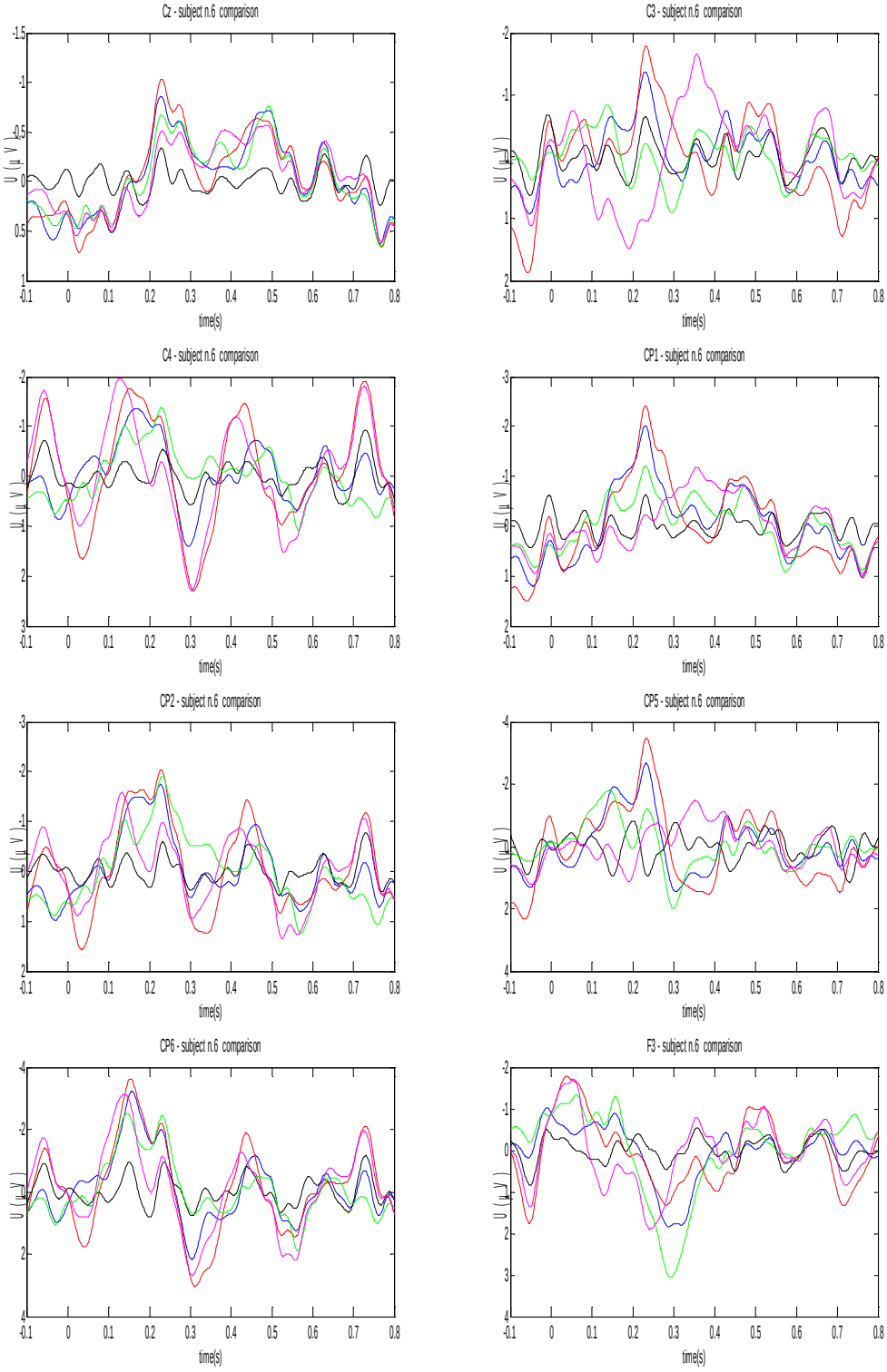

Fig 9 Comparison of EPs, red(after imaging artifact removal), blue(after BCG removal with Brainvision)), black(after artifact template subtraction method), green(after BCG removal with ICA(Brainvision)), violet(after BCG removal by ICA+Allen) – subject n.6(1/4)

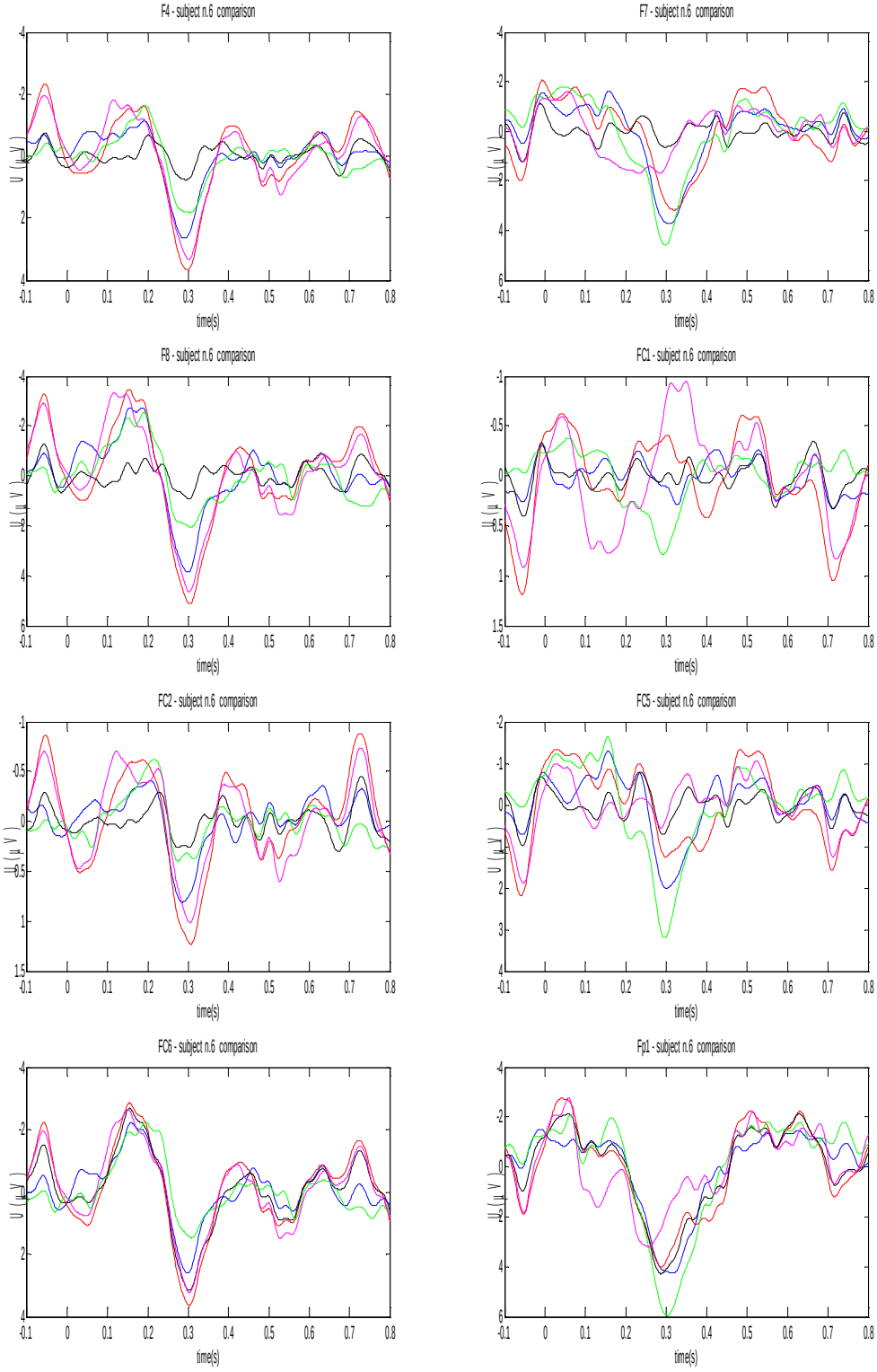

Fig 10 Comparison of EPs, red(after imaging artifact removal), blue(after BCG removal with Brainvision)), black(after artifact template subtraction method), green(after BCG removal with ICA(Brainvision)), violet(after BCG removal by ICA+Allen) – subject n.6(2/4)

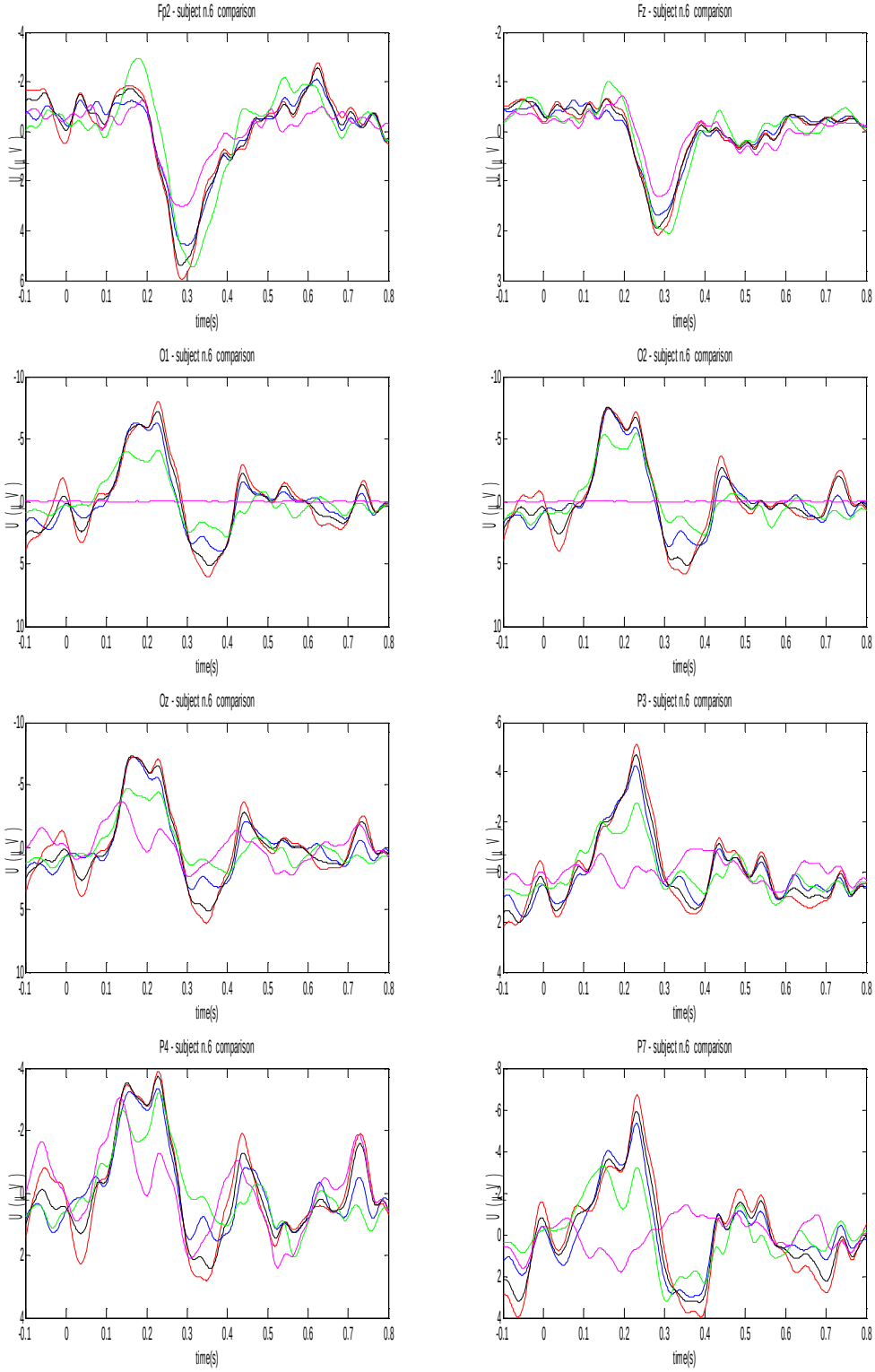

Fig 11 Comparison of EPs, red(after imaging artifact removal), blue(after BCG removal with Brainvision)), black(after artifact template subtraction method), green(after BCG removal with ICA(Brainvision)), violet(after BCG removal by ICA+Allen) – subject n.6(3/4)

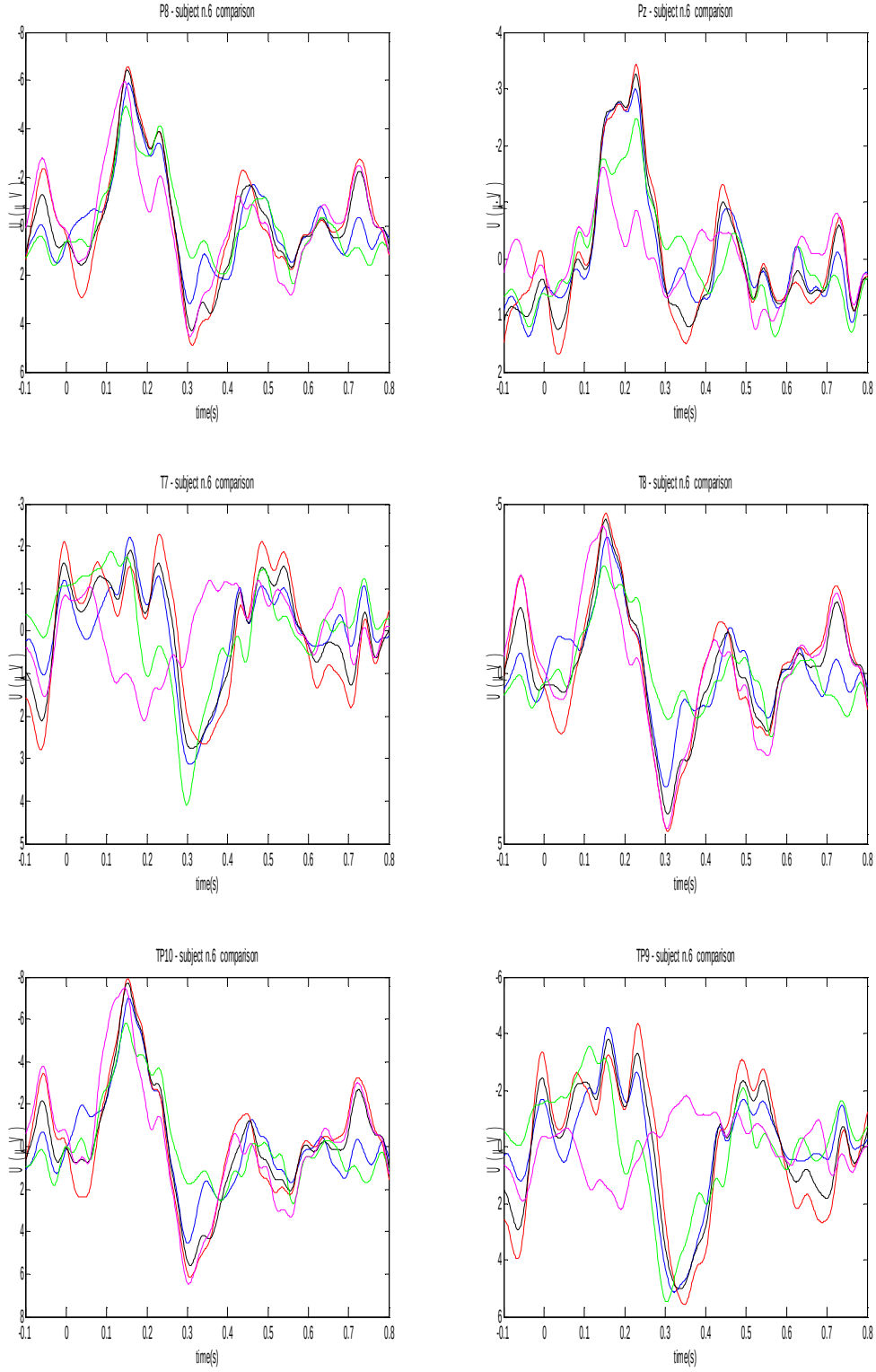

Fig 12 Comparison of EPs, red(after imaging artifact removal), blue(after BCG removal with Brainvision)), black(after artifact template subtraction method), green(after BCG removal with ICA(Brainvision)), violet(after BCG removal by ICA+Allen) – subject n.6(4/4)

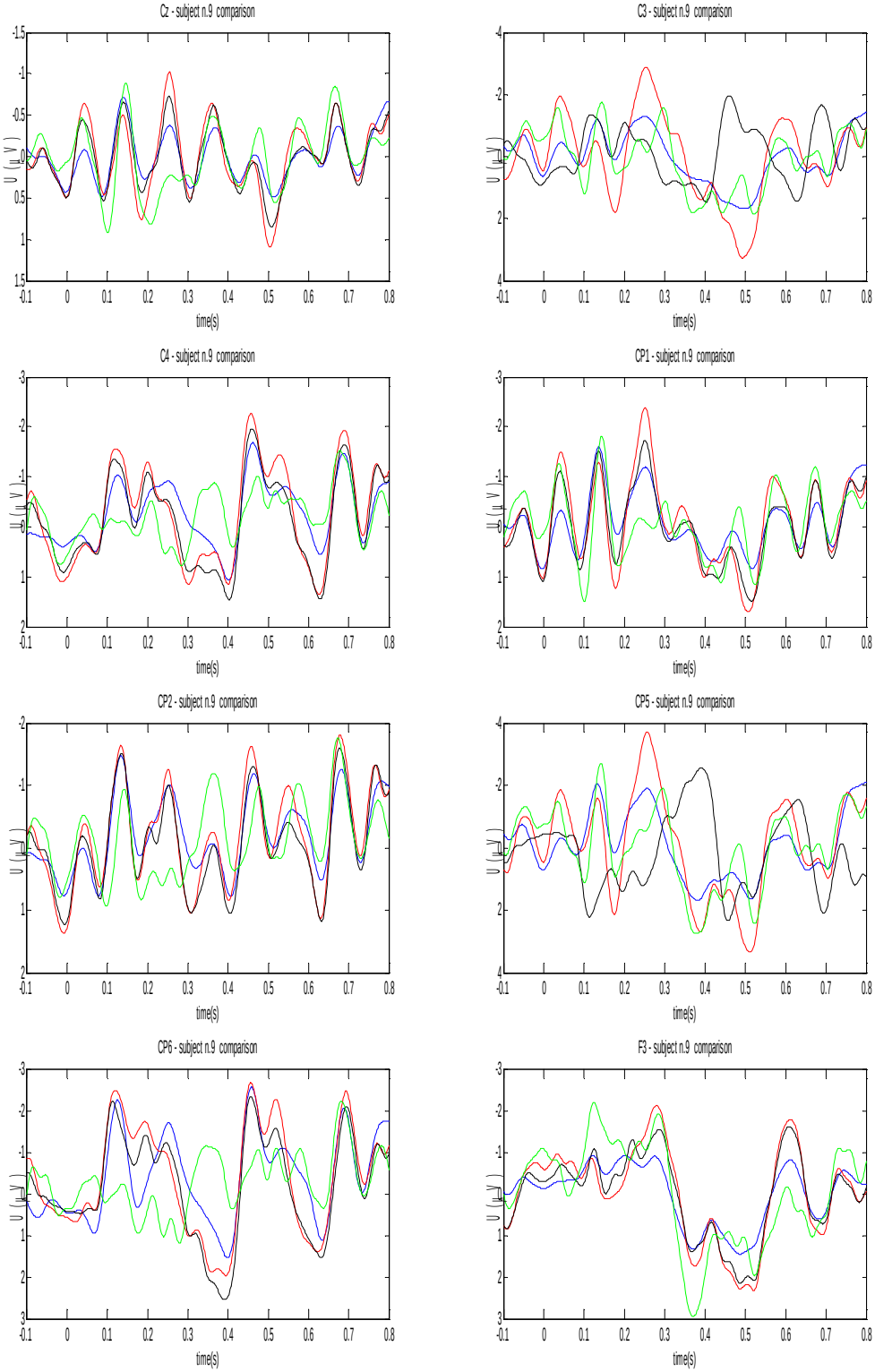

Fig 13 Comparison of EPs, red(after imaging artifact removal), blue(after BCG removal with Brainvision)), black(after artifact template subtraction method), green(after BCG removal with ICA(Brainvision)) – subject n.9(1/4)

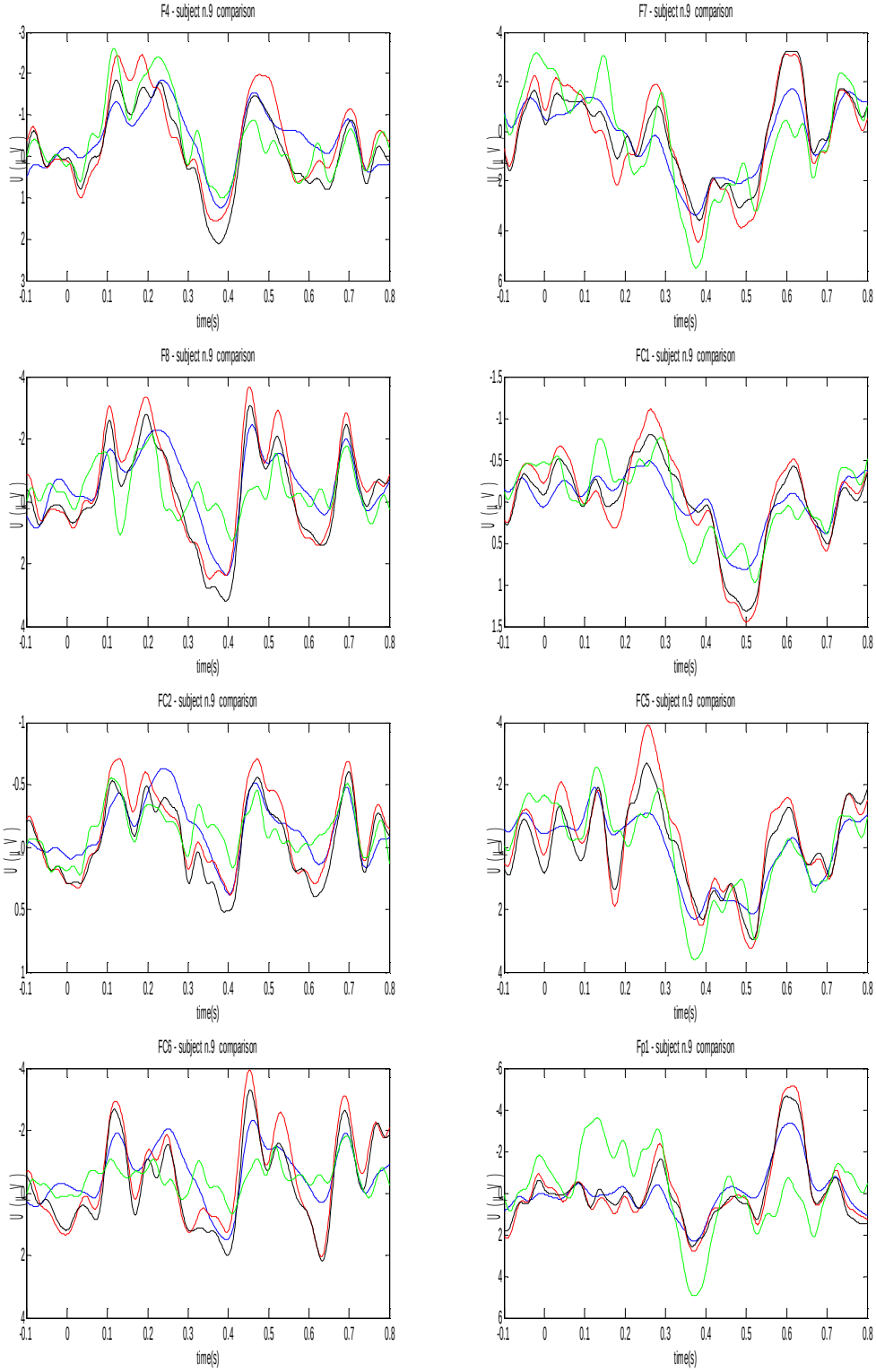

Fig 14 Comparison of EPs, red(after imaging artifact removal), blue(after BCG removal with Brainvision)), black(after artifact template subtraction method), green(after BCG removal with ICA(Brainvision)) – subject n.9(2/4)

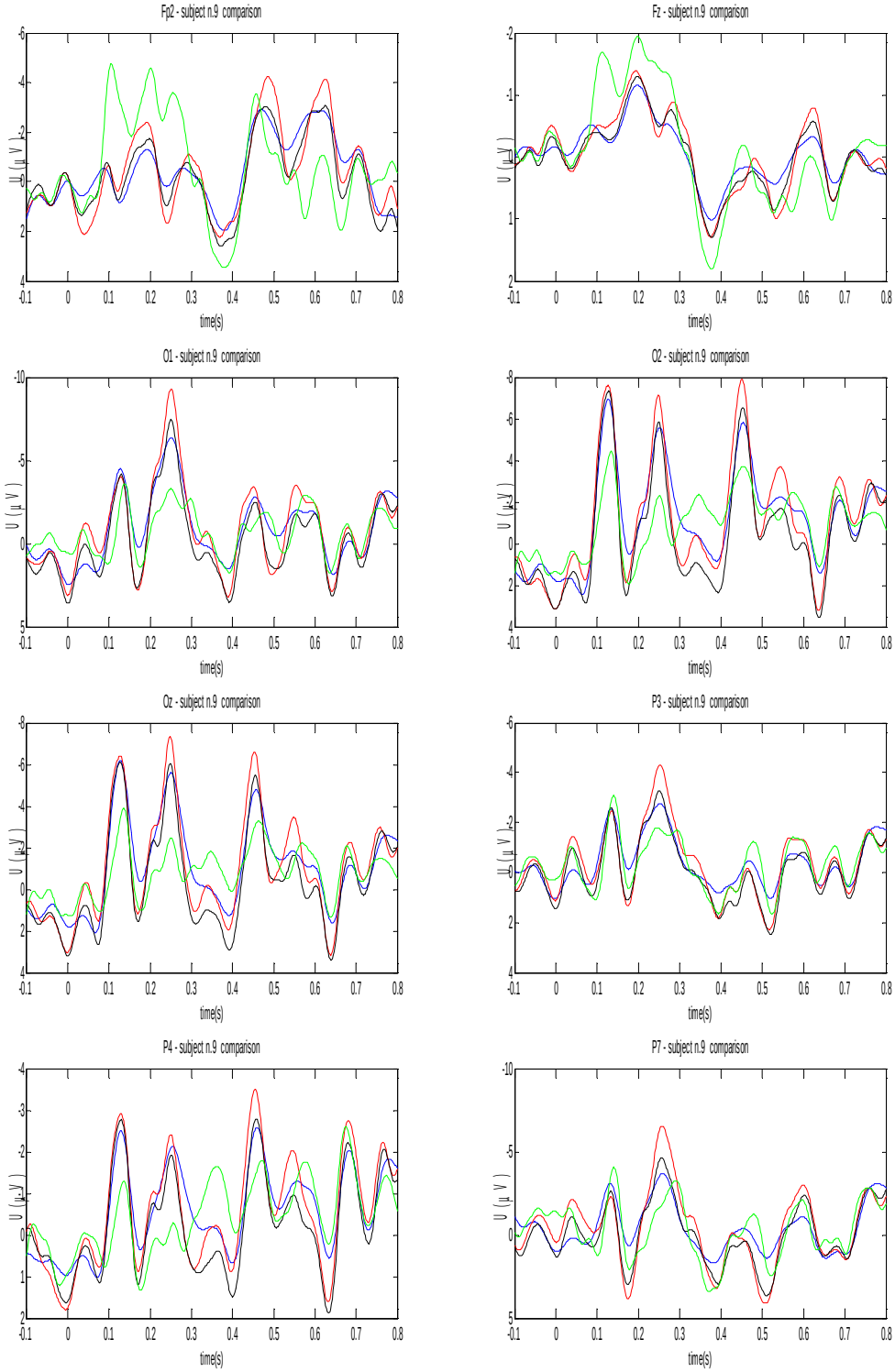

Fig 15 Comparison of EPs, red(after imaging artifact removal), blue(after BCG removal with Brainvision)), black(after artifact template subtraction method), green(after BCG removal with ICA(Brainvision)) – subject n.9(3/4)

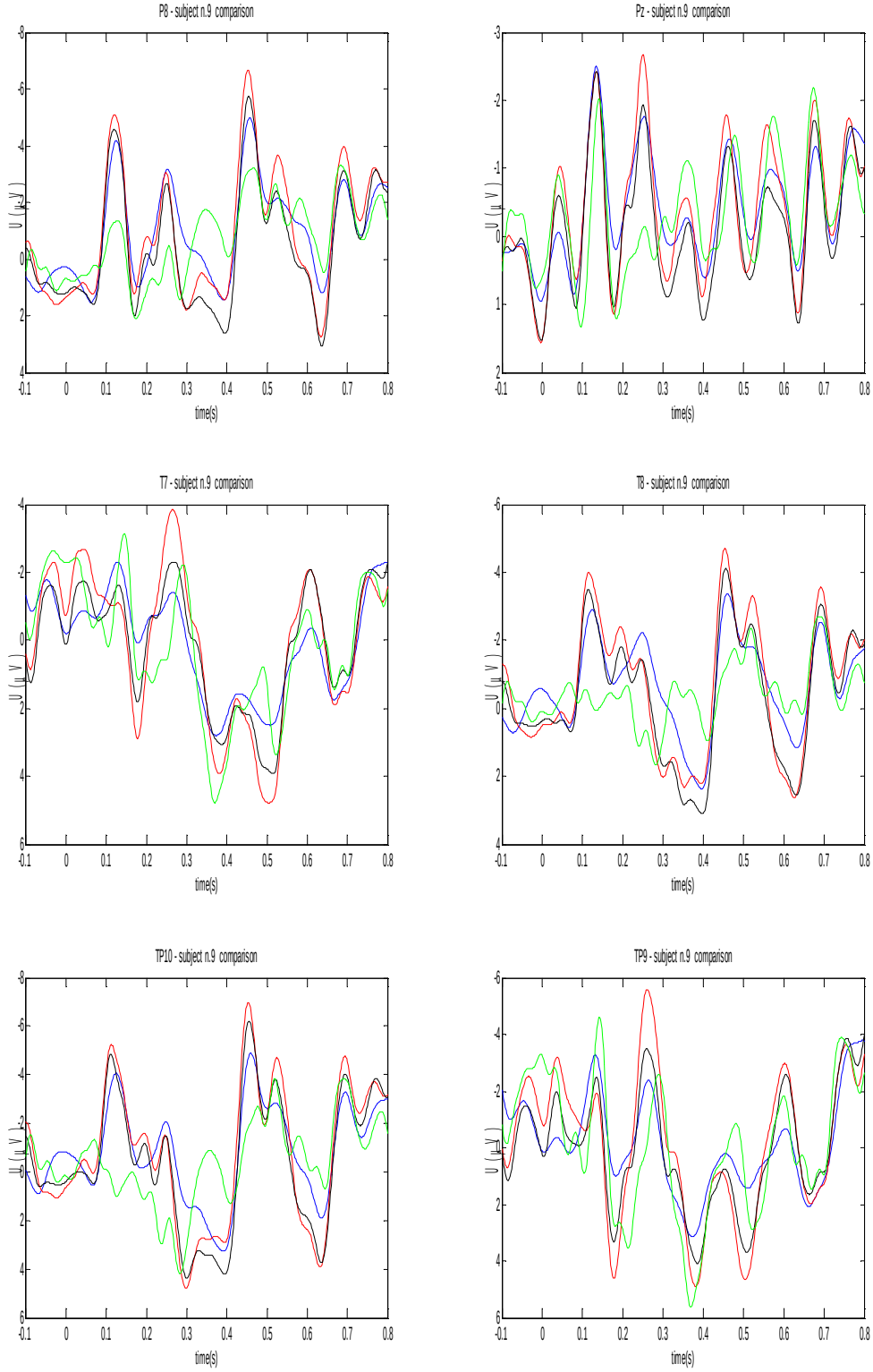

Fig 16 Comparison of EPs, red(after imaging artifact removal), blue(after BCG removal with Brainvision)), black(after artifact template subtraction method), green(after BCG removal with ICA(Brainvision)) – subject n.9(4/4)

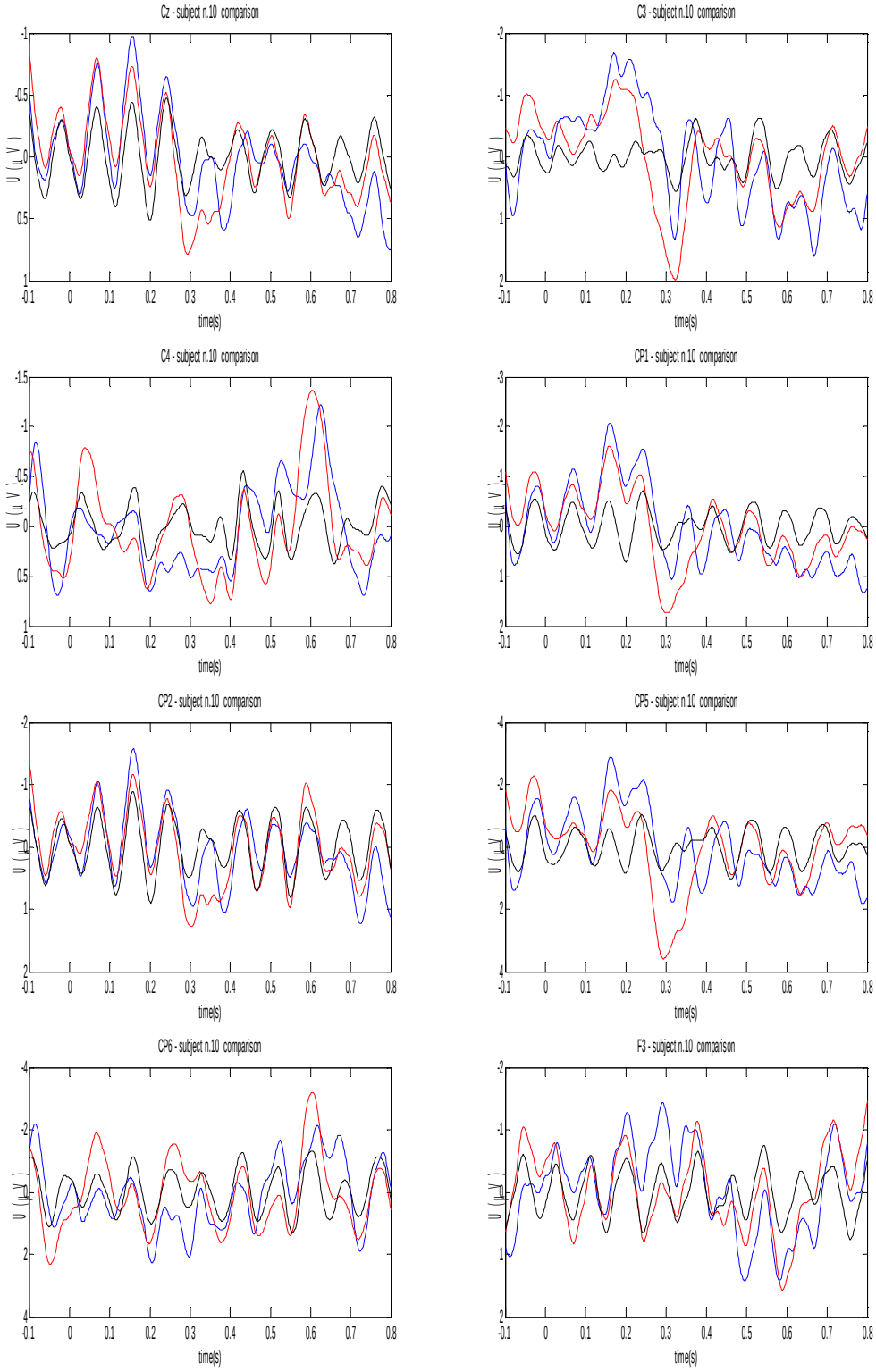

Fig 17 Comparison of EPs, red(after imaging artifact removal), blue(after BCG removal with ICA(Brainvision)), black(after artifact template subtraction method) – subject n.10(1/4)

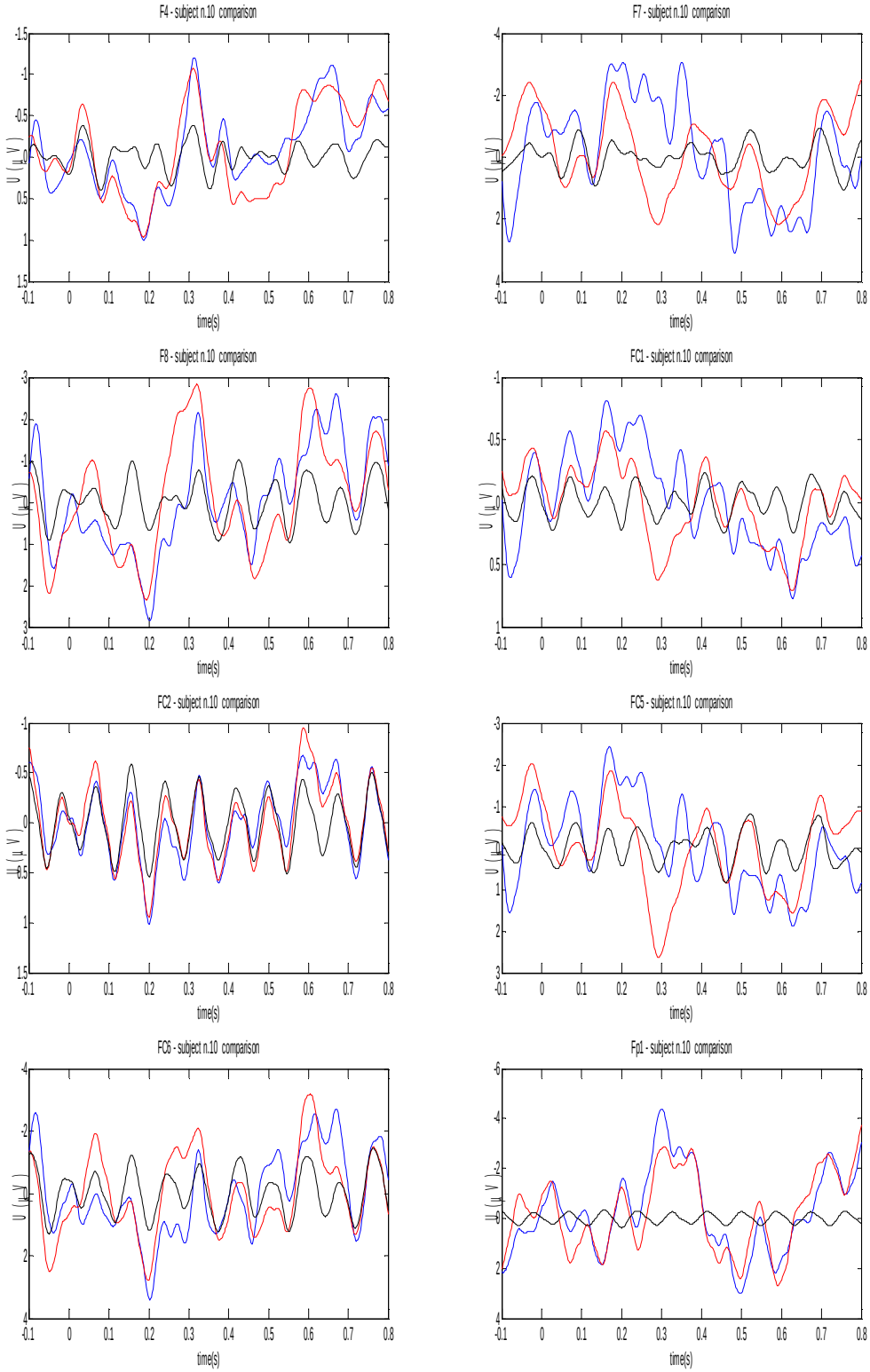

Fig 18 Comparison of EPs, red(after imaging artifact removal), blue(after BCG removal with ICA(Brainvision)), black(after artifact template subtraction method) – subject n.10(2/4)

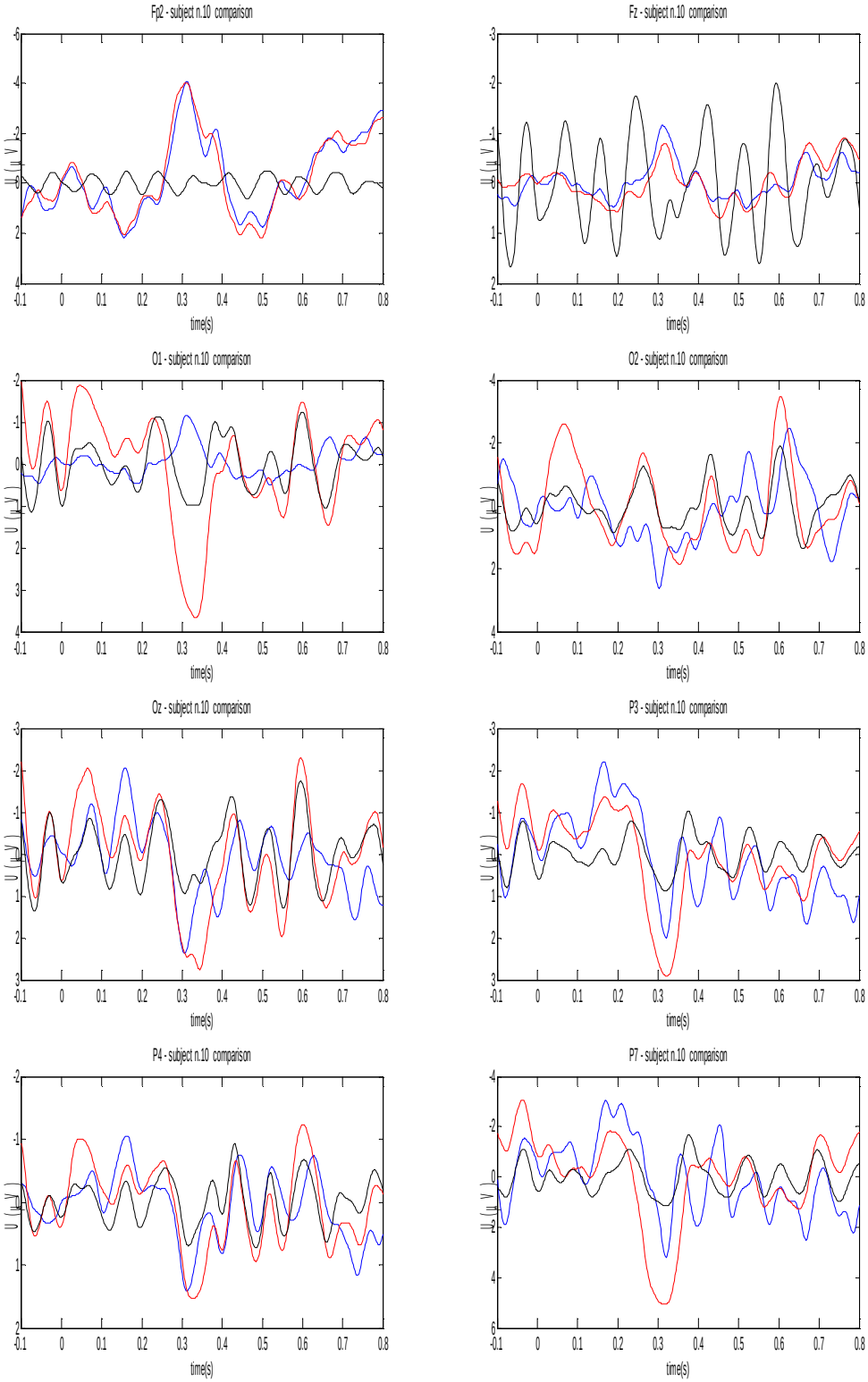

Fig 19 Comparison of EPs, red(after imaging artifact removal), blue(after BCG removal with ICA(Brainvision)), black(after artifact template subtraction method) – subject n.10(3/4)

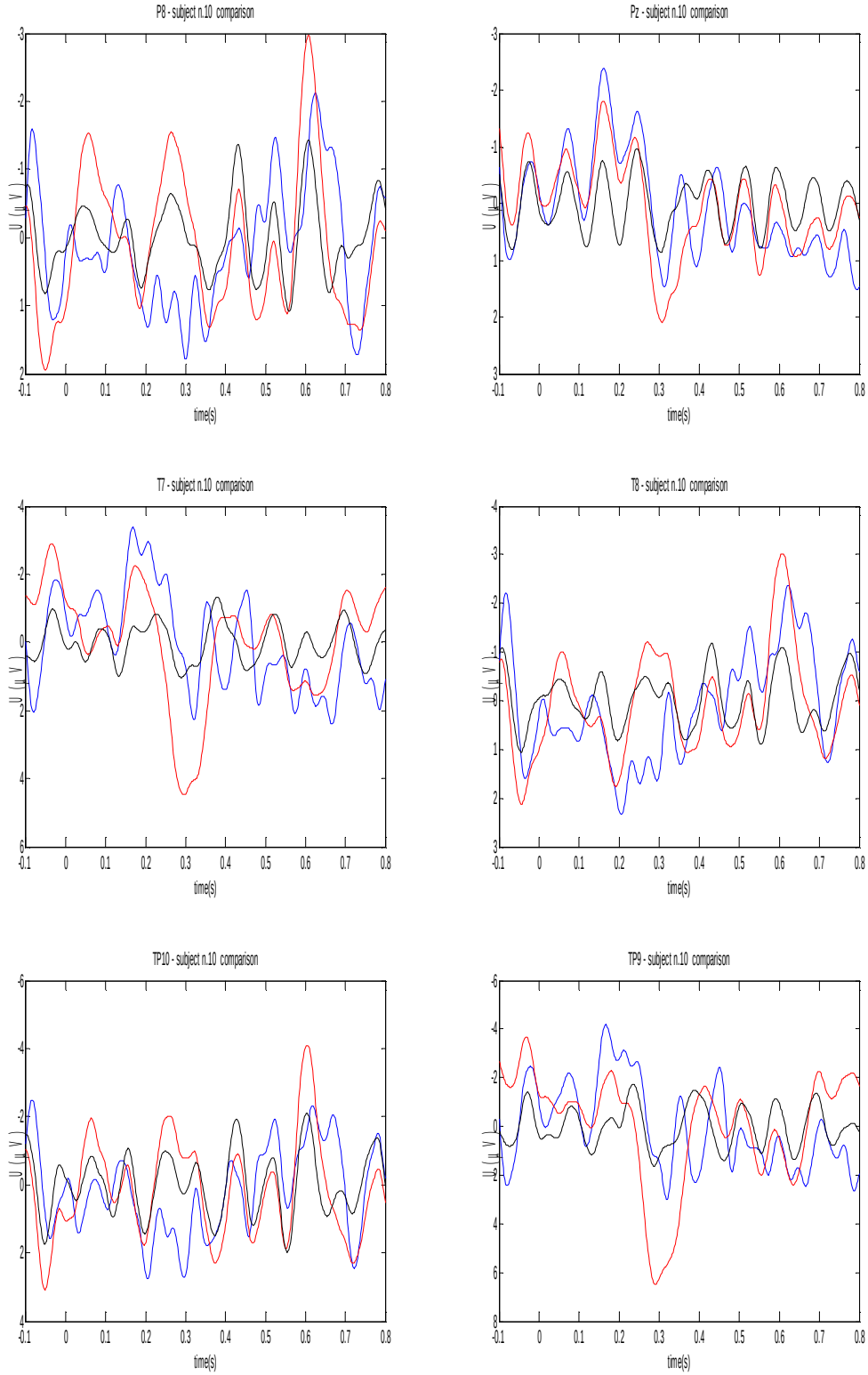

Fig 20 Comparison of EPs, red(after imaging artifact removal), blue(after BCG removal with ICA(Brainvision)), black(after artifact template subtraction method) – subject n.10(4/4)

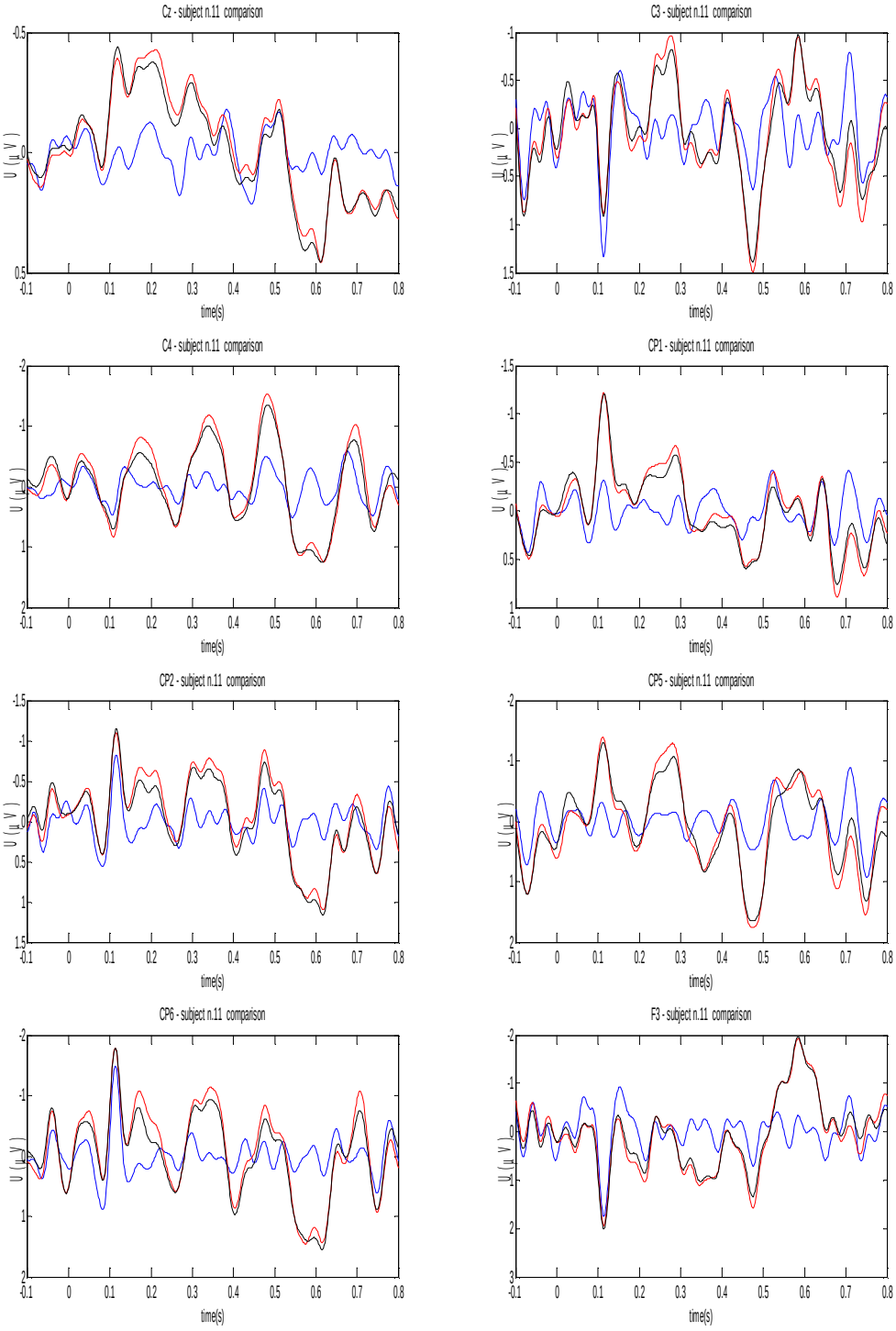

Fig 21 Comparison of EPs, red(after imaging artifact removal), blue(after BCG removal with ICA(Brainvision), black(after artifact template subtraction method) – subject n.11(1/4)

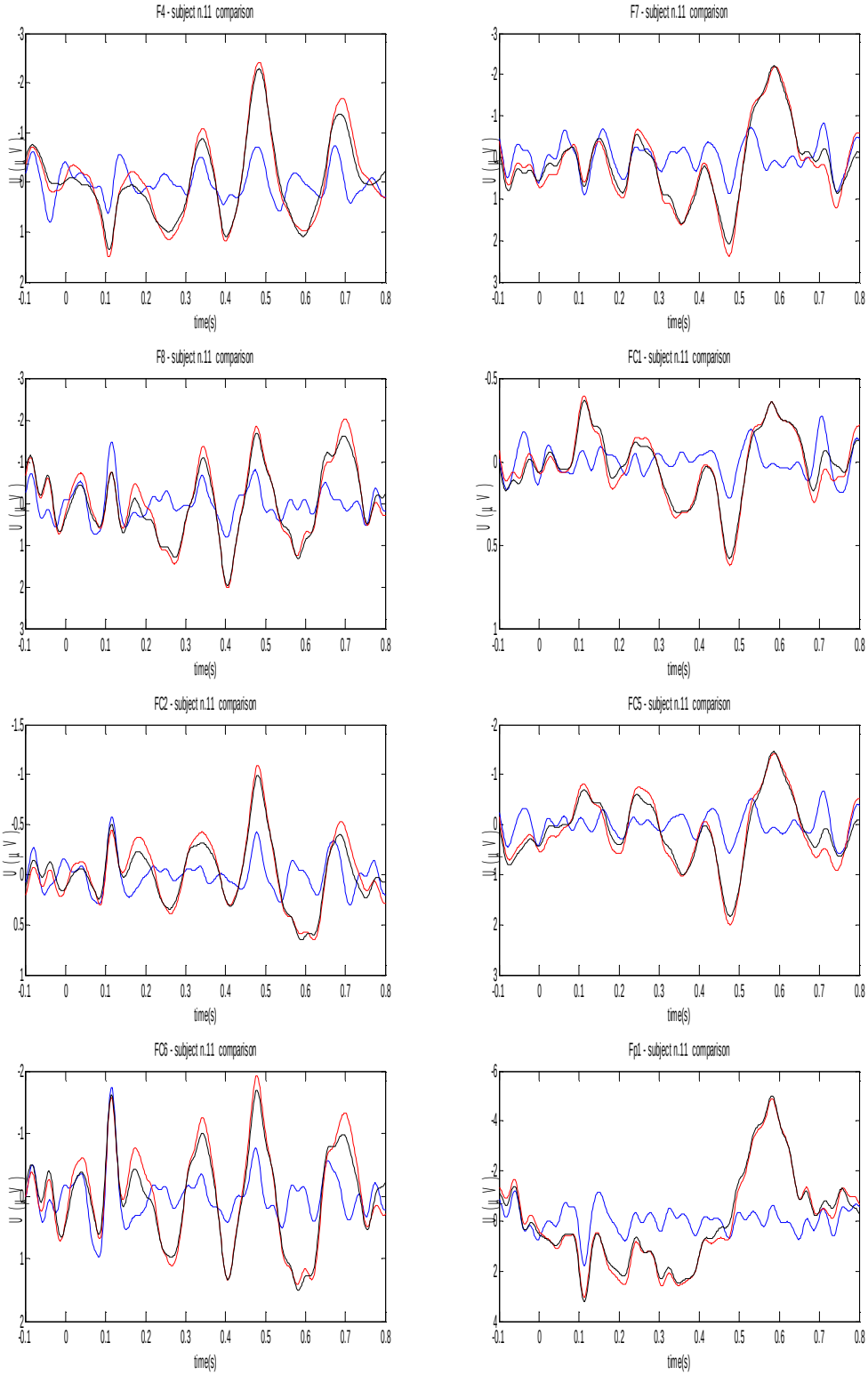

Fig 22 Comparison of EPs, red(after imaging artifact removal), blue(after BCG removal with ICA(Brainvision), black(after artifact template subtraction method) – subject n.11(2/4)

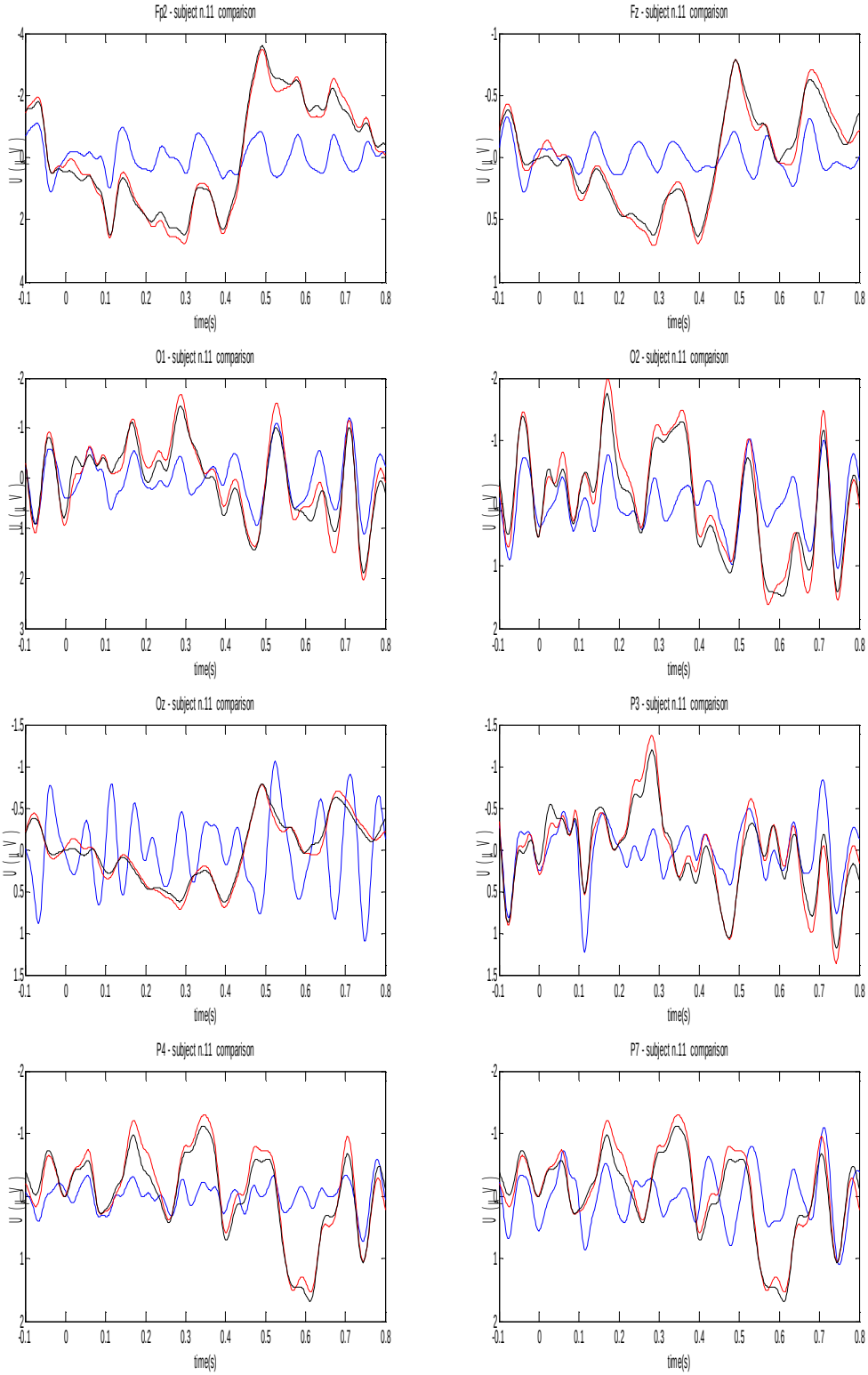

Fig 23 Comparison of EPs, red(after imaging artifact removal), blue(after BCG removal with ICA(Brainvision), black(after artifact template subtraction method) – subject n11(3/4)

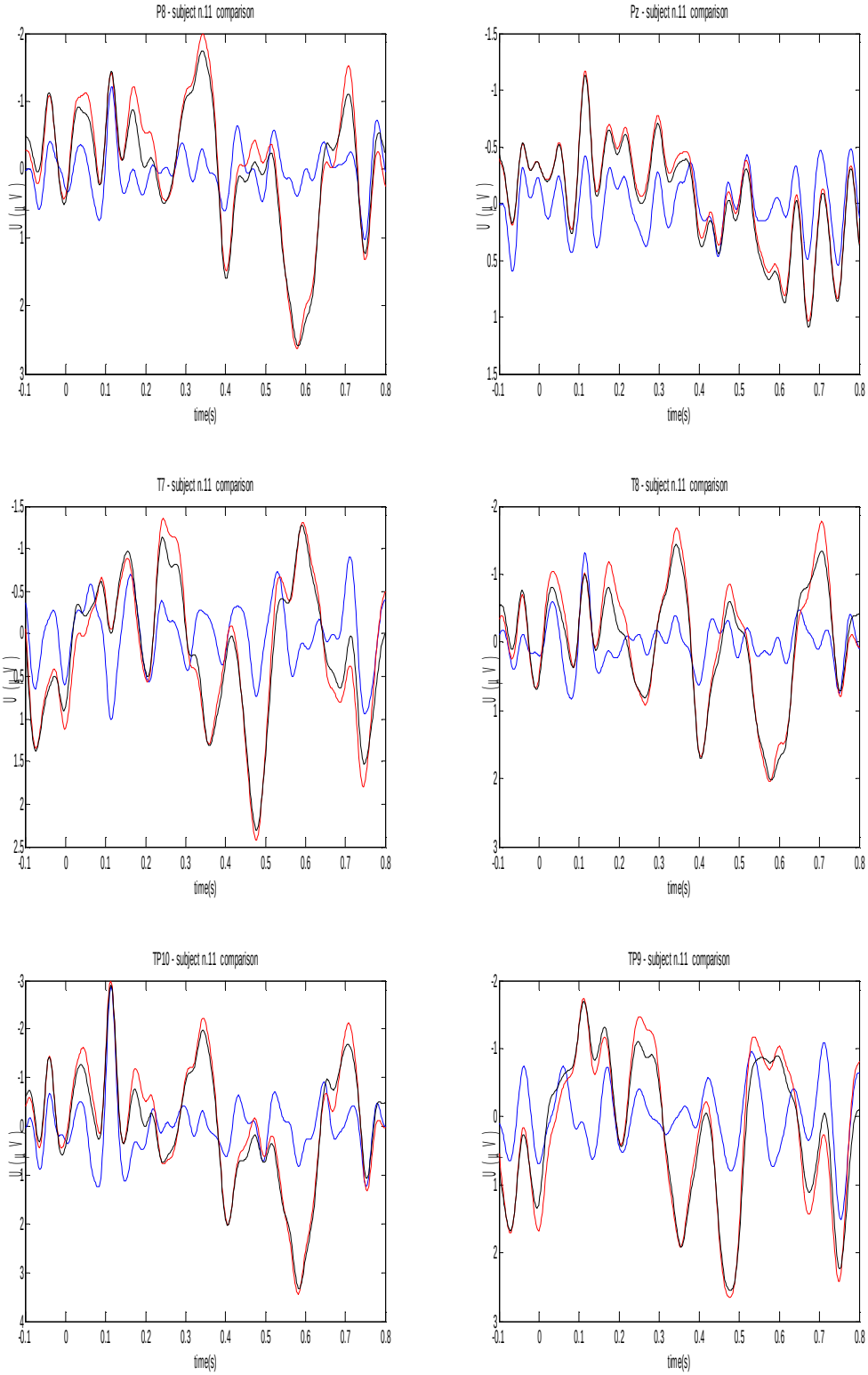

Fig 24 Comparison of EPs, red(after imaging artifact removal), blue(after BCG removal with ICA(Brainvision)), black(after artifact template subtraction method) – subject n.11(4/4)